MOLECULAR BIOLOGY DEPARTMENT

Molecular Causes and Mechanisms of Genomic Instability in G1-deregulated Cell Cycles

PhD Thesis

Fábia Araújo Gomes

Madrid, 2016

Molecular Biology Department
Faculty of Science
Universidad Autonoma de Madrid

Molecular Causes and Mechanisms of Genomic Instability in G1-deregulated Cell Cycles

Fábia Araújo Gomes
Cellular and Molecular Biology, B.S.;
Biomedical Sciences, M.S.

Director:
Dr. José Arturo Calzada García

Spanish National Centre for Biotechnology (CNB-CSIC)
Madrid, 2016

Aos meus pais e irmão

ACKNOWLEDGEMENTS

First, I would like to thank my supervisor Arturo for making this project possible and being a constant source of support and for his perspective, insight and helpful discussions. Also for answering my constant questions and incite me to be critics and rigorous with my work.

I would like to thank ex former members of the Lab that were of undoubtedly help for the development of this project: Pilar for all the work support, Fernando for his time, helpful discussions and cups of coffees between experiments; and Angel for his help and technical support. I would also like to thank to all students that had passed by the Lab and contributed in some way to this work, Niki, Azmane, Maria Luísa, Héctor, Arantxa, Deborah and Pablo.

I would like to thank José Antonio Tercero and Maria Gomez from the CBM-UAM and Karim Labib from Cancer Research UK for advice, help and material support.

I would also like to thank my colleagues and friends in the CNB. In particular, I'm very grateful to Elena, who has been a wealth of encouragement, advice and affection. To Maria, Vero, Andrea, Esther, Rúben, Carmén, Sofia, Ruggero, Daya, Estel for the all the good moments we spend together, for their enthusiasm for science and their friendship who made these years memorable.

To Mariangela, Alejandra and Carol, my "chicas BiMi", thank you for your friendship, all the afternoon coffees, trips and the good time we spent together in Madrid.

The support of all my friends has been invaluable. Margarida, Joana, Catarina, Leonor, Bruno and João thank you for all your motivation, valuable friendship and for being my best and dearest friends.

To my lovely boyfriend Yuri, thank you for being a constant source of encouragement and affection, also for being present during this important journey of my life.

Finalmente, queria agradecer a toda a minha família pelo apoio que recebi ao longo desta jornada académica. Em particular aos meus pais, Ana e Augusto, e querido irmão Hugo, por estarem sempre presentes, por me ensinarem o valor do esforço, por acreditarem em mim e apoiarem as minhas decisões. Sem vocês, esta tese não teria sido possível. Muito obrigada.

This work would not have been possible without the financial support and Fellowship from the Fundação para a Ciência e Tecnologia (Portuguese government), which I am grateful to for the opportunity to pursue my Ph.D.

FCT Fundação para a Ciência e a Tecnologia
MINISTÉRIO DA CIÊNCIA, TECNOLOGIA E ENSINO SUPERIOR

POPH

QREN QUADRO DE REFERÊNCIA ESTRATÉGICO NACIONAL PORTUGAL 2007.2013

UNIÃO EUROPEIA
Fundo Social Europeu

SUMMARY

Eukaryotic DNA replication initiates at numerous sites called origins and is tightly regulated so that chromosomes are accurately replicated only once per cell cycle. Absence of active cyclin-dependent kinase (CDK) complexes from late mitosis and during G1 allows the licensing of origins for their potential activation later in S phase. At the G1/S transition, rising levels of CDK activity block additional origin licensing and promote the activation of a subset of licensed origins, together with Dbf4-dependent kinase (DDK) activity. Origin activation follows a spatiotemporal program during S phase that is highly conserved in cell populations but partially stochastic in individual cells, and presumed to largely influence the timely completion of DNA replication due to exceeding numbers of licensed origins available to counteract hindered forks. Replication completion is critical to the genome integrity, as cells allowed to enter mitosis with on-going forks might suffer from chromosome breaks upon premature segregation during anaphase.

In both yeast and mammals, genomic instability arises when the G1/S transition is deregulated, as cells escaping this control have proliferative advantages and a mutator phenotype. Indeed, cancer cells often show mutations in G1/S regulators and perturbed DNA replication; furthermore, genomic instability is a hallmark of cancer. However, the molecular mechanism by which G1-phase deregulation causes genomic instability remains poorly understood. To study this question, we used budding yeast cells lacking the CDK inhibitor Sic1, a central regulator of the G1 phase and orthologous to $p27^{Kip1}$ in mammals, as eukaryotic model of oncogenic cell cycles. Here we show that in the absence of Sic1, cells loose functional origin redundancy that directly causes chromosomal instability. Moreover, we report that the differential loss of origin redundancy along the genome delays the completion of DNA synthesis at specific chromosomal regions. Importantly, these defects at sites containing elements delaying fork-progression commit chromosomes to fragility. Finally, we show that chromosomal instability in cells lacking Sic1 can be supressed by retaining cells prior to anaphase entry without alleviating G1-phenotype and origin activity defects, consistent with uncoupled DNA replication completion and mitosis entry. We conclude that in G1/S deregulated cells, chromosomal regions with an irregular distribution of inefficient origins are delayed in completing replication by lacking of functional origin redundancy that causes genomic instability. Moreover, additional obstacles to fork elongation at these regions may impede DNA replication completion and commit these sites to fragility by resulting in chromosome breaks during mitosis, which is considered a driving force of oncogenesis.

PRESENTACIÓN

La replicación del DNA eucariota se inicia en numerosos sitios llamados orígenes y se regula para que los cromosomas se repliquen una única vez por ciclo celular. La ausencia de complejos quinasa dependientes de ciclina (CDK) activos desde el final de mitosis y durante la fase G1 permite el licenciamiento de los orígenes, para su potencial disparo en fase S. El aumento de los niveles de actividad CDK en la transición G1/S bloquea nuevos licenciamientos y promueve el disparo de una parte de los orígenes licenciados, juntamente con la actividad de la quinasa dependiente de Dbf4 (DDK). La activación de orígenes en fase S sigue un programa espacio-temporal, muy conservado en poblaciones celulares pero estocástico en células individuales, que presumiblemente permite la finalización a tiempo de la replicación gracias al exceso de orígenes licenciados disponibles para rescatar horquillas paradas. Completar la replicación es crítico para la integridad del genoma, ya que células entrando en mitosis con horquillas activas podrían sufrir rupturas cromosómicas durante una segregación prematura en anafase.

En levaduras y en mamíferos hay inestabilidad genómica cuando se desregula la transición G1/S, porque estas células tienen ventajas proliferativas y un fenotipo mutador. De hecho, las células cancerosas tienen alteraciones frecuentes de los reguladores de G1/S y muestran una replicación aberrante del DNA; además, la inestabilidad genómica es una propiedad del cáncer. Sin embargo, el mecanismo molecular por el que un G1 desregulado causa inestabilidad es poco conocido. Para estudiarlo, hemos utilizado levaduras carentes del inhibidor de CDK Sic1, un regulador central de G1 y ortólogo de $p27^{Kip1}$ en células de mamífero, como modelo eucariota de ciclos celulares oncogénicos. Mostramos que en ausencia de Sic1 la pérdida de redundancia de orígenes causa directamente inestabilidad cromosómica. Además, mostramos que la pérdida diferencial de redundancia de orígenes en el genoma retrasa la finalización de la replicación en regiones cromosómicas específicas. Importantemente, este defecto convierte estas zonas en frágiles frente a elementos que retrasan la replicación. Finalmente, mostramos que la inestabilidad cromosómica en estas células se suprime retrasando la entrada en mitosis, consistente con un desacoplamiento entre finalización de la síntesis del DNA y la entrada en mitosis. Concluimos que en células desreguladas en G1/S, la distribución irregular de orígenes ineficientes reduce su redundancia, retrasa la finalización de la síntesis de DNA en regiones específicas del genoma, y causa su inestabilidad. Además, impedimentos a la progresión de horquillas añaden fragilidad adicional a estos sitios que pueden romper en mitosis y posiblemente promover la oncogénesis.

TABLE OF CONTENTS

ABBREVIATIONS

2D-Gels	Two-dimensional Electrophoresis Gel
Ade	Adenine
APC	Anaphase Promoting Complex
ARS	Autonomous Replication Sequence
Az	Azide
α-F	α-factor
bp	Base pair
BSA	Bovine Serum Albumin
CAN	L-Canavanine
CAPS	N-cyclohexyl-3-aminopropanesulfonic Acid
CKI	CDK Inhibitor
CDK	Cyclin-Dependent Kinases
Chr	Chromosome
DAPI	4′,6-Diamidino-2-phenylindole Dihydrochloride
dCTP	Deoxycytidine Triphosphate
DDK	Dbf4-Dependent Kinase
DNA Pol ε	DNA polymerase ε
dNTPs	Deoxyribonucleotides
EDTA	Ethylenediamine Tetraacetic Acid
EtBr	Ethidium Bromide
ERCs	Extrachromosomal rDNA Circles
FACS	Fluorescence Associated Cell Sorting
FALCOR	Fluctuation AnaLysis CalculatOR
FOA	5-Fluoroorotic Acid
Gal	Galactose
GCR	Gross Chromosomal Rearrangements
Glu	Glucose
His	Histidine
HRP	Horseradish Peroxidase
HphNT	Hygromycin
HU	Hydroxyurea
KanMX4	Kanamycin
kb	Kilo base pair
LB	Luria Broth

Leu	Leucine
M	Mitosis
MAT	Mating-type
Mcm	Minichromosome Maintenance Complex
MSS-MLE	Ma-Sandri-Sarkar Maximum Likelihood Estimator
NIB	Nuclear Isolation Buffer
Noc	Nocodazole
ORC	Origin Recognition Complex
OriDB	DNA Replication Origin Database
PBS	Phosphate-Buffered Saline
PCR	Polymerase Chain Reaction
PEM	Pipes EGTA $MgSO_4$
PEMBAL	PEM BSA Azyde Lysine
PEMS	PEM Sorbitol
PEMS-DIG	PEMS Digestion
PFGE	Pulsed-Field Gel Electrophoresis
Pgk1	3-phosphoglycerate kinase
PI	Propidium Iodide
Pre-IC	Pre-Initiation Complex
Pre-RC	Pre-Replicative Complex / Pre-Replication Complex
Raff	Raffinose
rDNA	Ribosomal DNA
rRNA	Ribosomal RNA
RFB	Replication Fork Barrier
RI	Replication Intermediates
S	Synthesis
SAC	Spindle Assembly Checkpoint
SDS	Sodium Dodecyl Sulphate
SDS-PAGE	SDS-Polyacrylamide Gel Electrophoresis
SGD	Saccharomyces Genome Database
SSC	Saline Sodium Citrate
ssDNA	Single-Stranded DNA
dsDNA	Double-Stranded DNA
TAE	Tris-Acetate EDTA
TE	Tris-EDTA
TBE	Tris-Boric acid-EDTA

TPBS	Tween PBS
Trp	Tryptophan
TUB	Tubulin
Ura	Uracil
wt	Wild-type
YP	Yeast extract Peptone
YPA	Yeast extract Peptone Adenine
YPAD	Yeast extract Peptone Adenine Glucose
YPARG	Yeast extract Peptone Adenine Raffinose Galactose
YNB	Yeast Nitrogen Base

NOMENCLATURE

All strain names are written in italic.

Gene names are written in italic with capital letters: e.g. *SIC1*.

Protein names start with a capital letter followed by lowercase letters: e.g. Sic1.

Protein depletion is written in italic with lowercase letters: e.g.: *sic1*.

Deletion mutants are indicated by the name of the gene deleted in italic with lowercase letters followed by the symbol Δ: e.g. *sic1*Δ.

Genetic substitutions are indicated by the name of the gene deleted in italic with lowercase letters followed by the symbols Δ:: and the name of the inserted gene in italic with capital letters: e.g. *ars507*Δ*::ARS305*.

INTRODUCTION

1. Cell Division Cycle and Eukaryotic DNA replication

Eukaryotes have very large genomes distributed into numerous chromosomes. To preserve the integrity of the genetic material across generations it is crucial that eukaryotic cells entirely replicate their whole DNA exactly once per cell cycle, free of errors and in a time fashion to ensure perfect synchrony with mitosis. Therefore, the eukaryotic cell cycle is controlled at many levels.

Eukaryotic cell-cycle transitions are controlled by oscillating waves of cyclin-dependent kinases (CDK) activity. CDKs are serine/threonine kinases whose activity depends on their association to cyclins, their regulatory subunits. In budding yeast, a single CDK (Cdc28) can bind to three different G1 cyclins (Cln1-3), two S phase cyclins (Clb5-6) and four mitotic cyclins (Clb1-4) to form G1-, S- and M-CDK active complexes, respectively. G1-CDKs control entry into the cell cycle and passage through START, a specific point at which cells become committed to the cell division (Nasmyth, 1993; Reed, 1992), S-CDKs are responsible for the progression into and through S phase (Nasmyth, 1993; Schwob and Nasmyth, 1993), and M-CDKs promote mitosis (Fitch et al., 1992; Ghiara et al., 1991; Richardson et al., 1992; Surana et al., 1991). Importantly, abnormalities in cellular processes caused by error-prone cell's machinery (e.g. fork collapse upon perturbations in DNA replication), metabolic environment (e.g. oxidation of DNA) or external agents (e.g. carcinogens) are sensed by surveillance mechanisms called "checkpoints" that inhibit or slow cell-cycle progression until these anomalies are correctly repaired or assembled (Lowndes and Murguia, 2000; Tercero et al., 2003). Furthermore, eukaryotes display also control mechanisms of chromosomal DNA synthesis, like the tight regulation of replication initiation that determines where, when and how replication initiates (Bell and Dutta, 2002; Fragkos et al., 2015; Siddiqui et al., 2013).

1.1 Model of Replication Initiation Control

The first model that proposed a regulatory control of the replication initiation was presented by Jacob, Cuzin, and Brenner nearly fifty years ago in the so-called replicon theory (Jacob et al., 1963). The model predicted that a *trans*-acting protein called the "initiator" would bind to a specific DNA sequence called the "replicator", promoting the unwinding of DNA and activating replication. The model was validated in prokaryotes with the identification of the initiator protein dnaA and the replicator oriC in *E. coli* (Baker et al., 1986; Fuller et al., 1984; Messer et al., 1979). In eukaryotes, chromosomal replication is more complex than in prokaryotes because timely duplication of their larger and fragmented genomes requires that replication starts at multiple locations distributed through chromosomes, instead of a single site as it

frequently occurs in bacterial genomes (Gao and Zhang, 2007). For instance, sites of replication initiation can vary from around 800 in yeast to 30,000 to 50,000 in human cells (Mechali, 2010; Siow et al., 2012). Nevertheless, the replicon theory also applies to eukaryotes. The first evidence of an eukaryotic replicator was the identification of specific genomic sequences necessary for replication initiation in the budding yeast *Saccharomyces cerevisiae* called autonomous replication sequences (ARS) (Stinchcomb et al., 1979). Later, a single eukaryotic initiator was identified capable of recognizing and binding to ARS, the six-subunit origin recognition complex (ORC) that is conserved from yeasts to humans (Chesnokov, 2007). The interaction of ORC with the ARS elements recruits specific proteins resulting in the assembly of pre-replicative complexes (pre-RCs) onto origins that are indispensable for origin DNA unwinding and the formation of the replisome for DNA synthesis (Kawakami and Katayama, 2010; Mendez and Stillman, 2003; Remus et al., 2009).

1.2 Passage through START and the Commitment to the Cell Cycle

START is a point of no return where cells become irreversible committed to a new round of cell division (Nasmyth, 1993). Passage through START is initiated by G1-CDKs (Dirick et al., 1995; Stuart and Wittenberg, 1995; Tyers et al., 1993) and several events occur at this point: cells duplicate their spindle pole bodies, start to form new buds, activate the G1 transcription machinery and initiate DNA synthesis (Toone et al., 1997). At the G1/S transition, Clb5 and Clb6 are the relevant cyclins for the activation of DNA replication, along with DDK activity (Bell and Dutta, 2002). *CLB5* and *CLB6* are expressed at the same time as *CLN1* and *CLN2* in G1 phase; however, Clb5,6/Cdc28 complexes are maintained inactive due to inhibition by Sic1 (Schwob et al., 1994).

Sic1 is a CDK inhibitor (CKI) that directly binds to and inactivates Clb/Cdc28, but not Cln/Cdc28 complexes (Mendenhall, 1993). Sic1 must be degraded before cells can initiate DNA synthesis (Donovan et al., 1994; Schneider et al., 1996; Schwob et al., 1994), which is achieved via simultaneous phosphorylation on multiple CDK consensus sites by Cln/Cdc28 (Nash et al., 2001) and subsequent degradation through SCF-mediated polyubiquitination and proteolysis by Clb/Cdc28 (Feldman et al., 1997; Koivomagi et al., 2011; Verma et al., 1997). Sic1 accumulates in late M and G1 phases and is largely degraded at the G1/S transition, remaining undetectable throughout S, G2 and early mitosis (Donovan et al., 1994; Schwob et al., 1994). In late mitosis, Sic1 cooperates with Cdh1 and promote exit from mitosis by contributing to shut off waves of M-CDKs, while Cdh1 targets mitotic cyclins for ubiquitin-mediated degradation through the APC/C (Jaspersen et al., 1998; Kramer et al., 1998; Ross and Cohen-Fix, 2003; Schwab et al., 1997). Moreover, at the G1/S boundary, Sic1 directly binds to and

inhibits S-CDKs, thereby controlling the correct timing of S phase activation (Figure 2) (Schwob et al., 1994).

2. Replication Initiation in Budding Yeast

The nature of origin sequences where DNA replication initiates still are the focus of intense search (Leonard and Mechali, 2013). Only in *S. cerevisiae* origins display an identified consensus sequence, that were first identified as 100 to 200 bp ARS elements by providing autonomous replication episomic plasmids (Stinchcomb et al., 1979). Subsequent studies on ARS elements in their native chromosomal position showed that some, but not all, of those sites function as true chromosomal replication origins and are required for DNA replication initiation (Brewer and Fangman, 1991; Dubey et al., 1991; Ferguson et al., 1991; Huberman et al., 1988).

2.1 Structure and Determinants of Origin Function

ARS sequences are very A/T-rich and consist of modular structures containing a conserved domain of 11 to 17 bp called the ARS consensus sequence (ACS), as well as multiple B elements which sequence varies between different ARS (DePamphilis, 1993; Marahrens and Stillman, 1992; Newlon and Theis, 1993). The ACS is essential for origin function and is the binding site for ORC (Bell and Stillman, 1992; Diffley and Cocker, 1992). Most origins contain a single ACS although some origins were found to carry multiple ACSs and recruit multiple ORC complexes (Newlon and Theis, 1993). Only a few hundreds of the conserved thousands ACS widespread on chromosomes successfully bind to ORC and initiate replication (Linskens and Huberman, 1988), indicating that the ACS is insufficient to define a functional origin. Indeed, the recruitment of ORC to origins also depends on its interaction with the B elements surrounding the ACS (Figure 1) (Bell and Stillman, 1992; Diffley and Cocker, 1992). B elements can be subdivided into three domains: the B1 domain that acts together with the ACS for ORC binding (Bell and Stillman, 1992; Diffley and Cocker, 1992; Rao and Stillman, 1995; Rowley et al., 1995); the B2 element that is suggested to be involved in origin unwinding (Wilmes and Bell, 2002; Zou and Stillman, 2000) and the B3 element that plays a role in transcription and can influence chromatin structure and nucleosome assembly (Ganapathi et al., 2011; Miyake et al., 2002). In addition to sequence specificity for ORC binding, chromatin modulation also play an important role in the specification and choice of initiation sites through the nucleosomal configuration (Yoshida et al., 2013). Origins activity requires the presence of a nucleosome exclusion region near the ACS that is possibly provided by its A/T-rich domain (Kaplan et al., 2009; Zhang et al., 2009). Also, ORC binding is necessary to shape an asymmetric

pattern of nucleosomes on both sides of the ACS and create a ~130 bp nucleosome-free region that provides space for the other proteins needed for the pre-RC assembly (Berbenetz et al., 2010; Eaton et al., 2010; Thoma et al., 1984). Studies on *ARS1* showed that allowing nucleosomes to overlap the origin disrupts its activity (Hu et al., 1999; Simpson, 1990; Venditti et al., 1994) and when nucleosomes are moved away from their ORC-binding sites, the activity of *ARS1* is reduced (Lipford and Bell, 2001), suggesting that ORC is a determinant for nucleosomes positioning and positively influences origin function.

2.2 The Two-step Activation of Origins

The main steps in DNA replication initiation are the unwound of the double stranded DNA (dsDNA) at origins and the recruitment of the replication machinery to synthesise the DNA. Eukaryotic cells require an active replicative helicase to unwind the dsDNA at origins and most proteins involved in this process are conserved among eukaryotes (Bell and Dutta, 2002). The molecular mechanisms implicated in origin activation (helicase loading and activation) are very well understood in *S. cerevisiae* and involve a two-step reaction (see Tanaka and Araki (2013) for a general review): firstly, the assembly of a putative helicase (the pre-RC complex) at origins in a reaction known as origin 'licensing'; and secondly, the conversion of the pre-RC into an active helicase in a reaction called origin 'firing' that is capable of unwind the dsDNA at origins (Figure 1).

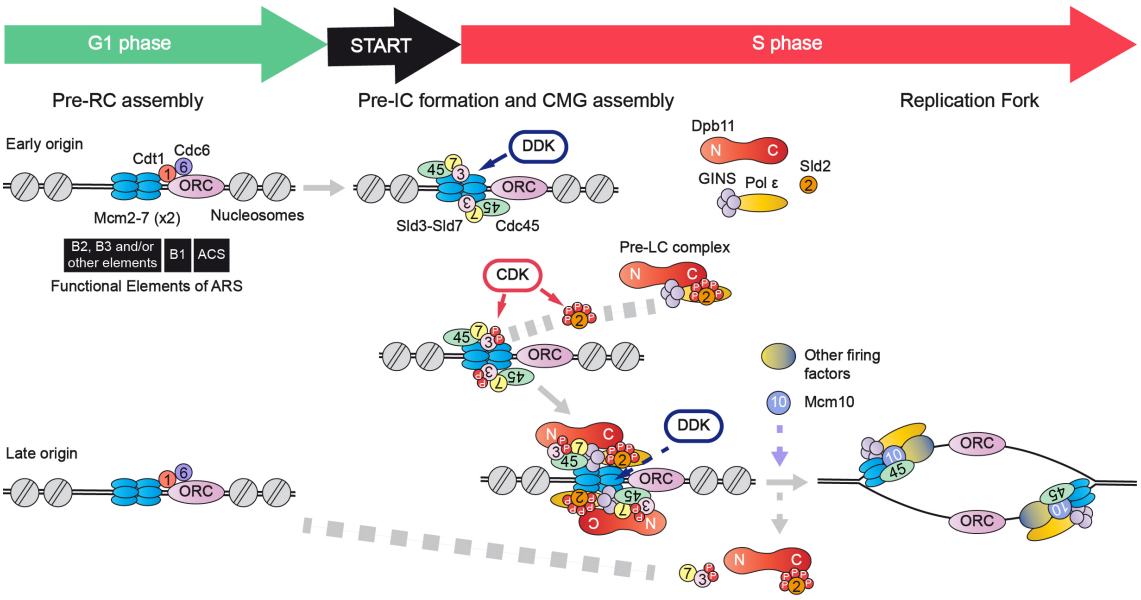

Figure 1: Biochemical steps of origin licensing and firing in budding yeast. Schematic representation of the components involved in the pre-RC assembly onto origins during G1 and the formation of the pre-IC and CMG assembly necessary for the initiation of DNA replication during S phase (Based on Tanaka and Araki (2013) and Yoshida et al. (2013)). See text for details.

Origin licensing depends on the recruitment of two proteins, Cdc6 and Cdt1, to ORC-bound origins. Together, these three licensing factors direct and load the core components of the replicative helicase Mcm2–7 around origins, forming the pre-RC (Tye, 1999). The Mcm2–7 complex is loaded onto origins as a head-to-head double-hexamer that surrounds the dsDNA (Evrin et al., 2009; Remus et al., 2009). However, the Mcm2–7 complex at the pre-RC does not show DNA helicase activity and is unable to unwind the origin dsDNA. Cells must pass through START to activate the Mcm2-7 complex into an active helicase (origin firing) by converting the pre-RC into the pre-initiation complex (pre-IC), a complex formed just before the initiation of DNA replication (Diffley, 1996; Muzi-Falconi et al., 1996; Zou and Stillman, 1998). The formation of the pre-IC involves the recruitment and association of Cdc45 and GINS with the Mcm2–7, forming a tight complex, the Cdc45-Mcm2-7-GINS (CMG) complex (Gambus et al., 2006; Moyer et al., 2006). At least five additional factors are essential for the CMG assembly, namely Sld2, Sld3, Sld7, Dpb11 and DNA polymerase ε (DNA pol ε) (Muramatsu et al., 2010). Cdc45 associates with the pre-RC via Sld3 and Sld7 (Kamimura et al., 2001; Tanaka et al., 2011b), while Sld2, Dpb11, GINS and DNA pol ε assemble and form a separated complex, the pre-loading complex (pre-LC) (Muramatsu et al., 2010) that recruits GINS to the pre-RC to form the CMG complex (Figure 1).

The formation of the pre-IC activates the replicative helicase through the dissociation of the double Mcm2–7 hexamer into two active helicases that encircles the single stranded DNA to unwind the dsDNA (Fu et al., 2011). After origin unwinding, several proteins are recruited and bidirectional replication forks are established to elongate the leading and lagging strands (Burgers, 2009). After firing or passive replication, pre-RCs are disassembled and origins remain in an unlicensed post-replicative state (post-RC), which corresponds to the binding of ORC only, and are maintained in the post-RC state in the rest of S phase, G2 and mitosis (Diffley et al., 1994).

2.3 Replication Initiation is Regulated During the Cell Cycle

During S phase, eukaryotic cells must prevent the re-licensing of replicated origins to block re-replication. Studies that artificially allowed cells to re-license origins found that multiple forks initiating from the same origin causes DNA re-replication leading to gene amplification and promoting genome instability, a feature present at many human cancers (Green et al., 2010; Lengauer et al., 1998; Li and Blow, 2005; Melixetian et al., 2004; Mihaylov et al., 2002; Nguyen et al., 2001; Nishitani and Nurse, 1995; Vaziri et al., 2003). Hence, it seems that controlling origin activity is key to

maintain the integrity of eukaryotic chromosomes and avoid genomic instability. Re-licensing (and re-replication) is prevented because the two steps of origin activation (helicase loading and activation) are timely separated in a way that cannot occur simultaneously (Diffley, 2004).

2.3.1 CDK Activity Control Origin Licensing and Firing

CDKs play a dual role in replication initiation control (Figure 1). Origin licensing can only occur from late M up to late G1 phase during the CDK-free window because the assembly of pre-RCs at origins is inhibited by any CDK activity (Dahmann and Futcher, 1995; Detweiler and Li, 1998; Nguyen et al., 2001; Tanaka and Diffley, 2002). On the contrary, origin firing is only allowed in the S-CDK active period and is thereby restricted to S phase (Bell and Dutta, 2002; Mendez and Stillman, 2003). Furthermore, because the licensing system is inactivated before entry into S phase and CDKs are active during the rest of the cell cycle, pre-RCs cannot be formed onto origins once S phase has started, which prevents a fired origin to re-fire. Notably, Sic1 is crucial during G1 phase to keep a CDK-free window that allows licensing of origins that depends on the absence of CDK activity to assemble pre-RCs (Lengronne and Schwob, 2002).

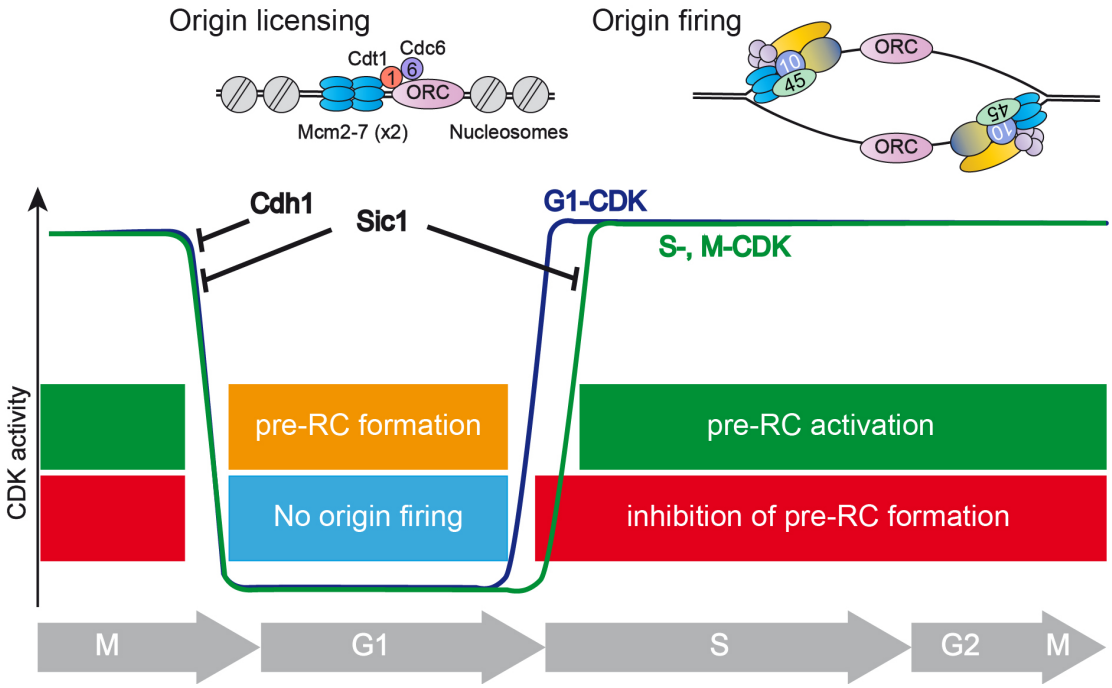

Figure 2: Regulation of DNA replication initiation by CDK activity. CDK activity is low or absent during a period of G1 allowing origin licensing, but is high throughout late G1, S, G2 and mitosis preventing licensing and promoting origin firing during S phase. A CDK-free window during G1 is necessary for the pre-RC assembly onto origins (licensing), while S-CDK activity at the G1/S transition is essential to activate origins (firing) and initiate DNA synthesis. Activation of G1-CDKs and S-CDKs from late G1 phase inhibits pre-RC assembly to impede origin re-licensing (Based on Diffley (2004) and Tanaka and Araki (2010)).

When activated, CDKs phosphorylate several initiation proteins to inhibit the pre-RC assembly: Clb/Cdc28 phosphorylate Orc2, Orc6 and Mcm2-7 (Detweiler and Li, 1998; Nguyen et al., 2001) and inhibits the interaction between ORC and Cdt1 (Chen et al., 2007) impeding the load of the Mcm2-7 complex onto origins (Chen and Bell, 2011); whereas Cln,Clb/Cdc28 phosphorylate Cdc6 and promote its degradation by the SCF^{Cdc4} complex (Calzada et al., 2000; Drury et al., 1997; Elsasser et al., 1999; Perkins et al., 2001). Additionally, during G2, the phosphorylation of CDK consensus sites in Mcm3 promotes the transportation of Mcm2-7 associated with Cdt1 out of the nucleolus (Labib et al., 1999; Liku et al., 2005; Nguyen et al., 2000).

At the G1/S transition, Clb5,6/Cdc28 are activated and phosphorylate Sld2 and Sld3, promoting their interaction with Dpb11 to form the Sld2-Dpb11-Sld3 complex (Masumoto et al., 2002; Tak et al., 2006; Tanaka et al., 2007; Zegerman and Diffley, 2007). The formation of this complex promoted by CDK is important for two different but related processes: on one hand, the interaction between phosphorylated Sld2 and Dpb11 leads to the pre-LC assembly that seems to form independently of the pre-RC (Muramatsu et al., 2010); on the other hand, the phosphorylation of Sld3, that is associated with Cdc45 at the pre-RC, promotes its interaction with Dpb11 in the pre-LC, eventually recruiting GINS to origins to form the CGM complex (Figure 1). Importantly, the association of the pre-LC with origins requires the previous association of Sld3 and Cdc45 with the pre-RC, which is promoted by DDK.

2.3.2 DDK Activity Controls the Temporal Activation of Origins

DDK consists of a Cdc7 catalytic subunit and its activator Dbf4 (Sclafani, 2000). DDK activity is regulated by Dbf4 levels that increase at G1/S boundary, are kept high during S phase, and decreases from late mitosis (Cheng et al., 1999; Ferreira et al., 2000; Oshiro et al., 1999). The increasing levels of DDK activity at the G1/S transition and during S phase are essential to promote the activation of origins and drives replication. DDK promotes the interaction between Sld3, Sld7 and Cdc45 that form a complex and recruits Cdc45 to the pre-RC formed at origins (Figure 1) (Heller et al., 2011; Tanaka et al., 2011a). The exact mechanism by which this occurs is unknown but biochemical and genetic evidences suggest that DDK phosphorylates several subunits of the Mcm2–7 complex in the pre-RC and modifies its structure, somehow enhancing the association of Sld3-Sld7-Cdc45 with origins (Hardy, 1997; Randell et al., 2010; Sheu and Stillman, 2010). Cdc45 binds to Sld3 during most of the cell cycle but Sld3 does not travel with the replication fork, unlike Cdc45 (Figure 1) (Kanemaki and Labib, 2006). Importantly, the interaction of Sld3-Sld7-Cdc45 with the pre-RC do not requires CDK activity or components of the pre-LC.

3. DNA replication timing programme in budding yeast

The interval during which eukaryotic chromosomes are replicated define S phase. Chromosomes replicate in segments called replicons that are activated in a unique temporal program that is stably transmitted to daughter cells and depends on the activation of origins within each replicon (Aladjem et al., 2002; Di Rienzi et al., 2012; Farkash-Amar et al., 2008; Liachko et al., 2010; Muller and Nieduszynski, 2012; Ryba et al., 2010; Xu et al., 2012; Yaffe et al., 2010). Because origins are not activated at the same time during S phase but instead follow a predictable temporal order, some replicons start to replicate at the onset of S phase while others begin replication at the middle or near the end of S phase (Fangman and Brewer, 1992). The coordination of the temporal control of DNA replication is referred to as the replication-timing program and is defined at early stages of the cell cycle.

3.1 The Usage of Origins is Flexible

Although all origins share the same machinery for their activation, they behave differently. During the G1 phase, hundreds of origins are licensed yet, only a subset of all licensed origins actually fires during S phase (Santocanale and Diffley, 1996). Importantly, the selection of origins to be activated each cell cycle varies from cell to cell within the same cell population, implying that origin usage is flexible (Friedman et al., 1997).

Some origins are more frequently activated than others, which led to the notion of origin efficiency to define the frequency at which an origin fires among a population of cells. According to this notion, origins can be classified into efficient, if they are frequently activated each cell cycle; inefficient, if they are infrequently activated or silent/dormant if never used (Friedman et al., 1997; Yamashita et al., 1997). Dormant origins are licensed origins that are not activated in normal cell cycles (silent), but are competent to fire in response to fork collapse or replication delay, thus acting as backup origins (Santocanale et al., 1999; Vujcic et al., 1999). According to the “origin redundancy model”, a large excess of potential origins are assembled before S phase in a way that any stretch of unreplicated DNA would remain competent for initiation during S phase, independently of licensing inhibiting mechanisms (Hyrien et al., 2003; Rhind, 2006). Therefore, the functional complementation among origins in initiating replication would ensure that no gaps on DNA remain unreplicated by the end of S phase and ultimately promote the timely completion of DNA replication. The activation of dormant origins, in particular, is considered a first line of defence against perturbations in DNA replication. For instance, when forks stall or its progression is delayed/inhibited, the activation of an adjacent dormant origin ensures the complete

synthesis of the chromosomal region therefore their availability during replication is crucial for the integrity of the genome (Blow et al., 2011).

3.2 Origin Activation and the Replication-Timing Program

The strict temporal program of replication is a heritable and robust epigenetic feature of almost all eukaryotic chromosomes (Hiratani and Gilbert, 2009). Importantly, it is the replication-timing program and not replication initiation that is conserved among species (Rhind and Gilbert, 2013). The fact that aberrant replication timing is present in many genetic diseases and human cancers suggests that careful control of replication dynamics is needed to avoid chromosomal abnormalities and preserve genome integrity (Donley and Thayer, 2013).

The replication-timing program is executed during S phase but established at a discrete point during G1, the START decision point in budding yeast and the time decision point in mammalian cells (Dimitrova and Gilbert, 1999; Raghuraman et al., 1997). However, the mechanism by which cells coordinate the firing of hundreds of origins and regulates the strict temporal program of replication is still largely unknown (Barberis et al., 2010). Many evidences suggest that the replication-timing program is largely dependent on the timely control of origin activation within each replicon together with origin location on chromosomes (Aparicio, 2013; McGuffee et al., 2013; Sclafani and Holzen, 2007). In fact, S phase in *S. cerevisiae* follows a temporal program dominated by the timing of origin firing, and broad chromosomal regions are replicated from clusters of origins that have very similar activity (Figure 3) (McGuffee et al., 2013).

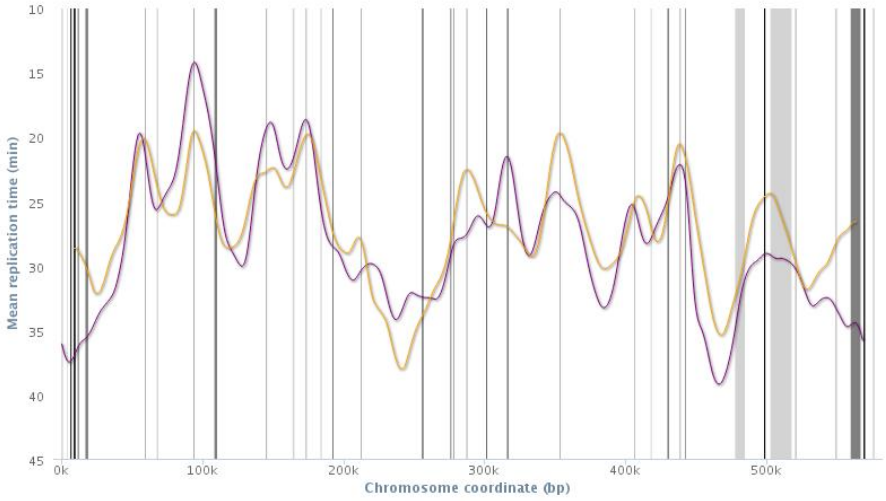

Figure 3: Genome-wide replication-timing program of *S. cerevisiae*. Only data for chromosome V is shown, evidencing that some regions replicate earlier that others (Siow, et al., 12).

Origins do not fire simultaneously at the beginning of S phase. Some origins fire shortly after S phase started (early-firing origins), whereas others are activated towards the end of S phase (late-firing origins) (Figure 3) (Raghuraman et al., 2001; Yabuki et al., 2002) and were defined based on whether origins fire (early) or not (late) in hydroxyurea (an inhibitor of ribonucleotide reductase for dNTP synthesis) that blocks DNA synthesis early in S phase (Feng et al., 2006; Santocanale and Diffley, 1998; Shirahige et al., 1998). Although more accurately, origins fire in a continuum from early to late S phase (Yoshida et al., 2013), the notion of early and late origins is still of broad use. Moreover, origins can either initiate replication actively by firing (active replication) or be passively replicated by an adjacent fork fired from a neighbour origin (passive replication). Therefore, origin efficiency corresponds to its frequency of active replication. In *S. cerevisiae*, early-firing origins are usually very efficient and late-firing origins are frequently inefficient. However, origin efficiency and timing can influence each other when origins are closely spaced (Brewer and Fangman, 1993; Friedman et al., 1997; Yamashita et al., 1997).

Timing of origins is referred to as the time at which an origin fires in S phase. The temporal program of origin activation can follow a deterministic model if the timing of origins occurs in a predictable order; or follow a stochastic model if origin firing is a matter of chance with no set order and origin timing rely on the random competition for critical initiation factors (Gomez, 2008; Rhind, 2006). Several evidences argue against a strictly stochastic model: different parts of the genome tend to replicate at specific times in S phase in bulk populations of cells (Raghuraman and Brewer, 2010) and in general, centromere-proximal regions replicate early in S phase while telomere-proximal regions replicate late (Ferguson et al., 1991; McCarroll and Fangman, 1988). Moreover, the sequential activation of origins is maintained in cells under replication stress conditions (Alvino et al., 2007; Poli et al., 2012). Furthermore, in *clb5Δ* yeast cells the kinetics of early-replicating regions remained unaffected whereas late-replicating regions were significantly delayed, contradicting a strictly stochastic model of origins activation, as it would predict that all origins would be equally affected after CDK activity depletion (McCune et al., 2008). These observations imply that the replication program of origin activation is robust and somehow predetermined. Nevertheless, evidences also exist against a strictly deterministic model: single-molecule analysis of replication in *S. cerevisiae* and in *S. pombe* showed that origin usage is extremely flexible between individual cells (Czajkowsky et al., 2008; Patel et al., 2006), also other studies found the existence of efficient late-firing and inefficiency early-firing origins (Friedman et al., 1996). However, although *S. cerevisiae* origins follow a staggered pattern of activation in S phase, the replication program is very

conserved at the population level (Czajkowsky et al., 2008; Tuduri et al., 2010). Accordingly, it seems that a mix of the two models its more likely to explain the temporal order of origin firing in *S. cerevisiae*: clusters of origins with similar activity are maintained together so that different regions of the genome replicate with similar timing within a population of cells, but stochastic events occur locally given by the overlap between peaks of early- and late-firing origins, resulting in a cell-to-cell variation in the precise order of origin activations (Raghuraman and Brewer, 2010).

3.3 Determinants of Origins Replication Timing

Several determinants, non-essential for the process of initiation of DNA replication, were found to influence origin specification (licensing) and choice (firing) and hence, origin timing. The timing of conversion of the pre-RC assembled at all potential origins into the pre-IC determines the timing of origin firing. Origin firing depends on its competence, which is the probability of an origin to acquire the necessary initiation factors to be activated in that cell cycle. Mechanistically, some of the proteins required for replisome assembly are limited and origins with more affinity for such factors were found to fire earlier in S phase (Mantiero et al., 2011; Patel et al., 2008; Tanaka et al., 2011a; Wu and Nurse, 2009).

3.3.1 *Cis*-acting elements

Cis-determinants on DNA were found to influence origin activity and provide diversity among origin activation time during S phase. Indeed, DNA sequences on origin can modulate ORC recruitment and pre-RC assembly during licensing and influence the timely selection and efficiency of origin activity during S phase. For instance, in *S. cerevisiae*, mutations on origin functional *cis*-acting domains caused a reduction in origin activity presumably by changing their capacity to attract and retain licensing factors (Huang and Kowalski, 1996; Newlon and Theis, 1993). Also, the later activation time of a subclass of origins was found to correlate positively with ORC-DNA interactions by chromatic-independent mechanisms (Hoggard et al., 2013), suggesting that *cis*-acting elements modulate origin function. It is possible that origins that are poor binding sites for ORC may fail to assemble pre-RCs in some cells or pre-RCs may have shorter half-times at some origins but not at others, and not be competent to fire in part of that cells population. In support of this, the *rDNA* ARS shows low efficiency (<20%) in its native context and its ACS shows a poor match to the consensus (Ivessa and Zakian, 2002). Replacing the native ACS with a better match to the consensus improves plasmid maintenance, suggesting that the poor efficiency is a result of poor competence to recruit ORC or other proteins (Miller et al., 1999). Consistently, distinct

sequence elements on origins influence their differential tolerance to mutations of licensing factors or to CDK deregulation in the G1 phase, supporting a hierarchy of preferential origin usage (Donato et al., 2006; Nieduszynski et al., 2005).

3.3.2 *Trans*-acting factors

Origin transplantation experiments showed that origin firing is influenced by its chromosomal context (Ferguson and Fangman, 1992; Friedman et al., 1996). Indeed, the histone acetylation (HDAC) surrounding chromatin was found to be a determinant of replication timing in budding yeast and other eukaryotes (Vogelauer et al., 2002). For instance, the loss of the class I HDAC Rpd3 results in precocious replication of many usually late-firing origins (Aparicio et al., 2004; Knott et al., 2009). Also, the class III HDAC Sir2 repress initiation at several non-telomeric origins, including origins at the *rDNA* locus (Crampton et al., 2008; Pappas et al., 2004; Pasero et al., 2002), although their mechanism of action remains unknown. Moreover, other HDAC such as Hst1-Sum1-Rfm1 complex promotes initiation at a number of origins (Weber et al., 2008), indicating that chromatin modulation clearly affects origin function in *S. cerevisiae*.

Besides HDACs, other factors have been implicated in replication timing control, such as those involved in transcriptional silencing delay or repression of initiation at subtelomeric origins (Stevenson and Gottschling, 1999; Zappulla et al., 2002). For instance, a Sir3-dependent process promotes the delay of origin activation at the vicinity of telomeres (Ferguson and Fangman, 1992; Stevenson and Gottschling, 1999). Also, cells deficient in the telomere binding protein Ku show advanced firing of subtelomeric origins, without interacting with origins or modifying histone acetylation (Cosgrove et al., 2002; Lian et al., 2011). Moreover, the telomeric proteins Rif1 and Taz1 are involved in late replication of fission yeast telomeres and at internal sites (Hayano et al., 2012; Tazumi et al., 2012), this function being conserved from yeasts to mammals (Cornacchia et al., 2012; Lian et al., 2011; Yamazaki et al., 2012).

In addition to chromatin modulation, the subnuclear localization of DNA sequences can also be involved in replication timing in a non-mutually exclusive way. In *S. cerevisiae*, late origins spend relatively more time near the nuclear periphery than do early origins and non-telomeric late-firing origins were found to relocate to the nuclear periphery in early G1 (Heun et al., 2001). Furthermore, telomeres were found to still replicate late in the absence of the Ctf18 RFC-like complex, even when moved from the nuclear periphery (Hiraga et al., 2006).

Moreover, higher-order structures in the nucleus such as telomeres and centromeres may also affect origin timing by concentrating key initiation factors preferentially at some regions. This is the case of the kinetochore component Ctf19

that advances replication timing recruiting DDK to centromeres, which in turn recruits Sld3 and Sld7 to pericentromeric replication origins (Natsume et al., 2013). Importantly, several initiation factors implicated in origin activation in budding yeast exist in limited amounts (Douglas and Diffley, 2012; Tanaka et al., 2011a), implying that late origins cannot fire until such factors are recycled from early origins. For instance, Cdc45 is one of those limiting factors that travel with forks after initiation (Aparicio et al., 1999; Pasero et al., 1999; Tercero et al., 2000), implying that Cdc45 cannot be recycled until completion of DNA replication at early domains. Also, the copy numbers of Sld3, Sld7, and Cdc45 (especially Sld3) are limited in comparison with the number of origins (Mantiero et al., 2011) and origins that associate with these proteins in early G1 were found to fire early in S phase (Tanaka et al., 2011a).

Thus, it seems that the pattern of origin firing in budding yeast depends on a combination of multiple *cis*- and *trans*-acting mechanism that act either locally (chromatin structure) or globally (higher organization of chromosomes) to modulate the ability of origins to compete for replication initiation. In addiction to that, the sequential activation of origins during S phase may also be regulated by checkpoints in response to replication stress (Yekezare et al., 2013). For instance, the central checkpoint kinases Mec1 and Rad53 in *S. cerevisiae* were found to inhibit late-firing replication origins in the presence of drugs that cause DNA damage (Santocanale and Diffley, 1998; Santocanale et al., 1999; Shirahige et al., 1998; Tercero and Diffley, 2001).

3.4 Genomic Localization of Replication Termination Sites

Replication terminates when two adjacent forks moving in opposite directions converge or when forks reach the end of a chromosome (Edenberg and Huberman, 1975). How and where convergent forks collide and replication terminates is poorly understood. At specific regions of the genome, both in prokaryotes and eukaryotes, termination is favoured at sites containing natural fork barriers that impede the passage of forks moving in one direction, increasing the probability of forks to collide and replication termination occurs precisely at the barrier (Hill and Marians, 1990; Linskens and Huberman, 1988). One example is the replication fork barrier (RFB) within the *S. cerevisiae* ribosomal DNA locus (*rDNA*) composed of approximately 150 repeat units arranged in tandem on chromosome XII. Each rDNA repeat unit encodes transcribed genes (35S and 5S rRNA subunits), non-transcribed regions (NTS1 And NTS2), one polar RFB and one ARS element (Takeuchi et al., 2003). During DNA replication, one in approximately five ARS sites is initiated and forks coming in opposite direction to transcription are arrested at the RFB to ensure that the rDNA locus is mainly replicated in the same direction as transcription (Brewer and Fangman, 1988; Linskens and

Huberman, 1988). However, sites where forks converge at RFBs to promote replication termination are only a small fraction of the genome and cannot explain all replication termination events. Foiani and collaborators proposed the existence of defined chromosomal termination regions (TERs) containing fork pausing sites that slow fork progression and restrict replication termination to the vicinity of these sites, coordinated by the Rrm3 DNA helicase and the Top2 DNA topoisomerase that alleviate the accumulation of X-shaped structures and prevent DNA breaks and genome rearrangements, respectively (Fachinetti et al., 2010). Contrary to this view, a more recent genome-wide study found no correlation between replication termination sites and *cis*-acting sequences or replication fork pausing, and propose that replication termination is a passive phenomenon that occurs midway between adjacent origins at positions largely dictated by their relative firing times (McGuffee et al., 2013).

In conclusion, although mechanisms underlying replication termination remain largely unknown, the idea of termination events being generally random, nonspecific sequences and dependent on the kinetics of origin firing seems to better describe what occurs in eukaryotic cells (Dewar et al., 2015; McGuffee et al., 2013; Santamaria et al., 2000; Zhu et al., 1992).

3.5 Monitoring the Timely Completion of DNA Replication Before Mitosis

Completion of DNA replication is essential to genome integrity as incompletely replicated chromosomes may break during anaphase if attempts to segregate sister chromatids that are still interconnected fail, resulting in double strand breaks (DSB) formation that is known to cause chromosomal instability (Bielinsky, 2003; Blow and Ge, 2009; Schwob, 2004). It has been proposed, but never demonstrated, that cells monitor the presence of unreplicated DNA or DNA synthesis itself, perhaps by detecting on-going forks, to delay mitotic onset until all chromosomes are fully replicated (Blow and Dutta, 2005; Hartwell and Weinert, 1989; Li and Deshaies, 1993). However, indirect evidences from several studies in which cells fail or delay to replicate the DNA but in despite this, undergo mitosis (Kelly et al., 1993; Piatti et al., 1995; Tavormina et al., 1997; Toyn et al., 1995) without being detected by checkpoints (Dulev et al., 2009; Lengronne and Schwob, 2002; Torres-Rosell et al., 2007b) support the hypothesis that unreplicated DNA does not directly prevent the mitotic onset.

The possible existence of a replication-completion checkpoint capable of prevent mitosis when DNA synthesis is incomplete has been studied mainly using drugs or mutations that interferes with replication fork progression. When DNA replication is perturbed, a conserved pathway (Mec1, Ddc2, Chk1, and Rad53 in budding yeast; ATR, ATRIP, Chk1, and Chk2 in mammals) arrest cells and stabilize forks in a process

involving the accumulation of RPA-coated single-stranded DNA (ssDNA) on stalled forks that trigger the DNA damage response (Bensimon et al., 2011; Ciccia and Elledge, 2010; Labib and De Piccoli, 2011; Polo and Jackson, 2011). However, it remains unclear whether this pathway is activated in the absence of DNA damage and if is capable of detecting normally progressing forks as it senses ssDNA on replication forks rather than unreplicated DNA (Nyberg et al., 2002). A recent study shed some light on this topic, using *S. cerevisiae* cells engineered to simulate on-going replication at the time of mitosis (Magiera et al., 2014). The study showed that late-replicating cells rely on S-phase, G2/M and Spindle-Assembly Checkpoints (SAC) for viability and that those mechanisms are active at a low level during S phase. The authors also show that the S-phase and SAC checkpoints can transiently delay chromosome segregation in unperturbed DNA replication by pathways involving Mec1 and Mad2 (Magiera et al., 2014). However, there is one caveat on this study: the mechanism delaying mitosis in those cells do not sense unreplicated DNA or DNA synthesis by itself. Instead, the presence of detached kinetochores at late-replicating centromeres is noticed by the SAC, which prevents anaphase entry. But centromeres generally replicate early during S phase in S. cerevisiae and consequently, centromere-proximal regions are less likely to be delayed in completing DNA synthesis during unperturbed replication. Keeping this is mind, it is still unclear if surveillance mechanisms exist capable of detecting on-going forks and prevent mitosis until chromosomes are fully replicated when delayed-replicating regions are not located at centromeres. It has been proposed the existence of a fork threshold for checkpoint activation during unperturbed cell cycles (Tercero et al., 2003). In cases of small amounts of on-going forks during G2-M (below a threshold level), the checkpoint fails to be activated and cells may rely on other mechanisms to ensure replication before mitosis such as the reservoir of unlicensed origin or the absence of centromeres replication (Magiera et al., 2014; Torres-Rosell et al., 2007b).

4. G1 phase Deregulation, Genomic Instability and Cancer

G0 is a quiescent state where cells remain when exit the cell cycle. The decision of a cell to progress from G0 to G1 represents a point of no return that commits cells to begin the next round of cell division. Studying the molecular mechanisms implicit on this important decision provides significant information to distinguish normal from abnormal proliferation (Malumbres and Barbacid 2001). Cancer cells frequently show unscheduled proliferation and genomic instability (GIN), defined as a tendency of the genome to acquire mutations and chromosomal abnormalities during the life cycle of cells (Shen, 2011). GIN frequently leads to chromosomal instability (CIN) that consists of changes in the numbers of chromosomes that arise after chromosomal segregation

defects during mitosis. Both GIN and CIN result in proliferative advantages and increased susceptibility to accumulate genetic alterations that contribute to tumour progression (Malumbres and Barbacid, 2009).

GIN is a cancer-enabling characteristic (Hanahan and Weinberg, 2011) but little is known about how it is generated and selected for during oncogenesis. Mechanisms controlling the cell cycle progression are often defective in cancer and have been studied extensively (Bartek and Lukas, 2007; Malumbres and Barbacid, 2009). In many genetic alterations and human cancers, proteins encoded by genes that regulate progression through the G1 phase are frequently mutated (Ho and Dowdy, 2002).

4.1 Decontrolled G1/S transition is Frequent in Cancer

The molecular analysis of human tumours revealed that cancer cells frequently display alterations in the expression of regulators involved in the G1/S transition (Malumbres and Barbacid 2001). Alterations include overexpression of cyclins and CDKs, as well as loss of CKI: the Rb-E2F pathway, the G1 cyclins, the INK and CIP/KIP families of CKI, the p53 and the ARF family (Sherr, 2000; Sherr and McCormick, 2002), underlying the importance of a precise and correct regulation of the G1/S transition to prevent human cancer. Cells escaping proper G1/S control have a proliferative advantage over normal cells and a mutator phenotype that may generate more mutations as they divide more often (Sidorova and Breeden, 2003). Both proliferative and mutator advantages are presumed to be necessary for a cell to acquire tumorigenic characteristics and become a cancer cell (Negrini et al., 2010). However, how the altered expression of G1/S regulators cooperates in tumour development is challenging and still unclear.

4.2 Perturbed DNA Replication Timing is Associated with Mutagenesis

The precocious G1/S transition often results in a sub-optimal S phase (Di Rienzi et al., 2009). DNA replication perturbation is a feature present at early stages of cancer development and current models propose that the replication-timing program significantly affects the distribution of mutations in cancer. Indeed, aberrant DNA replication timing is associated with altered gene expression, mutagenesis and genomic instability (Donley and Thayer, 2013). Mutagenesis refers to the acquisition of genetic changes that alter the DNA sequence, either spontaneously or as a result of exposure to mutagens. Mutation rate varies widely in the genome (Hellmann et al., 2005; Prendergast et al., 2007) and several studies have confirmed that replication-timing program is a potent force that influences mutation rates. Experiments in yeast established that late-replicating regions of the genome have higher rates of

spontaneous mutagenesis than early-replicating regions (Lang and Murray, 2011). Furthermore, the deletion of an early origin caused a slight increase in the rate of mutagenic events, possibly as a consequence of delaying replication, indicating that delaying the initiation of DNA replication is sufficient to increase its mutation rate (Lang and Murray 2011). Other experiments in mice and human demonstrated a similar correlation between mutagenesis and replication timing, with areas of single-nucleotide variance being concentrated at late-replicating regions (Chen et al., 2010; Cui et al., 2012; Stamatoyannopoulos et al., 2009; Watanabe et al., 2002).

Besides late-replicating regions, areas where early-replicating and late-replicating DNA converge are also hotspots for spontaneous mutagenesis (Hiratani et al., 2008; Watanabe and Maekawa, 2010). These regions lack of replication origins and are passively replicated by unidirectional forks fired from an adjacent early origin, increasing the probability of fork stalling and DNA damage. Importantly, many fusion genes and recurrent chromosome aberrations were found to coincide with or near these regions (Watanabe et al., 2009; Watanabe et al., 2002).

Cancer cells often show an aberrant asynchronous replication of loci that normally replicate synchronously (Amiel et al., 1999; Amiel et al., 1998). Moreover, a recent whole-genome study found that 9 to 18% of the genome undergoes a change in replication timing in leukemic cells compared to normal controls (Ryba et al., 2012). Changes in replication-timing program were detected on all chromosomes, near sites of genomic rearrangement and most of those changes were common to all samples, suggesting that altered replication at specific locations is an early epigenetic event in cancer development (Ryba et al., 2012). However, it remains to be addressed if the replication-timing changes observed in different types of cancers are a consequence of specific chromosomal features such as an asynchronous replication pattern or if, alternatively, results from nonspecific changes (Donley and Thayer, 2013). Interestingly, replication asynchrony was observed in pre-malignant cells in individuals pre-disposed to cancer or living in polluted areas with a high likelihood of getting cancer, suggesting that changes in the replication-timing program this may be an early event during carcinogenesis (Bras et al., 2008; Reish et al., 2003)

4.3 Abnormal DNA replication in Oncogenic Cell Cycles

Most activated oncogenes that deregulate entry into the cell cycle were found to continuously induce DNA DSBs in human precancerous lesions and cancers (Halazonetis et al., 2008). In yeast, deregulation of CDK activity compromises DNA replication and leads to formation of DNA DSBs and genomic instability (Lengronne and Schwob, 2002). By analogy, oncogenes could induce replication stress in human

precancerous lesions leading to the formation of DNA DSBs (Bartkova et al., 2006; Di Micco et al., 2006; Gorgoulis et al., 2005).

Work in budding yeast cells constitutively overexpressing Cln2 and the Cln2-1 mutant showed that this cells have inefficient pre-RC assembly and genomic instability (Tanaka and Diffley, 2002). Furthermore, the high levels of chromosomal rearrangements induced by Cln2-1 overexpression can be suppressed, at least partially, by the integration of a plasmid containing multiple origins, strongly suggesting that their genomic instability is produced by inhibition of origin firing (Tanaka and Diffley 2002). However, how mechanistically the defective usage of origins can cause genomic instability was not addressed. Also, both in yeast and higher eukaryotes, genomic instability often arise when cells are forced to enter S phase prematurely.

A CKI central to the control of the G1/S transition in budding yeast is Sic1, the functional and structural homologous of $p27^{Kip1}$ in mammals (Barberis et al., 2005). During G1 phase, Sic1 is key to maintain a CDK-free window of time that is critical for origin licensing. Although Sic1 is not essential, in cells lacking this CKI S phase starts prematurely, DNA replication initiate from fewer origins and takes longer compared to wild type cells (Ayuda-Duran et al., 2014; Lengronne and Schwob, 2002). Importantly, mitosis entry is not delayed and chromosomes frequently break and rearrange, showing a 100-fold increase in minichromosome loss and high rates of gross GCRs (Ayuda-Duran et al., 2014; Lengronne and Schwob, 2002; Nugroho and Mendenhall, 1994). It seems that precocious Clb5,6/Cdc28 activation at G1/S transition in cells lacking Sic1 is at the basis of chromosome rearrangements and genome instability through its inhibitory effect on pre-RC formation in late G1 phase (Schwob, 2004). Supporting this idea, a strain engineered to only allow the pre-RC formation in late G1 cannot survive without Sic1 and undergo terminal arrest with 1C DNA content (Lengronne and Schwob, 2002), suggesting that Sic1 is indispensable for origin licensing in late G1. Furthermore, the analysis of DNA fibbers by combing in *sic1*Δ cells showed that on average, the distance between replicons is 1.5 times longer compared to wild type (Lengronne and Schwob, 2002), suggesting they have fewer forks to duplicate the genome. After its extended S phase, *sic1*Δ cells enter mitosis on schedule but accumulate in mid-anaphase with Ddc1 foci (suggestive of DNA damage), intermediate length spindles and partial sister chromatid separation (Lengronne and Schwob, 2002). Importantly, the appearance of Ddc1 foci is dependent on the passage of cells throughout anaphase (Lengronne and Schwob, 2002). Moreover, it has been suggested that *sic1*Δ cells are unable to block mitosis because fail to activate a checkpoint response, as their viability was not significantly compromised after deleting Mec1 and Rad53 (Lengronne and Schwob, 2002).

4.4 Breakage Sites of Chromosomal Fragility are Associated with Origin Paucity and DNA Replication Stress

DNA replication stress is referred to as a state in the cell that leads to fork collapse that can be induced by an increase in the number of stalled forks (that eventually collapse) or by a decrease in the stability of stalled forks (Halazonetis et al., 2008). During DNA replication stress, the collapse of forks occurs preferentially at specific chromosomal loci called common fragile sites (CFS) (Arlt et al., 2006). CFS is a group of fragile sites in human chromosomes prone to breakage during mitosis (Sutherland and Richards, 1995). CFS are present in all individuals and stable in normal conditions, but are very sensitive to replication stress and are frequently rearranged in tumour cells, leading to genome rearrangements (Negrini et al., 2010). Moreover, CFS are late replicating regions sensitive to replication delays (Donley and Thayer, 2013), suggesting that forks progressing through those regions in G2 do not trigger a checkpoint to delay mitosis and the chromosomal breaks observed in metaphase is due to unreplicated DNA. Supporting this idea, their fragility has been linked with the replication program as most CFS were mapped at the junction of early and late-replicating chromosome bands at large regions void of replication origins (Debatisse et al., 2006). In addiction to that, other genomic features were also proposed to influence the expression of fragile sites, such as expandable DNA repeats, replication-transcription collisions or fork stalling at AT-rich sequences (Freudenreich, 2007; Mirkin and Mirkin, 2007; Ozeri-Galai et al., 2011).

Fragile sites were also found in budding yeast associated to slow replication (Cha and Kleckner, 2002). The mapping of rearrangement breakpoints in yeast coincides with replication slow zones such as transposable elements and their long terminal repeats (LTRs) and also fork pausing sites such as transference RNAs (tRNAs) and ARS sequences (Mirkin and Mirkin, 2007), suggesting that breaks occur at regions containing impediments to fork progression. The fork-stalling model of CFS expression explains how large regions with a paucity of replication initiation events ultimately cause chromosomal instability (Debatisse et al., 2012). The fork-stalling model of CFS expression propose that regions void of active origins are highly susceptible to fork elongation perturbations (Letessier et al., 2011b). As a consequence, inter-origin distances would increase such that forks need to replicate longer regions. Because long-travel forks are more prone to stall and could not be “rescued” by forks fired from nearby origins since dormant origins may not be available, replication might not be completed at those late-replicating regions before cells enter mitosis and chromosomes would break upon anaphase entry with partially unreplicated sister chromatids, committing cells to fragility (Letessier et al., 2011a).

5. Budding Yeast Cells Lacking G1 Regulators as a Model to Study the Causes and Mechanism of Instability in G1-deregulated Cell Cycles

Extensive study of G1 control in budding yeast and mammalian cells has revealed highly similar networks regulating cell commitment to enter the cell cycle (Johnson and Skotheim, 2013). Also, similar defects arise upon G1 phase deregulation (as compiled in section 4.3). Hence, conservation in the cell cycle regulation allows the strategy to use budding yeast lacking G1 regulators as a model to study the initial defects and molecular mechanism produced upon CDK deregulation during G1. Furthermore, other authors have employed budding yeast to study the consequences of CDK deregulation for genomic instability and the mechanism of deregulating G1 phase (Lengronne and Schwob, 2002; Nugroho and Mendenhall, 1994; Schwab et al., 1997; Skotheim et al., 2008; Tanaka and Diffley, 2002).

Budding yeast cells lacking the CKI and G1 phase regulator Sic1 show poor viability, reduced origins activity, S phase is premature and takes longer and their chromosomes frequently break or rearrange (Ayuda-Duran et al., 2014; Lengronne and Schwob, 2002; Nugroho and Mendenhall, 1994). However, cause-effect experiments are missing to determine whether deficient origin usage cause the genomic instability observed in G1-deregulated cell cycles. Also, what molecular abnormalities arise during a precocious but lengthened S phase that is conducted with fewer than normal forks in G1-deregulated cell cycles is poorly understood, as a detailed analysis on the kinetics of DNA replication is missing. Finally, it was hypothesized that G1-deregulated cells may enter mitosis prematurely with fewer on-going forks and escape the checkpoint, consequently failing to segregate partially unreplicated chromosomes during anaphase, resulting in genomic instability. Although, whether the delayed completion of replication and unscheduled entry in mitosis contribute to genomic instability upon G1 deregulation is still to be address.

OBJECTIVES

The main objective of this thesis was to study the causes and molecular mechanisms involved in the acquisition of genomic instability in budding yeast cells lacking the G1 phase regulator Sic1, to help deciphering what events occur at early stages of cancer development where decontrolled G1/S transition is frequent.

Hence the specific objectives of this thesis were the following:

1. Analyse whether cause-effect relationships link deficient origin activity to chromosomal instability in cells lacking Sic1.

2. Analyse the dynamics of DNA replication along large chromosomal regions in the first S phase after Sic1 depletion.

3. Characterize whether low origin efficiency triggers chromosomal instability upon fork-delaying elements in cells lacking Sic1.

4. Examine whether the chromosomal instability in cells lacking Sic1 could be compensate by delaying the mitosis entry.

MATERIALS AND METHODS

1. Bacterial Strains

Plasmids were transformed and amplified using competent *Escherichia coli* DH5α cells produced by the saline method (Kushner, 1978) or by the Inoue Method (Inoue et al., 1990).

2. Yeast Strains

All *Saccharomyces cerevisiae* strains used in this study are based on the W303-1a or S288C backgrounds and are derivatives of the parental YAC36 or RDKY3615 strains, respectively. A detailed description of all strains used in this study is shown in Table 1.

Table 1: Strains used in this study.

Strain	Background	Genotype	Source
YAC36	W303-1a	*MATa ade2-1 ura3-1 his3-11,15 trp1-1 leu2-3,112 can1-100*	K. Labib [1]
YAC198	W303-1a	*MATa ade2-1 ura3-1 his3-11,15 trp1-1 leu2-3,112 can1-100 yjl193w::HphNT sic1::[TRP1]GAL1,10p-SIC1*	(Ayuda-Duran et al., 2014)
YAC272	W303-1a	*MATa ade2-1 ura3-1 his3-11,15 trp1-1 leu2-3,112 can1-100 yjl193w::HphNT bar1Δ::URA3*	(Ayuda-Duran et al., 2014)
YAC276	W303-1a	*MATa ade2-1 ura3-1 his3-11,15 trp1-1 leu2-3,112 can1-100 yjl193w::HphNT bar1Δ::URA3 sic1::[TRP1]GAL1,10p-SIC1*	(Ayuda-Duran et al., 2014)
YAC316	W303-1b	*MATα ade2-1 ura3-1 his3-11,15 trp1-1 leu2-3,112 can1-100 yjl193w::HphNT sic1::[TRP1]GAL1,10p-SIC1 cdh1Δ::HIS3*	(Ayuda-Duran et al., 2014)
YAC852	W303-1a	*MATa ade2-1 ura3-1 his3-11,15 trp1-1 leu2-3,112*	This study
K1993	W303-1a	*MATa ade2-1 trp1-1 can1-100 leu2-3,112 his3-11,15 ura3 Gal+ psi+ ssd1-d cdc15-2*	(Koch et al., 1996)
YAC1098	W303-1	*MATa/α cdc15-2/CDC15 omns/OMNS ade2-1/ade2-1 ura3-1/ura3-1 his3-11,15/his3-11,15 trp1-1/trp1-1 leu2-3,112/leu2-3,112 can1-100/can1-100 SIC1/ sic1Δ::[TRP1]GAL1-10:SIC1 YJL193W/yjl193w::HphNT CDH1/cdh1Δ::HIS3*	This study
YAC1104	W303-1a	*MATa cdc15-2 ade2-1 ura3-1 his3-11,15 trp1-1 leu2-3,112 can1-100*	This study
YAC1106	W303-1b	*MATα cdc15-2 ade2-1 ura3-1 his3-11,15 trp1-1 leu2-3,112 can1-100*	This study
YAC1107	W303-1a	*MATa cdc15-2 ade2-1 ura3-1 his3-11,15 trp1-1 leu2-3,112 can1-100 sic1::[TRP1]GAL1,10p-SIC1*	This study
YAC1151	W303-1a	*MATa ade2-1 ura3-1 his3-11,15 trp1-1 leu2-3,112 V42219-42340Δ::[LEU2]RFB*	This study

[1] Cancer Research UK.

Strain	Background	*Genotype*	Source
YAC1164	W303-1a	*MATa ade2-1 ura3-1 his3-11,15 trp1-1 leu2-3,112 V42219-42340Δ::[LEU2]RFB hxt13::URA3*	This study
YAC1190	W303-1a	*MATa ade2-1 ura3-1 his3-11,15 trp1-1 leu2-3,112 V42219-42341Δ::[LEU2]RFB hxt13::URA3 sic1::[TRP1]GAL1,10p-SIC1*	This study
YAC1358	W303-1a	*MATa ade2-1 ura3-1 his3-11,15 trp1-1 leu2-3,112 V42219-42341Δ::RFB[LEU2] hxt13::URA3 cdc15Δ::CDC15-2*	This study
YAC1362	W303-1a	*MATa ade2-1 ura3-1 his3-11,15 trp1-1 leu2-3,112 V42219-42341Δ::RFB[LEU2] hxt13::URA3 cdc15Δ::CDC15-2 sic1::[TRP1]GAL1,10p-SIC1*	This study
RDKY3615	S288C	*MATa ura3-5, leu2Δ1 trp1Δ63 his3Δ200 lys2ΔBg, hom3-10 ade2Δ1 ade8 yel069::URA3*	(Chen and Kolodner, 1999)
YAC177	S288C	*MATa ura3-52 leu2Δ1 trp1Δ63 his3Δ200 lys2ΔBgl hom3-10 ade2Δ1 ade8 yel069::URA3 yjl193w::HphNT*	(Ayuda-Duran et al., 2014)
YAC217	S288C	*MATa ura3-52, leu2Δ1, trp1Δ63, his3Δ200, lys2ΔBgl, hom3-10, ade2Δ1, ade8, yel069::URA3, yjl193w::HphNT, sic1::[TRP1]GAL1,10p-SIC1*	(Ayuda-Duran et al., 2014)
YAC556	S288C	*MATa ura3-52, leu2Δ1, trp1Δ63, his3Δ200, lys2ΔBgl, hom3-10, ade2Δ1, ade8, yel069::URA3, yjl193w::HphNT ars507Δ::KanMX4*	This study
YAC558	S288C	*MATa, ura3-52, leu2Δ1, trp1Δ63, his3Δ200, lys2ΔBgl, hom3-10, ade2Δ1, ade8, yel069::URA3, yjl193w::HphNT, sic1::[TRP1]GAL1,10p-SIC1, ars507Δ::KanMX4*	This study
YAC560	S288C	*MATa, ura3-52Δ::KanMX4, leu2Δ1, trp1Δ63, his3Δ200, lys2ΔBgl, hom3-10, ade2Δ1, ade8, yel069::URA3, yjl193w::HphNT*	This study
YAC809	S288C	*MATa, ura3-52Δ::KanMX4, leu2Δ1, trp1Δ63 his3Δ200, lys2ΔBgl, hom3-10, ade2Δ1, ade8, yel069::URA3-1, yjl193w::HphNT*	This study
YAC874	S288C	*MATa, ura3-52Δ::KanMX4, leu2Δ1, trp1Δ63, his3Δ200, lys2ΔBgl, hom3-10, ade2Δ1, ade8, yel069::URA3-1, yjl193w::HphNT, ars507Δ::URA3*	This study
YAC884	S288C	*MATa ura3-52Δ::KanMX4 leu2Δ1 trp1Δ63 his3Δ200 lys2ΔBgl hom3-10 ade2Δ1 ade8 yel069::URA3-1 yjl193w::HphNT ars507Δ::ARS305*	This study
YAC899	S288C	*MATa ura3-52Δ::KanMX4 leu2Δ1 trp1Δ63 his3Δ200 lys2ΔBgl hom3-10 ade2Δ1 ade8 yel069::URA3, yjl193w::HphNT, ars507Δ::ARS305*	This study

Strain	Background	Genotype	Source
YAC921	S288C	*MATa ura3-52Δ::KanMX4 leu2Δ1 trp1Δ63 his3Δ200 lys2ΔBgl hom3-10 ade2Δ1 ade8 yel069::URA3 yjl193w::HphNT ars507Δ::ARS305 sic1::[TRP1]GAL1,10p-SIC1 7xARSH4[LEU2]*	This study
YAC1024	S288C	*MATa ura3-52, leu2Δ1, trp1Δ63, his3Δ200, lys2ΔBgl, hom3-10, ade2Δ1, ade8, yel069::URA3, yjl193w::HphNT, ars504.2Δ::LEU2*	This study
YAC1286	S288C	*MATa ura3-52, leu2Δ1, trp1Δ63, his3Δ200, lys2ΔBgl, hom3-10, ade2Δ1, ade8, yel069::URA3, yjl193w::HphNT sit1::pRS305-SIT1[LEU2]*	This study
YAC1290	S288C	*MATa ura3-52, leu2Δ1, trp1Δ63, his3Δ200, lys2ΔBgl, hom3-10, ade2Δ1, ade8, yel069::URA3, yjl193w::HphNT, sic1::(TRP1)GAL1,10p-SIC1, sit1::pRS305-SIT1[LEU2]*	This study
YAC1296	S288C	*MATa ura3-52, leu2Δ1, trp1Δ63, his3Δ200, lys2ΔBgl, hom3-10, ade2Δ1, ade8, yel069::URA3, yjl193w::HphNT, V42219-42340Δ::[LEU2]RFB*	This study
YAC1299	S288C	*MATa ura3-52, leu2Δ1, trp1Δ63, his3Δ200, lys2ΔBgl, hom3-10, ade2Δ1, ade8, yel069::URA3, yjl193w::HphNT V42219-42341Δ::[LEU2]RFB, sic1::[TRP1]GAL1,10p-SIC1*	This study
YAC1377	S288C	*MATa ura3-52, leu2Δ1, trp1Δ63, his3Δ200, lys2ΔBgl, hom3-10, ade2Δ1, ade8, yel069::URA3, yjl193w::HphNT, ars504.2Δ::LEU2, sic1::[TRP1]GAL1,10p-SIC1*	This study
YAC1302	S288C	*MATa ura3-52, leu2Δ1, trp1Δ63, his3Δ200, lys2ΔBgl, hom3-10, ade2Δ1, ade8, yel069::URA3, yjl193w::HphNT ars504.2Δ::ARS305[LEU2]*	This study
YAC1323	S288C	*MATa ura3-52Δ::KanMX4 leu2Δ1 trp1Δ63 his3Δ200 lys2ΔBgl hom3-10 ade2Δ1 ade8 yel069::URA3, yjl193w::HphNT ars504.2Δ:: ARS305[LEU2], sic1::(TRP1)GAL1,10p-SIC1*	This study
YAC1390	S288C	*MATa ura3-52, leu2Δ1, trp1Δ63, his3Δ200, lys2ΔBgl, hom3-10, ade2Δ1, ade8, yel069::URA3, yjl193w::HphNT V42219-42341Δ::LEU2-RFB, sit1::pRS303[HIS3]*	This study
YAC1394	S288C	*MATa ura3-52, leu2Δ1, trp1Δ63, his3Δ200, lys2ΔBgl, hom3-10, ade2Δ1, ade8, yel069::URA3, yjl193w::HphNT sit1::pRS305-7xARSH4[LEU2]*	This study
YAC1399	S288C	*MATa ura3-52, leu2Δ1, trp1Δ63, his3Δ200, lys2ΔBgl, hom3-10, ade2Δ1, ade8, yel069::URA3, yjl193w::HphNT, sic1::(TRP1)GAL1,10p-SIC1, sit1::pRS305-*	This study

Strain	Background	*Genotype*	Source
YAC1417	S288C	*MATa ura3-52, leu2Δ1, trp1Δ63, his3Δ200, lys2ΔBgl, hom3-10, ade2Δ1, ade8, yel069::URA3, yjl193w::HphNT V42219-42341Δ::LEU2-RFB, sic1::(TRP1)GAL1,10p-SIC1, sit1::pRS303[HIS3]*	This study
YAC1424	S288C	*MATa ura3-52, leu2∆1, trp1∆63, his3∆200, lys2∆Bgl, hom3-10, ade2∆1, ade8, yel069::URA3, yjl193w::HphNT clb2∆::HIS3*	This study
YAC1446	S288C	*MATa ura3-52, leu2∆1, trp1∆63, his3∆200, lys2∆Bgl, hom3-10, ade2∆1, ade8, yel069::URA3, yjl193w::HphNT, sic1::[TRP1]GAL1,10p-SIC1 clb2∆::HIS3*	This study
YAC1452	S288C	*MATa ura3-52, leu2Δ1, trp1Δ63, his3Δ200, lys2ΔBgl, hom3-10, ade2Δ1, ade8, yel069::URA3, yjl193w::HphNT V42219-42341Δ::LEU2-RFB, sit1::pRS303[HIS3]-7xARSH4*	This study
YAC1455	S288C	*MATa ura3-52, leu2Δ1, trp1Δ63, his3Δ200, lys2ΔBgl, hom3-10, ade2Δ1, ade8, yel069::URA3, yjl193w::HphNT V42219-42341Δ::LEU2-RFB, sic1::(TRP1)GAL1,10p-SIC1, sit1::pRS303[HIS3]-7xARSH4*	This study

3. Plasmids

Different plasmids from the pRS series (Sikorski and Hieter, 1989) were used in this study, particularly pRS303 (pBluescript, *HIS3*), pRS304 (pBluescript, *TRP1*) pRS305 (pBluescript, *LEU2*) and pRS306 (pBluescript, *URA3*). The plasmid pBH3 (Calzada et al., 2005) was used to insert a replication fork barrier (RFB) on chromosome V, and the plasmids pTZ19R (Mead et al., 1986) and pRS305 were used in the insertion of a tandem repeat of 7xARSH4 from pDK368-7 (Hogan and Koshland, 1992) on chromosome V.

The pGEM-T Easy system I vector (Promega) was used for the cloning of PCR products amplified with *Taq* polymerases.

4. Solutions

The detailed composition of unusual solutions used in this study is summarized in Table 2.

Table 2: Composition of solutions used in this study.

Solution	Composition
Az-STOP	0.5 M NaOH, 0.4 M EDTA, 0.2% Sodium Azide
Denaturing solution	0.5 M NaOH, 1.5 M NaCl
Hybridization buffer	1% SDS, 1 M NaCl, 10% Dextran Sulphate
NIB buffer	17% glicerol, 50 mM MOPS, 150 mM K acetate, 2 mM $MgCl_2$, 500 μg spermidine, 150 μM spermine. pH 6,8
PEM	100 mM Pipes, 1 mM EGTA, 1 mM $MgSO_4$, pH 6.9
PEMS	PEM supplemented with 1.2 M sorbitol
PEMS-DIG	PEMS supplemented with 0.1% 2-mercaptoethanol, 0.02% glusulase, 25 μg/ mL zymolyase 20T
PEMBAL	PEM supplemented with 1% BSA, 100 mM Lysine hydrochloride, 0.1% NaN_3, pH 6.9
Stripping solution	0.1 M NaOH, 1% SDS
SSC, 20x	0.3 M Sodium citrate, 3 M NaCl, pH 7,0
TBE, 10x	0.9 M Tris, 0.9 M Boric acid, 0.02 M EDTA, pH 8.3

5. Primers

Primers used in this study were synthesized by Sigma-Aldrich in desalt purification conditions (for short oligomers) or upon HPLC (for long oligomers) and are described in Table 3. Stocks were prepared at 100μM in 1xTE and maintained frozen.

Table 3: Primers used for the amplification by PCR of deletion cassettes, subcloning fragments or Southern probe synthesis.

Primer	Primer Sequence
5' SalI SIT1 cassette	GTCGACGGAATTTGAAGAGGTTGTCGTT
3' SalI SIT1 cassette	AATCTTTCCTATCTTTACTGC
5' ars507Δ::KanMX4	TAACATCTTTTTAAACAATCATAAATAGCACTTCTTATC ATACAACCTCATGATATCGAATTCCTGCAGC
3' ars507Δ::KanMX4	CCGCTTGTCCACAATCATGTAAATATAAATATTGAAACT TTTCACTTGTTTTCGACACTGGATGGCGGC
5' ars504.2Δ::LEU2	CATCGCTTATAATACGAACTAATTTATTTATGAACAAAG GCTTTGGAAAATCGAGGAGAACTTCTAGTAT
3' ars504.2Δ::LEU2	TTTTCGTCCCTGCATTGAGATCGCATCTGTCCCTGAGT AAACGATGCACATCGACTACGTCGTAAGGC
5' ura3-52Δ::KANMX4	AACATGAAATTGCCCAGTATTCTTAACCCAACTGCACA GAACAAAAACCTTGATATCGAATTCCTGCAGC
3' ura3-52Δ::KANMX4	GCTCTAATTTGTGAGTTTAGTATACATGCATTTACTTAT AATACAGTTTTTTCGACACTGGATGGCGGC
5' ura3-URA3	ACTTGTGTGCTTCATTGG
3' ura3-URA3	CGTTACAGAAAAGCAGGC
5' ars507Δ::URA3	TAACATCTTTTTAAACAATCATAAATAGCACTTCTTATC ATACAACCTCATTCAATTCATCATTTTTTTTTTATTC
3' ars507Δ::URA3	CCGCTTGTCCACAATCATGTAAATATAAATATTGAAACT TTTCACTTGTTGGGTAATAACTGATATAATTAAATTGAA GC
5' ura3Δ::ARS305	TAACATCTTTTTAAACAATCATAAATAGCACTTCTTATC ATACAACCTCATACAACAATATTAATAATAAGTAATAAA AAG

3' ura3Δ::ARS305	CCGCTTGTCCACAATCATGTAAATATAAATATTGAAACT TTTCACTTGTTGATCCTTTTTTTTATTGTGTTGG
5' ars504.2Δ::ARS305	CATCGCTTATAATACGAACTAATTTATTTATGAACAAAG GCTTTGGAAAAGAGGCCACAGCAAGACCGGC
3' ars504.2Δ::ARS305	TTTTCGTCCCTGCATTGAGATCGCATCTGTCCCTGAGT AAACGATGCACATCGACTACGTCGTAAGGC
5' BtwPS-RFB	GCTTTTTCAACAAGTCACCTAAATTTCCAAAGCCGAAA GCCCTGCTACTTCGAGGAGAACTTCTAGTAT
3' BtwPS-RFB	ATACTCTATATAGCACAGTAGTGTGATAAATAAAAAATT TTGCCAAGACTGGATCCTTCGTAGTATTTTTTTTC
5' Δclb2-HIS3	CAAGAAGCCTTTTATTGATTACCCCCTCTCTCTCTTCAT TGATCTTATAGCGGCATCAGAGCAGATTGTAC
3' Δclb2-HIS3	GGACATTTATCGATTATCGTTTTAGATATTTTAAGCATC TGCCCCTCTTCGTATTTCACACCGCATATGATC

6. Antibodies

Antibodies used in this study are listed in Table 4.

Table 4: List of antibodies and their dilutions used in western blot or immunofluorescence staining. Check all details, and include the reactivity details.

Name	Host and reactivity	Dilution of use	Catalogue Number and Company
Anti-Sic1	Rabbit polyclonal	1:2000	FL-284, Santa Cruz Biotechnology, Inc.
Anti-Rabbit-HRP	Donkey anti-rabbit	1:4000	NA934V, GE Healthcare
Anti-Pgk1	Anti-yeast, Mouse monoclonal 22C5-D8	1:20000	459250, Invitrogen, Molecular Probes
Anti-Mouse-HRP	Sheep anti-mouse	1:10000	NA931, GE Healthcare
Anti-α-tubulin	Mouse monoclonal	1:4000	T5168, Sigma-Aldrich
Anti-Cy3	Anti-mouse	1:1000	115-165-003, Jackson

7. Reagents and Enzymes

Nocodazole (M1404), β-glucuronidase (67770), proteinase K (P2308), spermine tetrahydrochloride (S1141) and spermidine (S0266) were purchased from Sigma-Aldrich; the Zymolyase 20T (120491-1) from AMS Biotechnology, and the dextran sulphate (M3183) from Genaxxon Bioscence.

Hygromycin B (10843555001), RNase A (10109169001), DNA MB grade (1146714001), Hexanucleotide mix (11277081001) and Klenow polymerase (11008404001) were obtained from Roche. The 1kb DNA ladder is from Invitrogen and the Precision Plus Protein Dual Colour Standards (161-0374) from Bio-Rad.

Restriction enzymes were purchased from New England Biolabs (NEB), Roche, Invitrogen, or Fermentas. The α-factor pheromone was synthesized in the Cancer Research UK facilities kindly provided by Prof. K. Labib (University of Dundee, UK).

All inorganic salts, acids, bases and organic compounds were obtained from Merck, Sigma-Aldrich or Formedium.

References for other reagents are included along this Section were appropriate.

8. Software and Databases

The SGD (http://www.yeastgenome.org) database is an online resource for genomic information on *S. cerevisiae*. The search and analysis tools integrated in the SGD were used in this study to access the sequence, chromosome coordinates of genes or origin replication sites, and also to help on primers and probes design.

The OriDB (http://www.oridb.org) is a database containing curated data of DNA replication origins in budding and fission yeast, obtained by genome-wide and origin mapping and characterization studies (Siow et al., 2012). The OriDB was used in this study to access the catalogue of confirmed and predicted replication origin sites identified in *S. cerevisiae*.

The Fluctuation AnaLysis CalculatOR or FALCOR (www.keshavsingh.org/protocols/FALCOR) (Hall et al., 2009) is a web tool that calculates the mutation rate from various mutation assays in bacteria and yeast using Luria-Delbruck Fluctuation Analysis (Luria and Delbrück, 1943). The Ma-Sandri-Sarkar Maximum Likelihood Estimator (MSS-MLE) (Sarkar et al., 1992) was used to estimate the mutation rates (Foster, 2006). The program FALCOR was used to estimate GCR rates with confidence intervals.

9. *E. coli* Growth Conditions and Plasmid Transformation

E. coli cells were routinely grown at 37 ºC in LB media (1% tryptone, 0.5% yeast extract and 1% NaCl) or LB agar plates (LB media with 2% agar-agar) supplemented with 100 µg/mL ampicillin. For plasmids amplification and transformation, competent *E. coli* DH5α cells were transformed with ligation mixtures or plasmids (Sambrook et al., 1989). For plasmid purification, minipreps from 1-2 mL aliquots of *E. coli* liquid cultures were performed using the "*E. coli* Boiling Lysis Plasmid Preparation" procedure (Sambrook et al., 1989)

10. Yeast Specific Methods

10.1 Media and Growth Conditions

Cells were routinely grown at 25 ºC in rich YP media (1% Yeast extract, DIFCO; 2% bacteriological-peptone, OXOID LP0037) media supplemented with a final

concentration of 40 mg/ L adenine (YPA) and 2% glucose (YPAD). 2% agar was added to prepare solid media. To grow conditional *GAL-SIC1* cells in Sic1-expressing conditions cells were grown in YPA media supplemented 1% raffinose (Formedium, RAF-03) and 0.3% galactose (Formedium, GAL-01) (YPARG) and in YPAD to deplete Sic1. Other cell growth conditions are detailed for each specific experiment. Cells carrying the c*dc15-2* thermo-sensitive mutation were grown in permissive conditions of 23 or 25 ºC, and incubated at the restrictive temperature of 37 ºC.

Cell growth and duplication time in liquid cultures was always monitored under the microscope by counting cell numbers using Neubauer counting chambers, and calculating the number of cells per millilitre (cells/ mL) (by the following formula: cell number per square x culture dilution x 2.5 x 10^5. explain this formula) according to manufacture's specifications.

Plates of synthetic minimal media with defined chemical composition were used to identify strains with selective markers or to isolate cell transformants during strain construction. Solid synthetic media contains Yeast Nitrogen Base without amino acids (DIFCO, 291940) (YNB) and agar (0.7% YNB, 2% agar-agar) complemented with all amino acids (Sigma) except one or several to check auxotrophies. For W303-1 strains, YNB-agar plates were supplemented with the amino acids according to the strain auxotrophy (see Table 1) at a final concentration of 40 mg/ L for uracil (Ura), tryptophan (Trp), adenine (Ade) and histidine (His); and 80 mg/ L for leucine (Leu) and 2% glucose (or 1% raffinose and 0.3% galactose for *GAL-SIC1* cells). For S288C strains, YNB-agar plates were prepared as before and supplemented with 1 mM methionine (Met), serine (Ser) and lysine (Lys) and 1.5 mM of threonine (Thr). To identify strains carrying the kanamycin (kanMX4) or hygromycin (HphNT) marker, cells were plated in YPA agar plates supplemented with 200 μg /mL geneticin (Gibco, G418) or hygromycin B (Calbiochem, 400051) respectively.

For sporulation, diploids were plated onto Rich Sporulation Medium (RSM) (0.25% yeast extract, 1.5% potassium acetate, 0.1% dextrose, 2% agar-agar) complemented with the following amino acids: 100 mg/ L phenylalanine, 50 mg/ L Ade and Ura, 25 mg/ L His, Leu, Lys, Trp, Met and arginine (Arg), and 10 mg/ L tyrosine (RSM plates).

For the GCR assay, cells were plated in synthetic minimal FOA-CAN agar plates (YNB media supplemented with 0.74 g/ L CSM-Arg (Qbiogene/Bio101, 4510-122), 20 mg/ L Ura, 1.1 g/ L 5-fluoorotic acid (Apollo Scientific, PC4054), 60 mg/ L sulphate salt L-canavanine (Sigma, C9758-5G) complemented with 2% glucose or 1% raffinose and 0.3% galactose for *GAL-SIC1* cells.

10.2 Yeast stocks

Cell aliquots of yeast strains were maintained for long-term storage in individual cryotubes (Nalgene) in an ordered collection frozen at -80 ºC in a solution of 30% glycerol.

10.3 Strain Construction

To obtain cells conditionally expressing the Sic1 protein, the *sic1::[TRP1]GAL1,10p-SIC1* cassette was transformed into cells of the appropriate parental cells by replacing a 19-bp DNA fragment immediately before the SIC1 ATG with an inducible *GAL1,10p* promoter preceded by the budding yeast *TRP1* marker (*TRP1-GAL1,10p* cassette) (Ayuda-Duran et al., 2014).

10.3.1 Construction of yeast strains with tandem repeats of *ARSH4* inserted on chromosome V

To integrate a plasmid containing tandem repeats of seven origins *ARSH4* (7xARSH4) in *SIT1* on chromosome V, we proceeded as follow: (1) To obtain the *pRS305-SIT1[LEU2]* plasmid, 1853-bp of the *SIT1* gene was amplified by PCR from the yeast genomic DNA (SGD coordinates 27689 - 29541 of the chromosome V) with primers 5' SalI *SIT1* cassette and 3' SalI *SIT1* cassette (Table 3), cloned into a pGEM-T Easy system plasmid and fully sequenced to confirm the absence of mutations inserted by PCR; the resulted plasmid was digested with SalI and HindIII and sub-cloned into the plasmid pRS305 containing the *LEU2* marker; (2) To obtain the *pRS305-7xARSH4[LEU2]* plasmid, the pDK368-7 (kindly provided by Douglas Koshland) containing a tandem of seven *ARS209* (*7xARSH4*) origins (Hogan and Koshland, 1992) was digested with PaeI and BoxI and the tandem was sub-cloned into the pTZ19R plasmid; (3) The resulted plasmid was digested with HindIII and XbaI, and ligated with the *pRS305-SIT1[LEU2]* plasmid previously digested with the same restriction enzymes, to obtain the *pRS305-SIT1-7xARSH4[LEU2]* integrative plasmid; (4) The resulted plasmid was integrated at the NheI site of *SIT1* on both YAC177 and YAC217 strains to obtain YAC1394 and YAC1399 strains, respectively; (5) The empty plasmid (*pRS305-SIT1[LEU2]* plasmid) was integrated at the NheI site of *SIT1* on both YAC177 and YAC217 strains to obtain YAC1286 and YAC1290 strains, respectively. The origin activity within the tandem 7xARSH4 was confirmed by 2D Gels (see 2D Gel Analysis) following hybridization with the pRS305 probe (Table 6) in all the resultant strains (Figure 17C and Figure 34C)

10.3.2 Construction of *ars507*Δ yeast strains

To delete the origin *ARS507* of chromosome V and generate the strains YAC556 and YAC558 strains, both YAC177 and YAC217 strains were transformed, respectively, with the *ars507*Δ*::KanMX4* deletion cassette, to replace a 234-bp DNA fragment containing *ARS507* (SGD coordinates 59283-59516 of the chromosome V) by the marker. The *ars507*Δ*::KanMX4* deletion cassette was amplified by PCR from the plasmid pRS305 containing the *KanMx4* marker, using primers 5' ars507Δ::KanMX4 and 3' ars507Δ::KanMX4 (Table 3) that include both flanking regions of *ARS507* region in 5' and 3', respectively. The origin inactivity at the *ars507*Δ locus was confirmed by 2D Gel analysis (see 2D Gel Analysis) following hybridization with the *ARS507* probe (Table 6) in all the resultant strains (Figure 12C).

10.3.3 Construction of *ars504.2*Δ yeast strains

To delete the origin *ARS504.2* of chromosome V, the YAC177 strain was transformed with the *ars504.2*Δ*::LEU2* deletion cassette to replace a 2505-bp DNA fragment containing ARS504.2 (SGD coordinates 10425-12929 of the chromosome V) by the *LEU2* marker and to obtain the YAC1024 strain. The *ars504.2*Δ*::LEU2* deletion cassette was obtained by PCR amplification of the *LEU2* marker from the plasmid pRS305, using primers 5' ars504.2Δ::LEU2 and 3' ars504.2Δ::LEU2 (Table 3) that include both flanking regions of the *ARS504.2*. To obtain the YAC1377 strain, the *sic1::[TRP1]GAL1,10p-SIC1* cassette was transformed into the YAC1164 strain (details of the replacement explained at the beginning of this section). The inactivity of the origin at the *ars504.2*Δ locus was confirmed by 2D Gels (see 2D Gel Analysis) following hybridization with the leu2Δ1 probe (Table 6) in all the resultant strains (Figure 15C).

10.3.4 Construction of yeast strains with *ARS507* replaced by *ARS305*

The substitution of *ARS507* with *ARS305* of chromosome III was obtained as follows: (1) Both *ura3-52* and *URA3* gene copies were eliminated from the YAC177 strain by sequential transformation with the *ura3-52*Δ*::KANMX4* and the *ura3*Δ*::URA3-1* deletion cassettes (details are described below), respectively, to obtain YAC560 and YAC809 strains, respectively; (2) *ARS507* was deleted by following a "pop-in, pop-out" strategy with the *URA3* marker by transforming the YAC809 strain with the *ars507*Δ*::URA3* deletion cassette (details are described below) to obtain the YAC874 strain; (3) The *URA3* marker was "pop-out" and replaced by the origin *ARS305* by transforming the YAC874 with the *ura3*Δ*::ARS305* cassette (the details are described bellow), to obtain the YAC884 strain; (4) The *URA3* marker was restored at the yel069

locus by transforming the YAC884 strain with the *ura3-1Δ::URA3* deletion cassette (the details are described below), to obtain the YAC899 strain.

The *ura3-52Δ::KanMX4* deletion cassette was amplified by PCR from the pRS305 carrying the *KanMX4* marker using primers 5' ura3-52Δ::KANMX4 and 3' ura3-52Δ::KANMX4 (Table 3) to replace the *ura3-52* by the *KanMX4* marker.

Both *ura3Δ::URA3-1* and *ura3-1Δ::URA3* deletion cassettes were amplified by PCR from yeast genomic DNA from deficient *ura3-1* or proficient *URA3* yeast cells, respectively, using primers 5' ura3Δ::URA3-1 and 3' ura3Δ::URA3-1 (Table 3). The *ars507Δ::URA3* deletion cassette was amplified by PCR from the pRS306 using primers 5' ars507Δ::URA3 and 3' ars507Δ::URA3 (Table 3) to replace a 234-bp DNA fragment containing ARS507 (SGD coordinates 59283-59516) by the *URA3* marker. The *ura3Δ::ARS305* cassette was constructed by PCR amplification of a 233-bp DNA fragment that include *ARS305* using primers 5' ura3Δ::ARS305 and 3' ura3Δ::ARS305 (Table 3), cloning the fragment into a pGEM-T Easy system plasmid, and sequencing the entire fragment to confirm that no undesired mutations were introduced by PCR, and digestion of the resulted plasmid with SacI and PstI.

To obtain the YAC921 strain, the *sic1::[TRP1]GAL1,10p-SIC1* cassette was transformed into cells of the YAC556 strain (details of the replacement explained at the beginning of this section).. The activity of *ARS305* at the *ars507Δ* locus was verified by 2D Gels (see 2D Gel analysis) with the ARS507 probe (Table 6) in all the resultant strains (Figure 13C).

10.3.5 Construction of yeast strains with *ARS504.2* replaced by *ARS305*

To substitute *ARS504.2* with *ARS305* of chromosome III, YAC556 and YAC558 strains were transformed with the *ars504.2Δ::ARS305[LEU2]* deletion cassette to replace a 2505-bp DNA fragment containing ARS504.2 (SGD coordinates 10425-12929 of the chromosome V) by the origin ARS305 followed by the *LEU2* marker and obtain YAC1379 and YAC1416 strains, respectively. In detail, the *ars504.2Δ::ARS305[LEU2]* deletion cassette was obtained by NotI digestion of the plasmid pRS305 cloned with a 234-bp DNA fragment containing ARS305 (SGD coordinates 39382-39615 of chromosome III) previously amplified by PCR using Pfu DNA polymerase (Promega) and primers 5' ars504.2Δ::ARS305 and 3' ars504.2Δ::ARS305 (Table3), and fully sequenced to verify that no undesired mutations were introduced by PCR. The activity of the ARS305 at the *ars504.2Δ* locus was confirmed by 2D Gel analysis (see 2D Gel Analysis) following hybridization with the leu2Δ1 probe (Table 6).

10.3.6 Construction of conditional temperature sensitive yeast mutants carrying the *cdc15-2* allele

To construct control *cdc15-2* (YAC1104) and *sic1 cdc15-2* (YAC1107) strains, the YAC316 MATα strain was cross-mated with the YAC1082 *MAT*a strain. The resulted diploid (YAC1098) was sporulated by plating cells onto RSM plates for 3 days at 25 ºC and then treated with glusulase (B-glucuronidase, SIGMA) at a concentration for Random Spore Analysis. Spores were genotyped by replica plating in synthetic minimal medium plates, and tested for the absence of growth on YPAD at 37 ºC and YPAD hygromycin plates (YAC1104) and for the absence of growth on YPAD at 37º C and on YPAD hygromycin plates, and for growth on YNB–TRP plates (YAC1107).

10.3.7 Construction of yeast strains carrying a *RFB* on chromosome V

To insert the *[LEU2]RFB* cassette on chromosome V between *PRB1* and *SOM1*, the *V42219-42341*Δ*::[LEU2]RFB* deletion cassette was constructed by PCR amplification from the plasmid pBH3 that contains a 450-bp DNA fragment with a *RFB* from the *rDNA* repeats of *S. cerevisiae* (SGD coordinates 460470**–**460919 of the chromosome XII) preceded by the *LEU2* marker from the plasmid pRS306 (Calzada et al., 2005), using the Pwo SuperYield DNA Polymerase (Sigma) and the 5' BtwPS-RFB and 3' BtwPS-RFB primers (Table 3). These plasmids include both flanking regions (upstream the 42219 coordinate, and downstream the 42341 coordinate of chromosome V) of the intergenic region between *PRB1* and *SOM1*. The resultant *V42219-42340*Δ*::[LEU2]RFB* deletion cassette was sub-cloned into the pGEM-T Easy system plasmid and fully sequenced to verify that no undesired mutations were introduced by PCR. This plasmid was NotI digested to liberate the insert and transformed into YAC852 and YAC177 strains to replace the 23-bp DNA fragment of the intergenic region between *PRB1* and *SOM1* (SGD coordinates 42219-42340 of the chromosome V) by the *[LEU2]RFB,* and to obtain the YAC1164 and YAC1196, respectively. To obtain the YAC1190 and YAC1299 strains, the *sic1::[TRP1]GAL1,10p-SIC1 cassette* was transformed into YAC1164 and YAC1296 strains (details of the replacement explained at the beginning of this section), respectively.

The efficiency of the RFB was confirmed in all the resultant strains (Figure 32B and Supplemental Figure 1B) using 2D Gels (see 2D Gel Analysis) following hybridization with the PCM1 probe (Table 6) by the appearance of a fork pausing spot.

10.3.8 Construction of conditional temperature sensitive yeast mutants carrying the *cdc15-2* allele and a *RFB* on chromosome V

To obtain the *RFB cdc15-2* (YAC1358) strain, the YAC1106 *MAT*α strain was cross-mated with the *MATa* YAC1164 strain. The resulted diploid was sporulated by incubation onto RSM plates and treated with glusulase for tetrad dissection analysis for spore micromanipulation (Singer Instruments). Tetrads were separated on YPAD plates and tested for their genotype by replica plating and selected for the absence growth on YPAD at 37º C and growth on YNB (-Leu) plates. The *sic1 RFB cdc15-2* (YAC1362) strain was obtained by transformation of the YAC1358 strain with the *sic1::[TRP1]GAL1,10p-SIC1* cassette (details of the replacement explained at the beginning of this section).

10.3.9 Construction of *clb2*Δ yeast strains

To delete *CLB2*, YAC177 and YAC217 strains were transformed with the *clb2*Δ*::HIS3* deletion cassette to replace a 1476-bp DNA fragment containing *CLB2* (SGD coordinates 771653-773128 of the chromosome XVI) with the *HIS3* marker and obtain YAC1424 and YAC1426 strains, respectively. The *clb2*Δ*::HIS3* deletion cassette was obtained by PCR amplification of the *HIS3* marker from the plasmid pRS303, using the primers 5' Δclb2-HIS3 and 3' Δclb2-HIS3 (Table 3) that include both flanking regions of the *CLB2* gene.

All cloning were verified by restriction enzyme plasmid digestion following mapping analysis. The correct integration of all deletion cassettes was confirmed by PCR (see "PCR for genotyping") and replica plating to check the appropriate auxotrophic markers, in all the resultant strains.

10.4 PCR for genotyping

The PCR technique was used to confirm the genotype of transformed or cross-mated strains. All PCRs were performed in a 2720 Thermal Cycler (Applied Biosystems) or GeneAmp PCR system 2400 (Perkin Elmer) using dNTPs (Roche, 1277049), BioTaq polymerase (Ecogen, BIO-21040) and the following thermal cycling conditions: 3 minutes at 94º C, 30 cycles of 1 min at 94 ºC, 1 minute at the appropriate temperature according to the melting temperature of the primers, and 1 min for each kb of the amplified product at 72º C, and finally 10-20 additional minutes at 72º C. To visualize the DNA bands, PCR products were run on a 1% TAE agarose gel and photographed using a UV transilluminator (Gel Doc XR+ Imaging System, Bio-Rad). Colony PCR was used to identify positive clones among yeast transformants that bear

the transformed DNA inserted in the desired positioning (including deletion cassettes). Briefly, a toothpick of cells of each transformant clone under examination from selective plates was introduced in the bottom of a 0.2 μL PCR tube and heated opened in a microwave for 90 seconds at 750 W. 10μL of the appropriate PCR mix containing an internal primer that anneals within the insert and an external primer that anneals flanking the desired insertion site (Figure 5) was added to each tube before PCR.

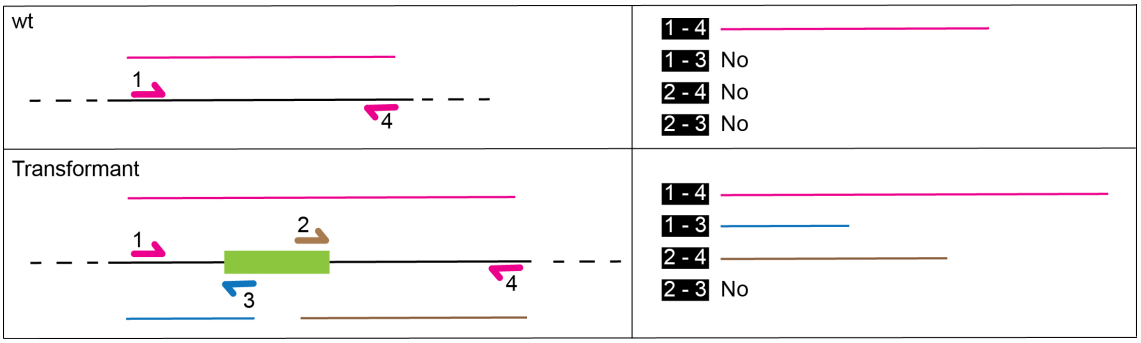

Figure 4: Schematic of the analysis for the correct integration of DNA inserts by PCR on genomic DNA. Primers 1-4 anneal with an external region of the DNA transformation *cassette*, primers 2-3 anneal with regions inside the DNA transformation *cassette*. The expected PCR bands are indicated on the right for negative (upper panel) or positive haploid transformants (middle panel) and for positive diploid transformants (lower panel).

Positive transformants from colony PCR were re-confirmed by using a more astringent PCR analysis. In brief, colonies from each candidate clone positive from colony PCR analysis were streaked in plates of rich media, and cells from a single colony were grown overnight in a 10 mL culture, centrifuged for 5 min at 3000 rpm, washed in sterile water and suspended in 200 μL of lysis solution (100mM NaCl, 10mM Tris pH 8.0, 1mM EDTA). To isolate and purify genomic DNA, 200 μL of glass beads and 200 μL of phenol/chloroform/Isoamyl alcohol 25:24:1, v/v (Ambion) were added to the cells and vortexed for 30 seconds. Then, 200 μL of 1x TE was added, the mixture vortexed for 5 seconds and centrifuged for 2 min at 3000 rpm. The aqueous layer was transferred to another tube, mixed with 2 volumes of 100% ethanol and centrifuged as before. The pellet was washed with 70% ethanol, suspended in 1x TE supplemented with 50 μg/ mL RNAse A (Roche), and incubated for 1 h at 37 ºC to dissolve DNA and degrade the RNA. Four distinct PCRs using all pairwise combinations of 4 different primers where two anneal inside the insert and two flanking the chromosome site of insertion (Figure 5). For simplicity, the sequences of all primers used to check DNA inserts by PCR are not specified in this text, since any region within the insert or any region flanking the insert can be used for primers design, but details can be provided upon request.

10.5 Dilution Spotting Assay

As a rapid approach to evaluate the growth ability of every new constructed strain, from two to four sister clones were examined for parallel growth among them and regarding parental and control strains. Cell suspensions of fresh strains were serially diluted from 3.33 x 10^6 to 3.33 x 10^3 cells/ mL, identical volumes (usually 10 µL) were spotted in YPAD and/or YPARG plates and allowed to growth at the desirable temperature until colonies form, usually during 48 hours. After that time, plates were scanned for cell growth evaluation.

10.6 Cell Cycle Synchronization

To synchronize control *cdc15-2* (YAC1104) and *sic1 cdc15-2* (YAC1107) cells, cell cultures of both strains were grown in YPARG until exponential phase, arrested in G2/M by incubation with 15 µg/ mL of the microtubule-depolymerizing drug nocodazole (Sigma, M1401) for 3.5 hours and shifted to YPAD containing 15 µg/ mL nocodazole for 1.5h to deplete Sic1 from *GAL-SIC1* cells while maintaining the nocodazole block. Then, cells were washed twice to eliminate the nocodazole by centrifugation at 3,000rpm for 3 minutes, resuspended in YPAD prewarmed at 37 ºC, and incubated at this temperature for 3.5 hours to inactivate Cdc15 and to arrest cells in telophase. Cells were then centrifuged as above and transferred to fresh YPAD at 23 ºC to synchronously release cells into the new cell cycle.

To block-and-release from *cdc15-2,* control *RFB cdc15-2* (YAC1358) and *GAL1-SIC1 RFB cdc15-2* (YAC1362) cells were grown in YPARG until exponential phase and shifted to YPAD for 3.5 hours at 37 ºC to arrest cells in telophase and to deplete Sic1 from *GAL1-SIC1* cells. Cells were collected by centrifugation at 3,000rpm for 3 minutes and resuspended in fresh YPAD at 23 ºC to synchronously release cells into G1 phase and samples were taken along their progression during a whole cell cycle during 190 minutes.

To arrest control *bar1Δ::URA3* (YAC272) and *GAL1-SIC1 bar1Δ::URA3* (YAC276) cells in G2/M, both cultures were grown in YPARG until exponential phase and shifted to YPAD pre-warmed at 37 ºC (to increase G1-phenotype defects in *sic1* cells) for 240 minutes to deplete Sic1 from *GAL1-SIC1* cells. Then, cells were arrested at G2/M by incubation with 15 µg/ mL nocodazole for 180 minutes and collected for 2D gels analysis.

10.7 Flow Cytometry Analysis

Fluorescence-activating cell sorting (FACS) analysis was employed to analyse the cell cycle distribution of cells within populations by quantitation of the DNA content.

For sample preparation, exponentially growing cells were fixed in 70% ethanol, centrifuged for 5 minutes at 13,200 rpm and incubated overnight at 37 ºC in 50 mM sodium citrate supplemented with 0.2 μg/ μL RNase (Roche, 10109169001). After the incubation time, cells were centrifuged 5 minutes at 13,200 rpm and incubated in 50 mM sodium citrate supplemented with 50 mM hydrochloric acid and 5 mg/ mL Pepsin (Merck, 107197) for 30 minutes at 37 ºC. Finally, cells were collected by centrifugation and resuspended in 50 mM sodium citrate supplemented with 2 μg/ mL propidium iodide, a DNA binding-dye. Stained samples were sonicated for 10 seconds in a low power frequency sonicator (Labsonic U, B. Braun) and analysed using the flow cytometer BD FACScalibur (BD Biosciences). 10,000 single events were acquired and analysed for forward-scattered light (FSC) to estimate cell size, and for FL2-H to measure the DNA content, using the BD CellQuest Pro software (BD Biosciences).

10.8 Immunofluorescence Staining of Tubulin

To detect microtubules and calculate the percentage of cells with anaphase spindles, 5 x 10^7 cells were fixed in 3,7% formaldehyde for 1 hour at room temperature and washed twice with 1x PEM (Table 2). Then, cells were sonicated (Labsonic U, B. Braun) for 10 seconds, centrifuged and incubated at 37 ºC for 15 to 40 minutes in 1 mL PEMS-DIG (Table II), until the cell wall was digested. After that time, cells were washed 3 times with 1 mL PEMS (Table 2) and incubated for 30 seconds in 1 mL PEMS supplemented with 1% Triton X-100 to permeabilize the cell membrane. For tubulin staining, cells were washed 3 times with 1 mL PEM, blocked for at least 30 minutes in 1 mL PEMBAL (Table 2), centrifuged and incubated overnight at 4 ºC with the anti-α-tubulin primary antibody (Table 4) in PEMBAL solution. After the incubation time, cells were washed twice with 1 mL PEMBAL supplemented with 0.1% Triton X-100, once with 1 mL PEMBAL, centrifuged and incubated for 1 hour in the dark at 37 ºC with the Anti-Cy3 fluorescent antibody (Table 4) in PEMBAL solution. Finally, cells were washed as before and suspended in PBS (Table 2). All centrifugations were performed at 7000 rpm for 1 minute. For fluorescent microscopy analyses, a drop of cells were mixed with the DNA-dye stain 4′,6-diamidino-2-phenylindole dihydrochloride (DAPI, Sigma-Aldrich D9542), set in a microscope slide and covered with a mounting medium containing anti-fade solution (ρ-phenylenediamine, Sigma-Aldrich P-1519) to minimize the photobleaching of fluorophores. The cover slip was sealed and analysed in a Confocal Microscope Leica MicroFluor using the phase contrast, DAPI and TxRed fluorescence filters. The percentage of cells with anaphase spindles (> 2 μm) was obtained by counting at least 100 cells each time point.

10.9 Two-dimensional Gel Analysis of DNA Replication Intermediates

To analyse DNA replicating molecules, total genomic DNA was extracted from cells, digested with restriction enzymes, separated on a neutral-neutral two-dimensional gel electrophoresis (referred as 2D Gel analysis or 2D gels in this text), Southern blotted and hybridized with probes to identify specific chromosomal regions at the left arm of chromosomes V and III (Figure 6 and Figure 7) and the *rDNA* locus on chromosome XII (Figure).

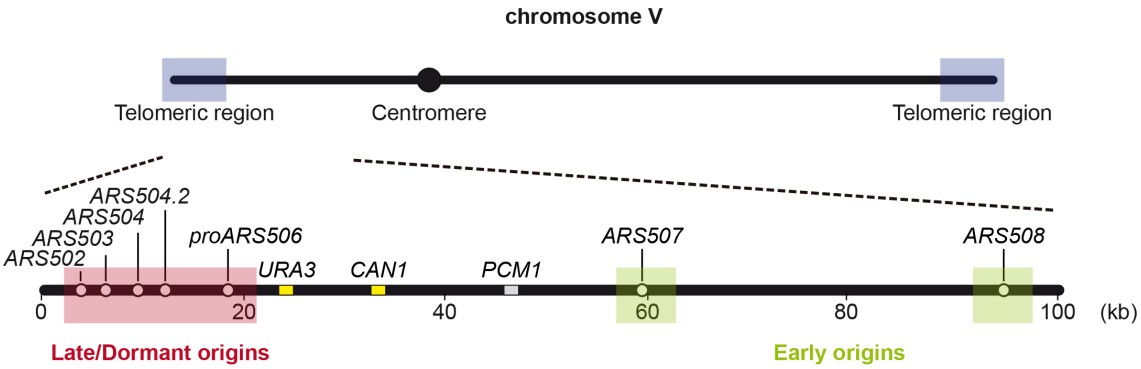

Figure 5: Schematic view of *S. cerevisiae* chromosome V. A zoom to the first 100 kb of the left arm of chromosome V is represented above. All ARS elements mapped in the region are indicated (open circles); the known activity of origins is indicated for early-firing (green) and late-firing/dormant origins (red). *CAN1* and *URA3* (yellow squares) represent the two markers used for the GCR assay and *PCM1* (grey square) is the first telomere-distal essential gene.

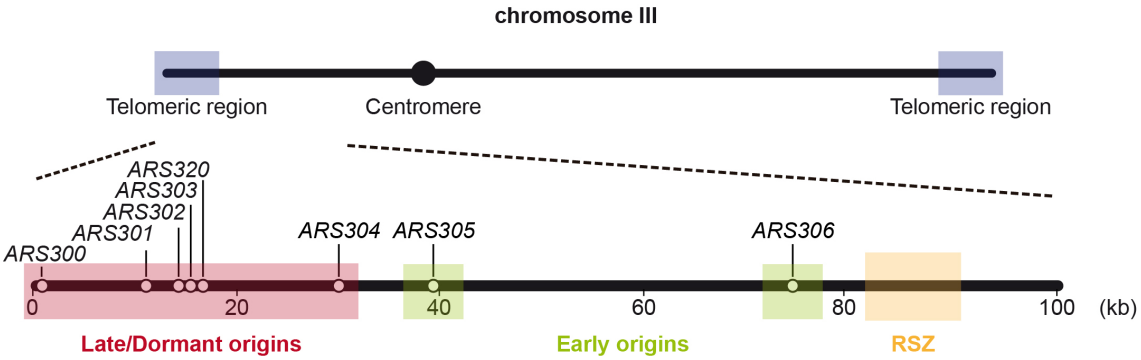

Figure 6: Schematic view of *S. cerevisiae* chromosome III. A zoom to the first 100 kb of the left arm of chromosome III is represented above. All ARS elements mapped in the region are indicated (open circles); the known activity of origins is indicated for early-firing (green) and late-firing/dormant origins (red). The previously identified replication slow zone (RSZ) is indicated in orange (Cha and Kleckner, 2002).

10.9.1 DNA Extraction

DNA samples were obtained using a modified "Nuclear isolation DNA Extraction" method (Friedman and Brewer, 1995; Lopes et al., 2001; Wu and Gilbert, 1995). Briefly, exponentially growing cells at a concentration of 1.6 x 10^7 cells/ mL were mixed with Az-STOP buffer (Table 2) to stop growth, centrifuged for 5 minutes at 3000 xg,

washed with cold Milli-Q water and centrifuged again for 5 minutes at 6000 xg. For cell wall disruption, the cell pellet was suspended in NIB buffer (Table 2) and repeated cycles of 30 seconds of vortexing and 30 seconds in ice were performed until most of the cells (more than 90%) were broken by microscopic observation. DNA was isolated from cells using the Blood & Cell Culture DNA Midi Kit (QIAGEN) following manufacturer's instructions, and suspended in 150 µL of 1x TE for 16 to 20 hours at room temperature.

10.9.2 DNA Digestion and Precipitation

2 µg (synchronous cultures) or 5 µg (asynchronous cultures) of DNA was digested with restriction enzymes for 4 hours with 75 units of the selected enzymes and appropriate restriction buffers. After digestion, the DNA was precipitated with potassium acetate/isopropanol, washed in 75% ethanol and suspended in 1x TE for 48 hours at room temperature. All the DNA digestions with specific restriction enzymes used in this Thesis to generate DNA fragments containing origin sites or genes of interest are summarized in Table 5.

Table 5: Chromosome features analysed in this thesis, DNA fragments and flanking restriction sites, and probes used during the Southern analysis.

Chr	Feature of interest	Restriction sites and DNA fragment	Probe
III	Origin *ARS300* and retrotransposon *Ty5*	KpnI-KpnI: 3.5 kb	YCLWTy5-1
III	Origins *ARS302*, *ARS303* and *ARS320*	ClaI-ClaI: 5.9 kb	HML ARS
III	Origin *ARS305*	ClaI-ClaI: 5.1 kb	PBN1
III	Origin *ARS306*	KpnI-ClaI: 3.6 kb	ARS306
III	Replication Slow Zone[1]	ClaI-ClaI: 3.2 kb	YCL021W-A
V	Origins *ARS503* and *ARS504*	ClaI-MluI: 4.5 kp	ARS503-504
V	Origin *ARS504.2*	MluI-ClaI: 4.8 kp	proARS504
V	Likely origin *proARS506*[2]	ClaI-ClaI: 6.3 kp	proARS506
V	*HXT13* gene	ClaI-ClaI: 5.2 kb	HXT13
V	*CIN8 gene*	XhoI-XhoI: 3.4 kb	CIN8
V	*LEU2-RFB*	ClaI-ClaI: 3.1 kb	PCM1
V	*SOM1* gene	ClaI-ClaI: 2.1 kp	SOM1
V	Origin *ARS507*	SacI-KpnI: 2.5 kp / XhoI-XhoI: 4.7 kp	ARS507
V	Origin *ARS508*	KpnI-ClaI: 2.4 kb	ARS508
V	*pRS305-7xARSH4*	SacI-SacI: 4.9 kb	pRS305
V	*pRS305-empty*	ClaI-ClaI: 4.2 kb	pRS305
V	*pRS303-7xARSH4*	SacI-ClaI: 6.13 kb	pRS305
V	*pRS303-empty*	KpnI-ClaI: 4.3 kb	pRS305
XII	*rDNA* locus	SacI-ClaI: 5.1 kb / ClaI-ClaI: 6.0 kb	rDNA

Note: Detailed information on probe localizations is described in Table 6.
[1] (Cha and Kleckner, 2002)
[2] Source: OriDB.

10.9.3 2D Gel Analysis

2D Gels (Figure 8) of digested DNA samples were performed as previously described (Brewer and Fangman, 1987; Calzada et al., 2005; Huberman, 1997). The first-dimension electrophoresis was run in a 0.4% agarose gel in 1x TBE without ethidium bromide (EtBr) during 36 to 38 hours at 20 V and the second-dimension electrophoresis was run for 7 hours in a 1% agarose gel in 1x TBE with 0.3 µg/ mL EtBr at 160 V, in a cold room at 4 ºC. After the transference, membranes were neutralised with 2x SSC for 30 minutes. To visualize particular replicating regions of interest, Southern analysis was performed by hybridising membranes with specific radioactive labelled probes (Table 6).

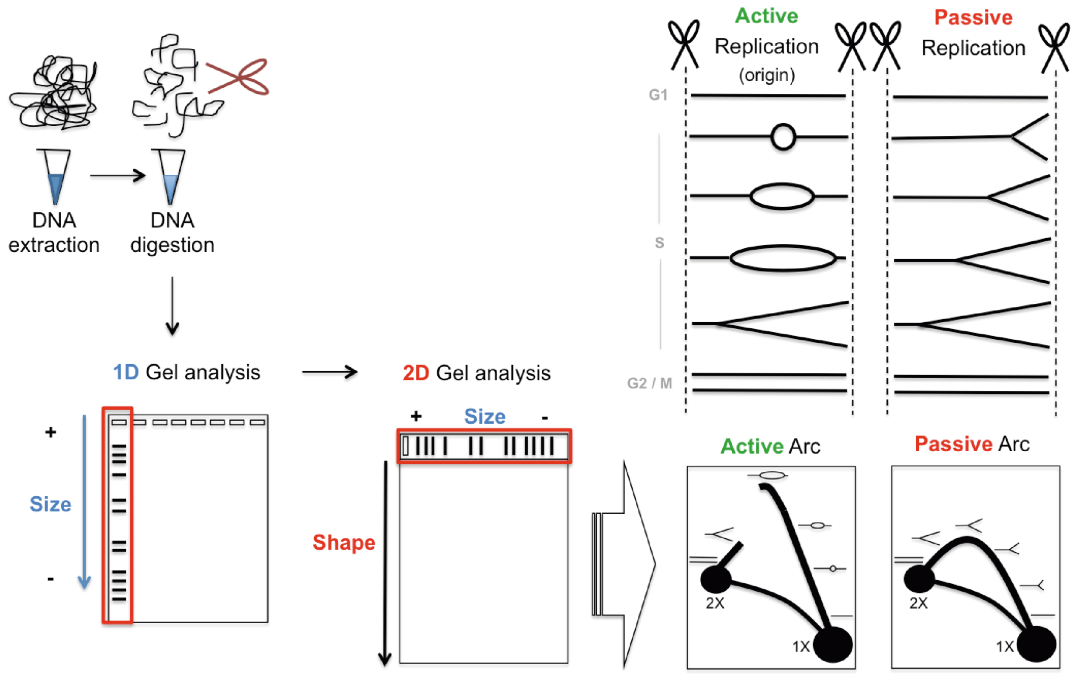

Figure 7: 2D Gel Electrophoresis. DNA samples containing replicating molecules were separated during the first dimension according to their size. Then, the agarose lane containing the size-separated DNA molecules was cut, inserted in the second agarose and run in a second dimension gel to resolve replication intermediates according to their structure.

10.9.4 Radioactive DNA Labelling for Probe Hybridisation

The DNA template for probe labelling was amplified from genomic DNA by PCR using the DFS-Taq polymerase (Bioron) and appropriate primers, in normal thermal cycling conditions (see above). A second PCR was performed in the same conditions using 1 µL of the former PCR product as a template. The resulting DNA product was examined to be unique, and purified using the JETquick PCR Product Purification Spin Kit (Genomed), following manufacturer's instructions. The DNA template was

radioactively labelled with dCTP [alpha ^{32}P]- 6000Ci/mmol (NEG-513Z, Perkin Elmer) using the Random Primed DNA Labelling Kit (Roche), according to the manufacturer's instructions. For all radioactive probes, approximately 25 ng of DNA template was used for each 2,5 μL of labelled dCTP [alpha ^{32}P], in a final reaction volume of 20 μL. Labelled probes were purified from the unincorporated dCTP [alpha ^{32}P] nucleotides using the Illustra ProbeQuant G50 Micro Columns Kit (ref, GE Healthcare), following manufacturer's instructions. All DNA probes synthesised and used in this study are listed in Table 6.

Table 6: DNA probes used for Southern analysis.

Probe	Chr	Chromosome Coordinates[1]
YCLWTy5-1	III	2,277-2,799 bp
HML ARS	III	14,040-14,991 bp
PBN1	III	34,848-35,590 bp
ARS306	III	73,001-73,958 bp
YCL021W-A	III	83,269-83,951 bp
leu2Δ1	III	91,522-9,1950 bp
ARS503-504	V	8,919-9,432 bp
proARS504	V	10,744-11,272 bp
proARS506	V	18,213-18,663 bp
HXT13	V	23,820-24,660 bp
CIN8	V	39,206-39,535 bp
SOM1	V	41,985-42,565 bp
PCM1	V	42,776-43,477 bp
ARS507	V	59,965-60,438 bp
ARS508	V	92,964-93,372 bp
rDNA	XII	466,856-467890 bp
pRS305	-	2588-30003 bp [2]

[1] According to the SGD (http://www.yeastgenome.org).
[2] Plasmid coordinates.

10.9.5 Probe Hybridisation

All hybridisations and washes were performed in a hybridization oven with rotation at 65 ºC. Membranes were pre-hybridized overnight in hybridization buffer (Table II) supplemented with 100 μg/ mL of denatured ssDNA (Roche) and hybridized overnight in the same solution complemented with the denatured radioactive labelled probe of interest (Table 6). After hybridization, membranes were washed twice with 2X SSC for 5 minutes each, twice with 2x SSC, 1% SDS for 30 minutes each, and finally with 0.1x SSC for 15 minutes. Membranes were exposed to Phosphor Storage Screens (BAS-MS imaging plates, Fujifilm) in cassettes and detected using a Phosphorimager (Personal Molecular Imager FX, Bio-Rad).

When necessary, membranes were stripped to remove the probe and re-hybridized with other probe. For probe stripping, membranes were incubated twice with

stripping solution (Table 2) heated at 42 ºC for 5 min each and washed with 0.1x SSC for 15 minutes.

10.9.6 Autoradiograms Quantification

Quantitative determination of origin efficiency was determined as previously described (Theis et al., 2010; Yamashita et al., 1997). For origin efficiency estimation, bubble-arc (active replication) and the Y-arc (passive replication) signals (Figure 8) were quantified using the volume free hand quantitative tool of the Quantity One software (Bio-Rad), resting the respective background and employing the following formula: bubble-arc/(bubble-arc+Y-arc). The region of large Ys was not included in the quantification of any of the bubble-arc or Y-arc signals because is a mix of both signals that result from the co-migration of passive replicating molecules (large Ys) and active replicating molecules (large Ys that result from bubbles resolution).

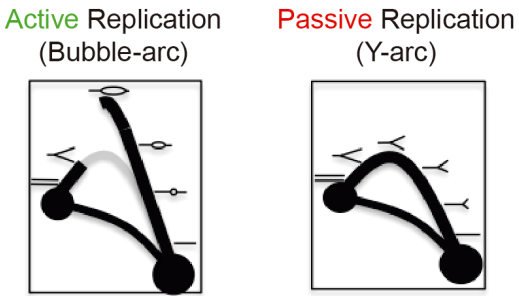

Figure 8: 2D gel analysis of active and passive replication. The expected images for probe hybridization against a DNA fragment containing an active origin (active replication, left panel) or passively replicated (passive replication, right panel). The type of replication intermediate formed in each case is show. The different migration pattern of intermediates in a 2D gel results in a continuous bubble- or Y-arc.

10.10 Western blot Analysis

Yeast proteins were extracted by the TCA method (Foiani, M. 1994) from 2.5 x 10^8 cells and separated on a 10% SDS-Polyacrylamide gel electrophoresis (SDS-PAGE). After the electrophoresis, proteins were transferred for 1.5 hour to nitrocellulose membranes (Hybond-ECL RPN303D, GE Healthcare) by electrophoretic wet transfer in 100 mM CAPS, 10% methanol.

For Sic1 detection, membranes were blocked for 1 hour in T-PBS milk (Table 2) and incubated with the anti-Sic1 primary antibody (Table 4) overnight at 4 ºC. After the incubation, membranes were washed 3 times 5 minutes with T-PBS (Table 2) and incubated for 1 hour with the anti-rabbit-HRP secondary antibody (Table 4) at room temperature. Membranes were then washed 2 times with T-PBS, 1 time 10 minutes with PBS and revealed with chemiluminescence reagents using the Western Lighting plus-ECL kit (Perkin Elmer, NEL104001EA) following manufacturer's instructions and

exposed to X-ray films (Konica Minolta Medical Films A plus, A9KN) for the appropriate time. Radiography films were scanned with a CanoScan 9000F (Canon) and Western blot bands were quantified using the Quantity One software (Bio-Rad).

3-phosphoglycerate kinase (Pgk1) was used as a loading control. For Pgk1 detection, the same membranes used for Sic1 detection were blocked for 1 hour in T-PBS milk, incubated for 1 hour with the anti-Pgk1 primary antibody (Table 4) and for 45 minutes with the anti-mouse-HRP secondary antibody (Table 4), including the same intermediate washings as before. Membranes were revealed, exposed and scanned as before.

10.11 Pulsed Field Gel Electrophoresis

To obtain intact chromosome-sized DNA for Pulsed Field Gel Electrophoresis (PFGE) analysis, plugs of agarose-embedded DNA were prepared using the CHEF Yeast Genomic DNA Plug Kit (Bio-Rad, 170-3593) following manufacturer's instructions. Succinctly, exponentially growing cells were harvested by centrifugation, suspended in cell suspension buffer and mixed with 2% CleanCut agarose equilibrated at 50 ºC, to a final concentration of 0.8%. The melted cells-agarose mixture was transferred to disposable plug molds and allowed to solidify at room temperature. To digest the cell wall and to degrade proteins, plugs were treated with lyticase for 2 hours at 37 ºC, rinsed with sterile water and incubated with proteinase K (Roche, 03115879001) for 4 days at 50 ºC. Finally, plugs were washed 5 times in 10 mM Tris, 50 mM EDTA, pH 7.5, for 1 hour each.

To resolve yeast chromosomes in a PFGE, plugs were loaded in a 1% Certified Megabase agarose (Bio-Rad, 161-3108) gel and run in a CHEF-DR II System (Bio-Rad) in 0.5x TBE recirculated at 14º C. The run time was 24 hours at 6 V/cm with a 60-120 second switch time ramp. *S. cerevisiae* Chromosomal DNA Ladder (CHEF DNA Size Standard 170-3605, Bio-Rad) and Lambda Concatemers Ladder (CHEF DNA Size Standard 170-3635, Bio-Rad) were used as PFGE markers. After the electrophoresis, the gel was stained with 1 µg/ mL EtBr in 0.5x TBE for 30 minutes, de-stained for exactly 30 minutes in 0.5x TBE and photographed using a UV Transilluminator (Gel Doc XR+Imaging System, Bio-Rad).

To study a particular chromosome, the chromosome-sized DNA was transferred to Hybond-XL membranes and hybridized with specific radioactively labelled probes (Table 6), as for 2D Gels, except that the gel was incubated with 0.25 N HCl for 25 min instead of 15 min.

10.12 Gross Chromosomal Rearrangements Assay

The GCR assay is a genetic screening that allows the isolation of mutants of haploid cells that spontaneously suffer gross chromosomal rearrangements of two markers (*CAN1* and *URA3*) placed on a non-essential region at the left arm of chromosome V (Chen and Kolodner, 1999) (Figure 10) by Fluctuation Analysis (Luria and Delbrück, 1943). Rearrangements detected with this assay include broken chromosomes healed by *de novo* telomere additions and a range of inter- and intra-chromosomal fusion events (Putnam and Kolodner, 2010). Further, statistical analysis of the observed number of mutants and the number of total viable cells in the experiment allows the estimation of the mutational events across the experiment and the mutation (GCR) rate per cell per generation.

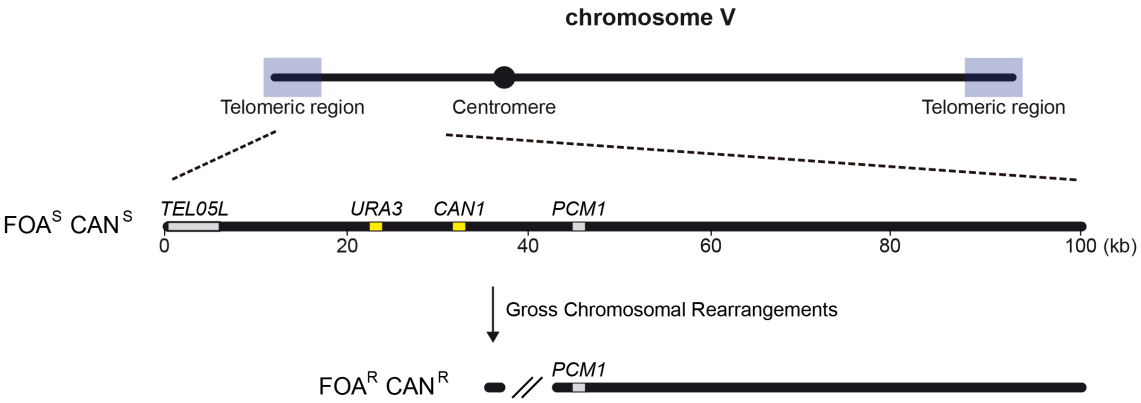

Figure 9: Assay for gross chromosomal rearrangements. The GCR assay measures the rate of simultaneous inactivation of two selective markers, *URA3* and *CAN1* (in yellow), placed on a non-essential end of the yeast chromosome V. Since the strain is haploid, cells cannot lose the entire chromosome V, which harbours many essential genes therefore, breakpoints formation occur between *CAN1* and the first telomere-distal essential gene, *PCM1* (in grey). The GCR rate is estimated from the number of cells resistant to both 5-FOA and L-canavanine (FOA^R CAN^R) that arise from the deletion of both *URA3* and *CAN1* marker genes, since the spontaneous point mutation rate of both markers can be calculated as 10^{12} to 10^{14} per generation, a rate far too low to be detected (Chen and Kolodner, 1999). GCR rates allow the detailed analysis of the contribution of different genes, proteins or pathways in the suppression of genomic instability.

For each GCR assay, at least five independent cultures were inoculated in an appropriate volume of YPAD liquid media (depending on the expected GCR) at a density of 2.5 x 10^5 cells*/* mL (latent phase), from mutant-free freshly growing single colonies cut from a Petri dish. Cells were grown at 25 ºC until stationary phase, usually 32 to 40 h. After that time, cells were counted in a Neubauer chamber to confirm they have reached the stationary phase and to calculate cell concentration and the total cell number per culture. 25 μL of a 1:10,000 dilution of the culture were plated in duplicate on YPAD plates, or YPARG plates for *GAL1-SIC1* cells, and incubated at 25 ºC for 7 days. The number of colonies formed in YPAD or YPARG plates was counted to

calculate the total number of viable cells. To identify yeast mutants carrying both FOA^R and CAN^R mutations, all cells from the remaining culture were collected, washed with sterile water, spread in synthetic minimal FOA-CAN media (see Media and Growth Conditions) at a maximum concentration of 5 x 10^8 cells per 150 mm Petri dish and incubated for 14 days at 25 ºC. After that time, the number of colonies was counted for each independent culture and the GCR rate was determined with the FALCOR software (see Software and Databases), using the MSS-MLE (Foster, 2006; Sarkar et al., 1992).

RESULTS

1. Paucity of initiation events causes chromosomal instability in cells lacking Sic1

It remains unknown if reduced origin activity is a direct cause of genomic instability. In support of this, a strong correlation exists at a chromosome region between the natural loss of origin firing in *sic1* cells and increased rates of GCR (Ayuda-Duran et al., 2014). Also, defective-licensing suppression experiments showed that increasing locally the distribution and density of origins reverts genomic instability (Tanaka and Diffley, 2002). However, no origin firing activity is shown posing the question on if suppression is due to restored origin activity and how. Thus, addressing whether cause-effect relationships apply or are instead unrelated although simultaneous events, is not known but critical to understand what is the molecular mechanism by which genomic instability appear in these cell populations.

To test whether the inefficient usage of origins in cells lacking Sic1 directly causes chromosomal instability, we have genetically manipulated the firing efficiency of individual replication origins within a chromosomal arm and analysed the effect on the GCR rates. Among the few genetic assays of genomic instability described, the GCR assay helped to discover the pathways involved in maintaining genomic stability in budding yeast cells (Chen and Kolodner, 1999; Kolodner et al., 2002). This assay is based on the simultaneous inactivation of two markers (*CAN1* and *URA3*) located on the left arm of chromosome V, and their location is depicted in Figure 10A. Hence, we concentrated on origins within this left arm of chromosome V. Originally designed in yeast cells of the S288C background, for comparative purposes all our following analyses of origin activities and origin manipulations were performed in the original Kolodner's S288C strain (RDKY3615).

Firstly, we studied the normal activity of origins within this chromosome arm. The exact positioning of all confirmed and likely DNA replication origins is known in *S. cerevisiae* cells, as found in several genome-wide studies, and is compiled in the Oridb (http://cerevisiae.oridb.org/). The relative positioning of all known origins in the left arm of chromosome V is shown in Figure 10A. As previously optimised in the group (Ayuda-Duran et al., 2014), we used Sic1-depleted cells (hereinafter referred to as *sic1* cells) to study the firing efficiency of all origins mapped in the first 100 kb of chromosome V by 2D gel analysis, in the first G1-deregulated cell cycle and in wt cells in parallel (see Material and Methods for growth details on wt and *sic1* cells). The activity of *ARS502* was omitted from this study given its localization very close to the telomere (very well conserved regions across chromosomes) that impedes finding a specific probe to this origin.

ARS507 and *ARS508* are the earliest firing origins in chromosome V (Raghuraman et al., 2001) and are very efficient, firing in more than 60% in wt cells (Ayuda-Duran et al., 2014). The 2D-gel analysis of origins *ARS507* and *ARS508* in *sic1* cells shows a firing deficiency of *ARS507* to nearly 30%, as the Y-arc signal is much more intense than the bubble-arc, when compared to the wt, while *ARS508* remains invariant as previously published (Ayuda-Duran et al., 2014) (Figure 10B).

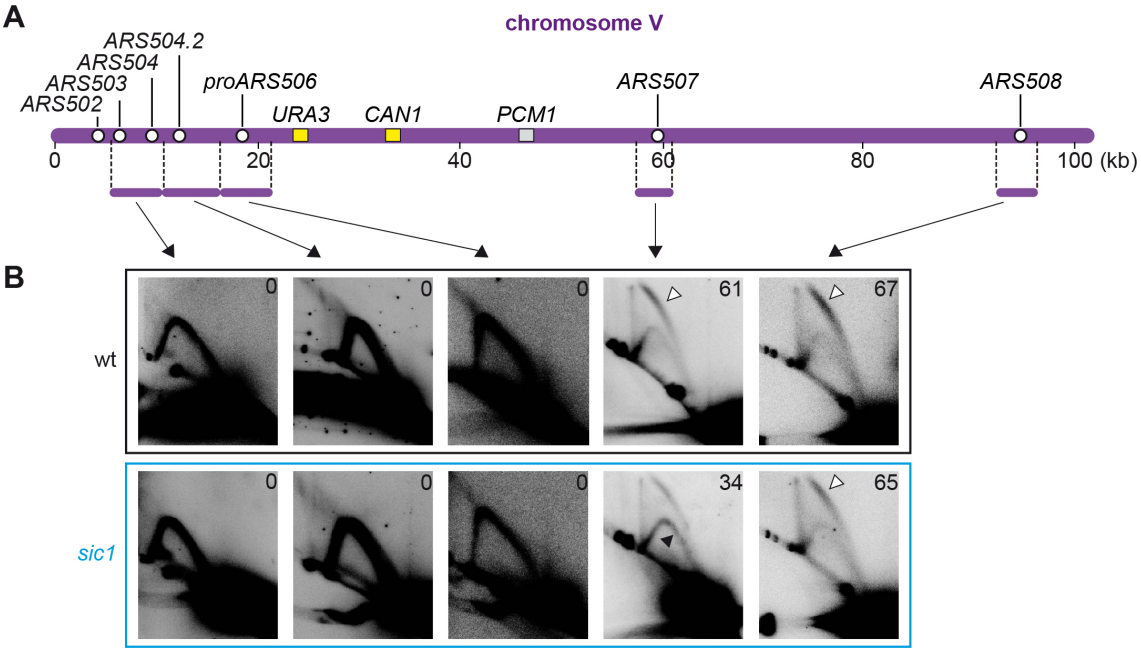

Figure 10: Deficient origin firing on the left arm of chromosome V in *sic1* cells. (A) Schematic view of the first 100 kb of chromosome V left arm. All ARS elements mapped in the region are indicated (open circles), *CAN1* and *URA3* (yellow squares) represent the two markers used for the GCR assay and *PCM1* (grey square) the first telomere-distal essential gene. Horizontal bars flanked by dashed lines represent the restriction fragments analysed. **(B)** 2D gel analysis of the indicated fragments in S288C wt (YAC177, upper panels) and *sic1* (YAC217, lower panels). Restriction enzyme digestions, fragments sizes and probes are described in Material and Methods. Firing efficiencies of origins were estimated from the ratio between intermediates along the bubble-arc and intermediates in the ascending arm of the Y-arc, and are indicated in the upper right corner of each panel. White arrowheads denote efficient origins and black arrowheads indicate loss of origin-firing efficiency.

Regarding the firing of late/dormant origins located at the subtelomeric region, bubble-arcs (active replication) were absent for *ARS503-ARS504*, *ARS504.2* and *proARS506* in both wt and *sic1* cells (Figure 10B), indicating that these origins are silent and probably replicated passively by forks fired from *ARS507*, *ARS508*, or other inner-chromosome origins as previously shown (Raghuraman et al., 2001).

Given the low firing efficiency of *ARS507* in *sic1* cells, we hypothesized if the instability of chromosome V in these cells is caused by the fail of this origin.

1.1 Inefficient firing of early origins causes chromosomal instability in *sic1 cells*

To study the causal contributions of inefficiency of early origins to chromosomal instability in *sic1* cells, we have manipulated the activity of *ARS507*, the most failing origin detected in the region. *ARS507* was deleted or its efficient firing was restored and their effect on chromosomal stability was analysed by measuring GCR rates on both cases. To delete *ARS507* in wt and *sic1* cells, we replaced a 234-bp DNA fragment containing the *ARS* element of the origin by the *KanMX4* marker (see Material and Methods for construction details), to obtain *ars507*Δ and *ars507*Δ *sic1* strains, respectively. Serial dilutions of equal cell numbers showed that the deletion of *ARS507* does not affect cell viability, as *ars507*Δ and *sic1 ars507*Δ cells grew similar to the respective parental strains onto glucose and raffinose galactose plates (Figure 11A). These findings agree with previous studies showing that deletions of different ARS elements had no deleterious effect and caused no change in the growth rate of cells (Dershowitz and Newlon, 1993).

To confirm that the deletion of *ARS507* fully removes origin activity, we studied the firing efficiency of the *ars507*Δ locus by 2D gel analysis in asynchronous *ars507*Δ or *sic1 ars507*Δ cells. As expected, we found that *ARS507* is inactive for firing in *ars507*Δ and *sic1 ars507*Δ cells given the absence of bubble-arcs in blots identifying the *ars507*Δ locus (Figure 11C), thus confirming the complete deletion of the origin. We also observed that no compensatory firing occurs in *ARS508,* as no differences between the bubble- and Y-arcs exist in either wt or *sic1* cells (Figure 11C) regarding the parental strains in Figure 10B, agreeing with *ARS508* firing earlier than *ARS507* (Raghuraman et al., 2001). Consistently with delayed replication of the subtelomeric region in chromosome V by *ARS507* loss, *ars507*Δ cells show bubble-arcs in 2D gel blots of *ARS504.2* and *proARS506*, indicating that those are dormant origins when *ARS507* is present (Santocanale et al., 1999; Vujcic et al., 1999). As these dormant origins fire in a subpopulation of *ars507*Δ cells (Figure 11B), we confirmed that forks emanating from *ARS507* normally replicate the subtelomeric region. This further demonstrates that the likely *proARS506* origin is a confirmed origin, and is hereinafter renamed as *ARS506*. Importantly, in *sic1 ars507*Δ cells, the activity of dormant origins was severely impaired (Figure 12B). Indeed, bubble-arcs remained undetectable in *ARS503-ARS504* and *ARS506* indicating that those origins remained inactive for firing, while in *ARS504.2* a bubble-arc is visible although the intensity is reduced in cells lacking Sic1 (Figure 11C, *sic1 ars507*Δ), regarding the control (Figure 11C, *ars507*Δ). The barely use of dormant origins in *sic1 ars507*Δ cells, compared to *ars507*Δ cells, demonstrates that cells lacking Sic1 fail to activate most of the available dormant origins at the subtelomeric region in response to origin paucity (*ars507*Δ*).* Thus we

conclude than *sic1* cells may misuse dormant origins in late replicating regions in response to a poor distribution and density of early efficient origins.

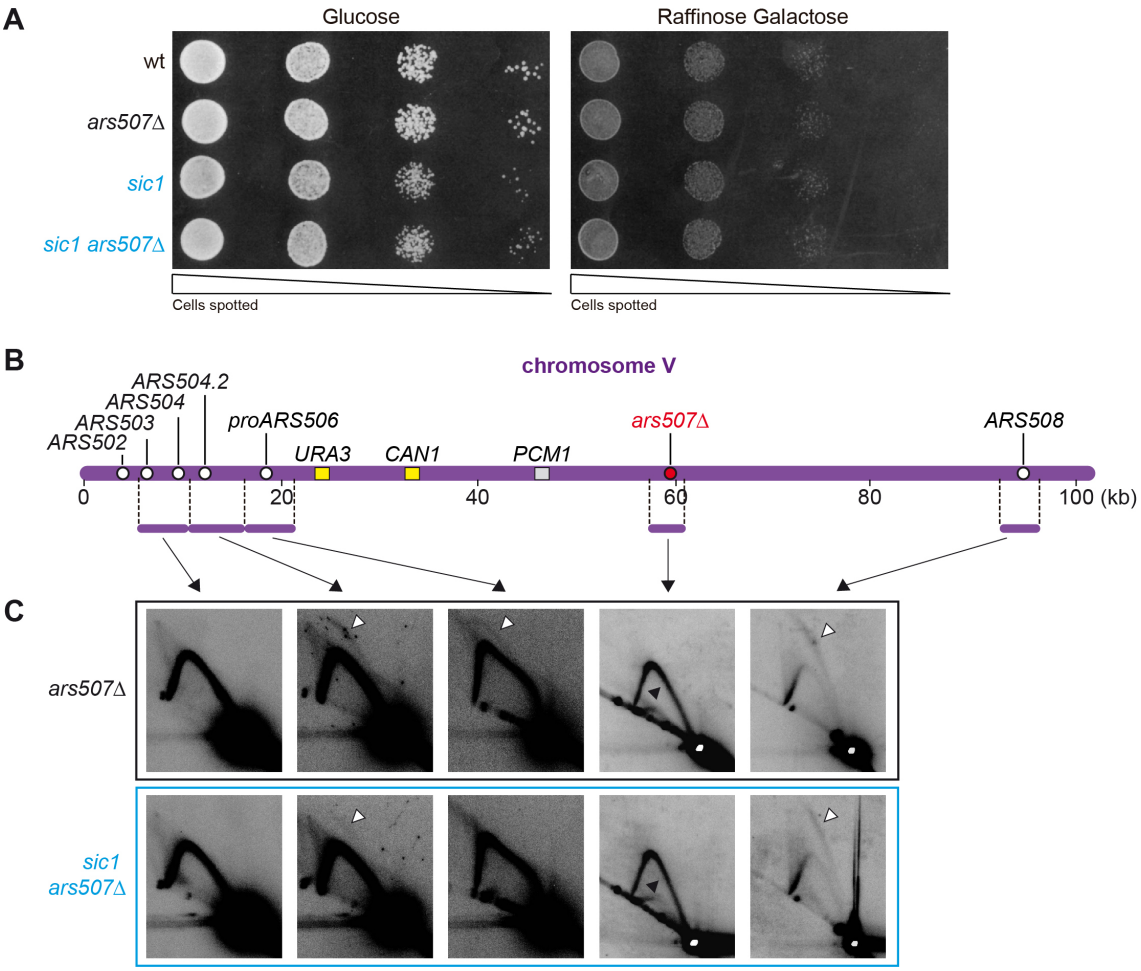

Figure 11: *ars507*Δ removes firing activity to the *ARS507* locus and dormant origins fail to activate in *sic1* cells. (A) Dilution spotting assay of S288C wt (YAC177), *ars507*Δ (YAC556), *sic1* (YAC217) and *sic1 ars507*Δ cells (YAC558). Plates were incubated for 2 days at 25º C and photographed. *GAL1,10p-SIC1* strains (in blue) deplete or moderately overexpress Sic1 onto YPAD (left) or YPARG (right) plates, respectively. **(B)** Schematic view of the first 100 kb of chromosome V left arm. The deletion of *ARS507* is indicated in red. **(C)** 2D gel analysis of the indicated fragments of strains in (A). Restriction enzyme digestions, fragments sizes and probes are described in Material and Methods. Firing efficiencies of origins were estimated as in **Figure 10**. White arrowheads denote efficient origins and black arrowheads indicate loss of origin-firing efficiency.

To increase the firing activity at the *ARS507* locus, we replaced the same 234-bp fragment containing *ARS507* as above, with a 234-bp fragment including *ARS305*, a very well characterized origin on chromosome III of known tolerance to Sic1-dependent CDK deregulation (Ayuda-Duran et al., 2014) (see Material and Methods for construction details). We used the spotting assay to test whether the viability of the newly constructed strains, *ars507*Δ*::ARS305* and *sic1 ars507*Δ*::ARS305*, was affected

Figure 12A) and 2D gel analysis to confirm that *ARS305* insertion restores efficient firing at this locus in *sic1* cells (Figure 12C).

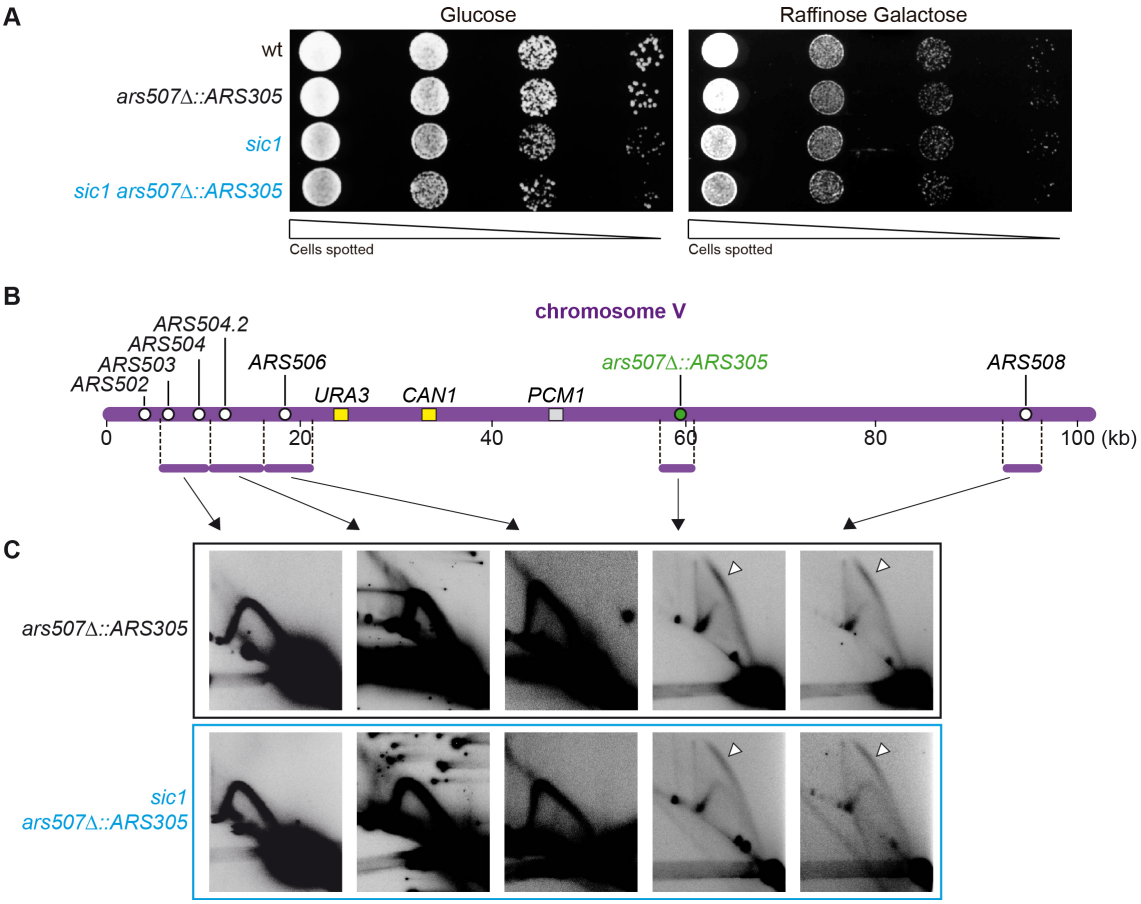

Figure 12: The replacement of *ARS507* by *ARS305* restores firing efficiency to the *ARS507* locus in *sic1* cells. (A) Dilution spotting assay of S288C wt (YAC177), *ars507Δ::ARS305* (YAC899), *sic1* (YAC217) and *sic1 ars507Δ::ARS305* cells (YAC921). Plates were incubated for 2 days at 25º C and photographed. *GAL1,10p-SIC1* strains (in blue) deplete or moderately overexpress Sic1 onto YPAD (left) or YPARG (right) plates, respectively. **(B)** Schematic view of the first 100 kb of chromosome V left arm. The substitution of *ARS507* with *ARS305* is indicated in green. **(C)** 2D gel analysis of the indicated fragments of strains in (A). Restriction enzyme digestions, fragments sizes and probes are described in Material and Methods. Firing efficiencies of origins were estimated as in **Figure 10**. White arrowheads denote efficient origins.

sic1 ars507Δ::ARS305 cells show efficient firing at *ARS305* relocated on chromosome V (Figure 12C), with a higher firing efficiency when compared to *ARS507* in *sic1* cells (compare the relative intensities of bubble- and Y-arcs of *ARS507* in *sic1* cells in Figure 10B). This indicates that the firing efficiency is restored at the *ARS507* locus in *sic1* cells and that our approach is valid.

Then, to address the activity of origins surrounding *ARS305* relocated at the *ars507Δ* locus, we analysed the firing efficiency of *ARS503-504*, *ARS504.2*, *ARS506* and *ARS508* in the same cells by 2D-gel analysis (Figure 12C). We observed that, in all cases, bubble- and Y-arc signals were very similar to natural chromosome V cells

(Figure 10B), showing that the firing efficiencies of all origins within the region was not disturbed after replacing *ARS507* with *ARS305*.

Finally, to address whether the deletion or increased firing efficiency at *ARS507* affected the chromosomal instability of *sic1* cells, we performed the GCR assay on *sic1 ars507*Δ and *sic1 ars507*Δ*::ARS305* strains (see Material and Methods for details on the GCR assay). We found that the GCR rate of *sic1* cells increased to 4.0-fold after deleting *ARS507* (Figure 13, *sic1 ars507*Δ), indicating that the firing inefficiency of this origin strongly affects the stability of the chromosomal arm. Given the simultaneous deficient firing of dormant origins in *sic1* cells, we suggest that both defects contribute to the increase in GCR rates. Strikingly, the GCR rate decreased to 0.3-fold in *sic1* cells when *ARS507* was replaced by *ARS305* (Figure 13, *sic1 ars507*Δ*::ARS305*), indicating that the increase of firing efficiency at *ARS507* strongly suppresses the instability of *sic1* cells. However, the GCR rate is not completely suppressed (0-fold), so we do not discard the possibility that other features might contribute to the chromosomal instability of *sic1* cells, like the failure of dormant origins. Taken together, these results demonstrate that the activity of *ARS507* in *sic1* cells significantly affects the stability of chromosome V left arm and suggests that the failure of dormant origin might also contribute to the instability of the region.

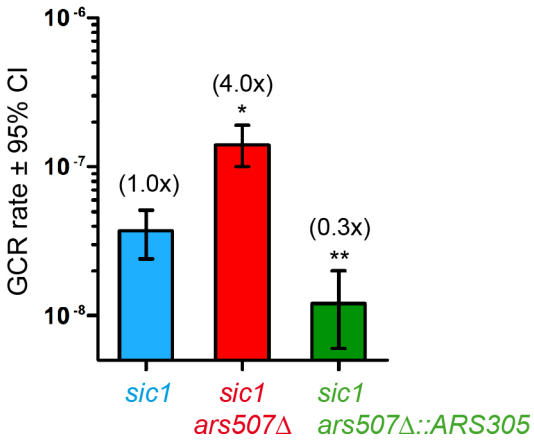

Figure 13: The lack of *ARS507* causes high chromosomal instability to the left arm of chromosome V in *sic1* cells but is significantly suppressed after replacing *ARS507* with *ARS305*. Rates of GCR were determined in at least five independent cultures of S288C wt (YAC177), *sic1* (YAC217), *sic1 ars507*Δ (YAC556) and *sic1 ars507*Δ*::ARS305* (YAC921) cells. The indicated values of GCR rates are per cell per generation. Error bars represent 95% confidence intervals. Asterisks indicate statistical significance: *, p<0.02; **, p<0.001. Numbers in parenthesis denote fold increase with respect to wt.

1.2 Dormant origins firing is defective in *sic1* cells and causes high chromosomal instability

The incapacity of most *sic1* cells to activate dormant origins when *ARS507* is deleted suggests that inefficient activity of dormant origins may occur and contribute to chromosomal instability in *sic1* cells. To test this hypothesis, we studied the role of dormant origins in the chromosomal instability of *sic1* cells by either deleting or increasing firing efficiency from dormant origins, and measured the GCR rate in both cases. We chose *ARS504.2*, the most efficient dormant origin in *ars507*Δ cells (Figure 11C) and the only dormant origin with detectable activity in *sic1 ars507*Δ cells (Figure 11C). To delete *ARS504.2*, we replaced a 2505-bp DNA fragment containing the ARS sequence by the *LEU2* marker in wt and *sic1* cells, to obtain *ars504.2*Δ and *sic1 ars504.2*Δ cells, respectivelly (see Material and Methods for construction details). Using the spotting assay, we confirmed that the viability of the newly constructed strains was not affected (Figure 14A).

Then, we studied the firing efficiency of origins on chromosome V left arm by 2D gels in these cells. We observed that bubble-arcs at the *ars504.2*Δ fragment were not detected in *ars504.2*Δ or *sic1 ars504.2*Δ cells (Figure 14C) indicating absence of active firing at this locus, thus we concluded that *ARS504.2* was efficiently deleted. At *ARS507* and *ARS508*, we observed similar differences in efficiency between control and *sic1* cells regarding parental strains (compare Figure 14C with Figure 10B). Interestingly, the lack of bubble-arcs at *ARS503/ARS504* and *ARS506* denotes the absence of firing activity in both strains (Figure 14C), indicating that they were not required to compensate the deletion of *ARS504.2*. Although we do not discard the possibility of bubble-arc signals were below the threshold detection levels, we can conclude that the firing activity of dormant origins in *sic1 ars504.2*Δ cells did not increased with respect to *sic1* cells (Figure 10B) to compensate the loss of *ARS504.2*.

In parallel, to increase the firing activity at the *ARS504.2* locus we substituted the same 2505-bp fragment as above, by a fragment of 234 bp containing *ARS305* flanked by the *LEU2* marker (see Material and Methods for construction details). Although this construction did not affect cell viability (Figure 16A) bubble-arcs were undetectable at the *ars504.2*Δ*::ARS305* locus when analysed by 2D gels (Figure 16C) indicating that *ARS305* is inactive when relocated at the subtelomeric region, possibly because of its proximity to the end of the chromosome (Ferguson and Fangman, 1992). Thus, we considered the approach invalid.

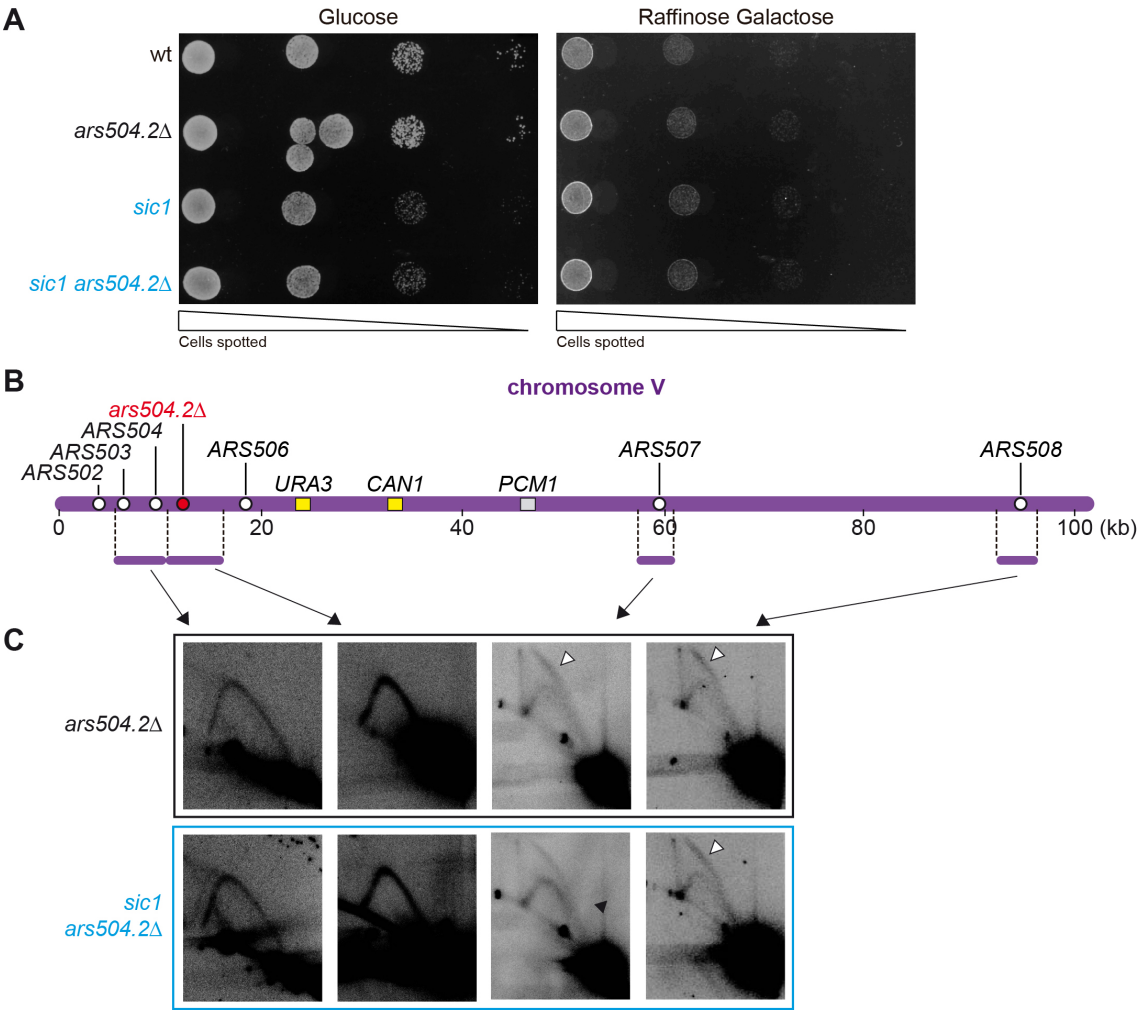

Figure 14: The usage of origins on chromosome V left arm remains unaffected after deleting *ARS504.2*. (A) Dilution spotting assay of S288C wt (YAC177), *ars504.2*Δ (YAC1024), *sic1* (YAC217) and *sic1 ars504.2*Δ cells (YAC1377). Plates were incubated for 2 days at 25º C and photographed. *GAL1,10p-SIC1* strains (in blue) deplete or moderately overexpress Sic1 onto YPAD (left) or YPARG (right) plates, respectively. **(B)** Schematic view of the first 100 kb of chromosome V left arm. The deletion of *ARS504.2* on chromosome V is indicated in red. **(C)** 2D gel analysis of the indicated fragments of strains in (A). Restriction enzyme digestions, fragments sizes and probes are described in Material and Methods. Firing efficiencies of origins were estimated as in Figure 11. White arrowheads denote efficient origins and black arrowheads indicate loss of origin-firing efficiency.

As an alternative approach, we took advantage of the previously described integration of a plasmid containing multiple origins at the *SIT1* locus, a gene localized between the *URA3* and *CAN1* markers on chromosome V (Tanaka and Diffley, 2002) (Figure 16B). The authors of this study inserted a plasmid containing a tandem of seven origins *ARSH4* (*7xARSH4*) (Hogan and Koshland, 1992) at *SIT1* in budding yeast cells overexpressing the G1-cyclin Cln2 to significantly decrease GCR rates and suggest that its instability was due to low origin activity (Tanaka and Diffley, 2002). Following this rationale, we constructed the plasmid *pRS305-7xARSH4* and integrated a single copy at *SIT1* to obtain isogenic control *7xARSH4* and *sic1 7xARSH4* cells (see

Material and Methods for construction details). The same plasmid without origins was used as a control and integrated at the same locus to obtain control *empty* and *sic1 empty* cells. In any case, the viability of the strains was affected (Figure 16A).

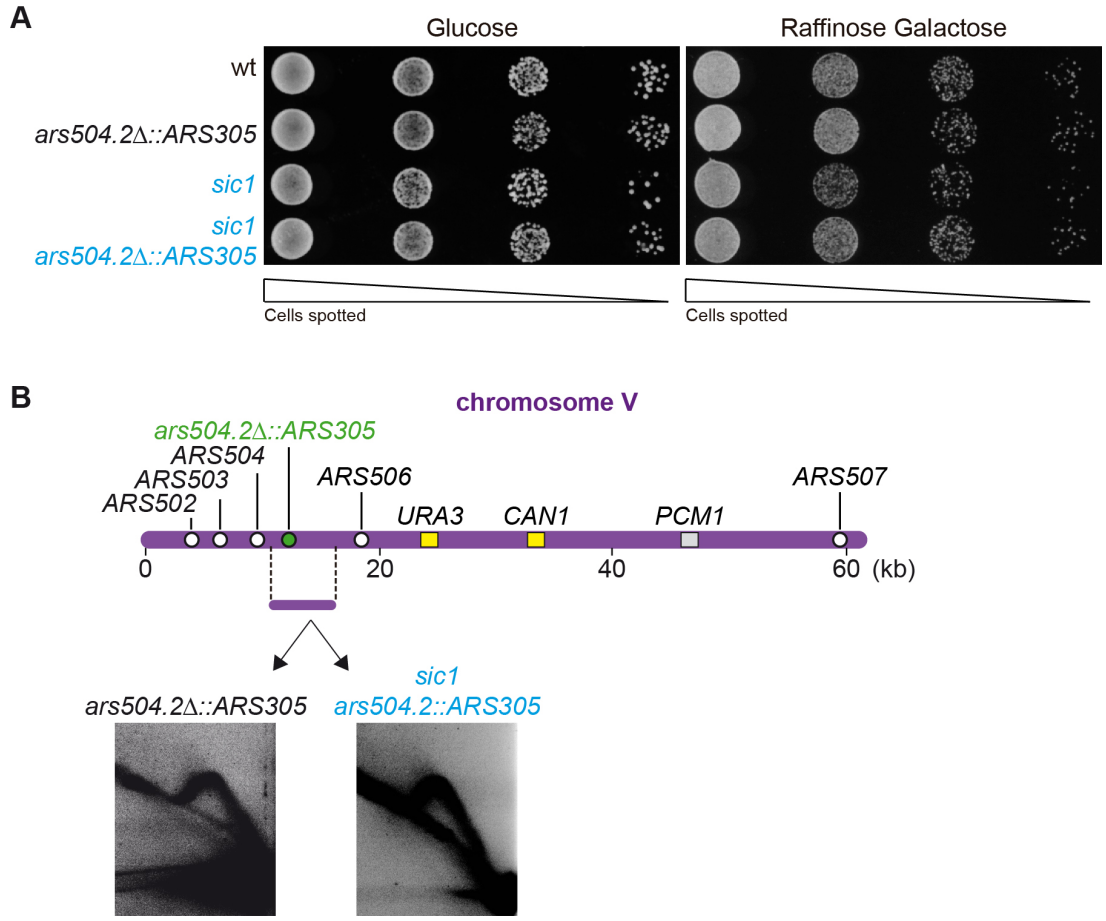

Figure 15: *ARS305* relocated at the *ars504.2*Δ locus is inactive for firing. (A) Dilution spotting assay of S288C wt (YAC177), *ars504.2Δ::ARS305* (YAC1302), *sic1* (YAC217) and *sic1 ars504.2Δ::ARS305* cells (YAC1323). Plates were incubated for 2 days at 25º C and photographed. *GAL1,10p-SIC1* strains (in blue) deplete or moderately overexpress Sic1 onto YPAD (left) or YPARG (right) plates, respectively. **(B)** Schematic view of the first 100 kb of chromosome V left arm. The substitution of *ARS504.2* with ARS305 is indicated in green. **(C)** 2D gel analysis of the indicated fragment of strains in (A). Restriction enzyme digestion, fragment size and probe are described in Material and Methods.

To analyse whether the multiple origins were active, we analysed the presence of bubble-arcs within the plasmid *pRS305-7xARSH4* or the control *pRS305-empty* 2D-gel analysis in control and *sic1* cells (Figure 16C). Importantly, the tandem of origins remained silent in control cells, but in *sic1* cells a bubble-arc was detected denoting active replication, so we concluded that the tandem of origins functions as dormant origins. This result indicates the need of dormant origins in *sic1* cells, but not in control cells, and strongly suggests that replication is delayed at the subtelomeric region in *sic1* cells.

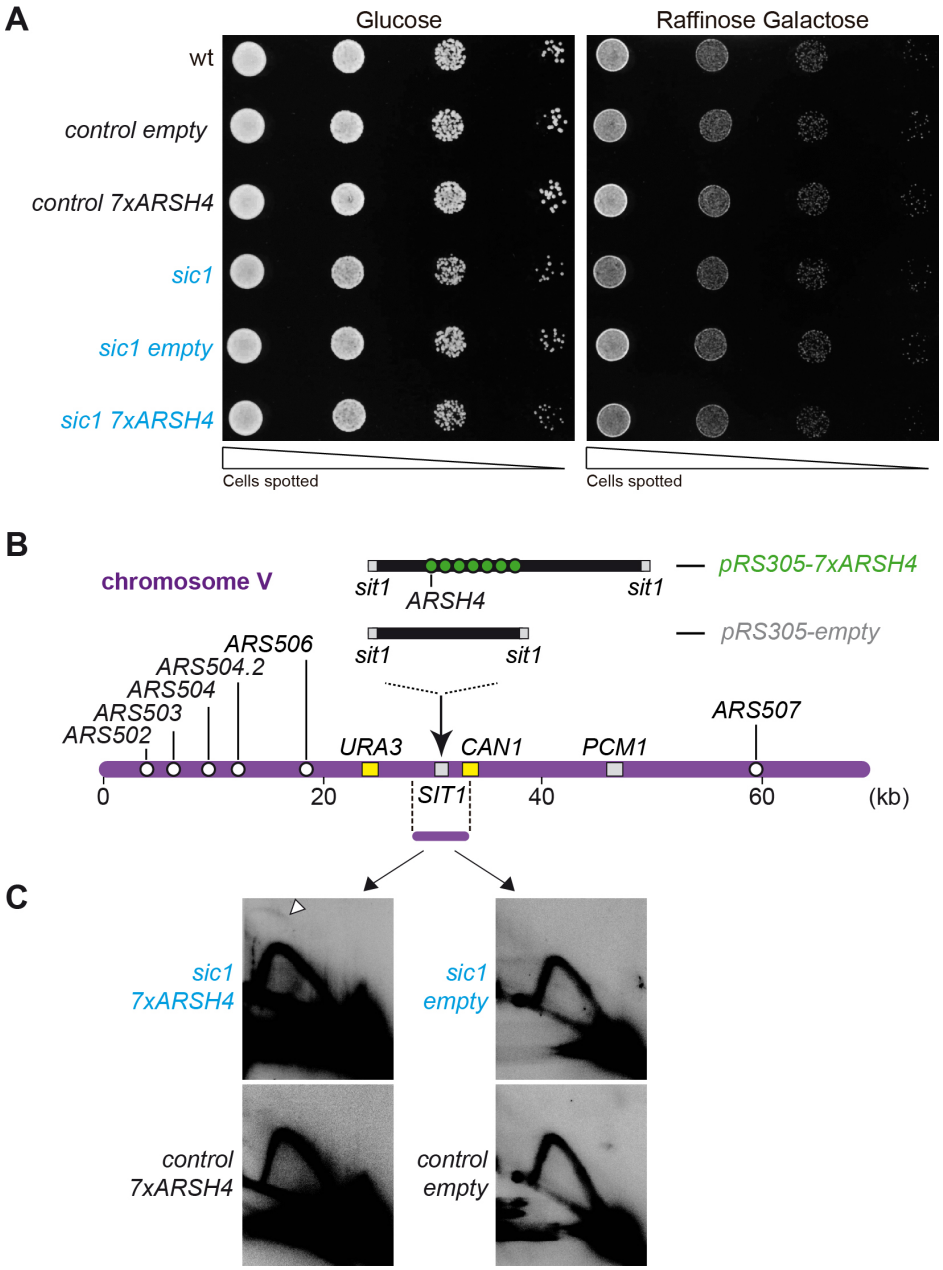

Figure 16: A tandem of origins (*7xARSH4)* integrated in the left arm of chromosome V remains dormant in control cells but fires in *sic1* cells. (A) Dilution spotting assay of S288C wt (YAC177), control *empty* (YAC1286), control *7xARSH4* (YAC1394), *sic1* (YAC217), *sic1 empty* (YAC1290) and *sic1 7xARSH4* cells (YAC1399). Plates were incubated for 2 days at 25º C and photographed. *GAL1,10p-SIC1* strains (in blue) deplete or moderately overexpress Sic1 onto YPAD (left) or YPARG (right) plates, respectively. (B) Schematic view of the first 100 kb of chromosome V left arm. The integration of the plasmid containing the tandem of origins (*pRS305-7xARSH4*) or the empty plasmid (*pRS305-empty*) at *SIT1* is indicated in green and grey, respectively. (C) 2D gel analysis of the indicated fragment of strains in (A). Restriction enzyme digestions, fragments sizes and probes are described in Material and Methods. Firing efficiencies of origins were estimated as in **Figure 10**. The white arrowhead denotes origin firing.

We then tested whether the deletion of *ARS504.2* or the increased firing of the tandem of dormant origins *7xARSH4* integrated at the subtelomeric region influences the chromosomal instability of *sic1* cells, using the GCR assay. The deletion of

ARS504.2 in *sic1* cells resulted in a significantly 3.0-fold increased in the GCR rate with respect to *sic1* cells (Figure 17, *sic1 ars504.2*Δ) showing that the loss of this dormant origin severely affects the stability of this chromosome arm. This is a surprising result as no active firing of *ARS504.2* was detected in *sic1* cells (Figure 10B), except if its firing activity is below the threshold of detection by 2D gels. Hence, there is a strong potential for the loss of dormant origins in causing chromosome instability in *sic1* cells. Furthermore, the fact that the GCR rate of *sic1 ars504.2*Δ cells is very similar to that of *sic1 ARS507*Δ cells (see Figure 13) indicates that the loss of dormant origins in *sic1* cells threatens the chromosome stability similarly to losing early efficient origins. Moreover, supporting this idea, the insertion of multiple origins at the subtelomeric region almost completely suppressed the GCR rate in *sic1* cells (Figure 17, 0.3x in *sic1 7xARSH4* compared to 1.4-x in the *sic1 empty*). Therefore we conclude that the loss of dormant origin activity in *sic1* cells is a contributing cause of genomic instability in these cells.

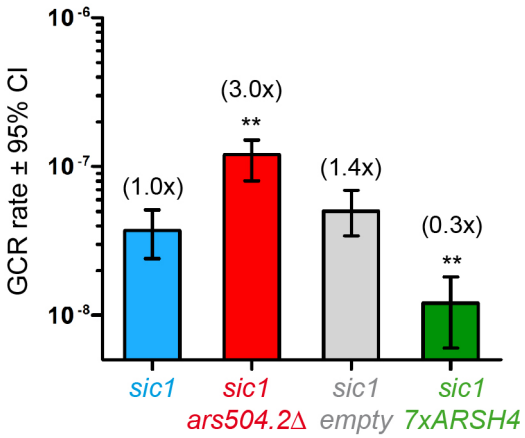

Figure 17: Dormant origin firing is critical to prevent the chromosomal instability in *sic1* cells. Rates of GCR were determined in at least five independent cultures of S288C wt (YAC177), *sic1* (YAC217), *sic1 ars504.2*Δ (YAC1377), *sic1 empty* (YAC1290) and *sic1 7xARSH4* (YAC1399) cells. The indicated values of GCR rates are per cell per generation. Error bars represent 95% confidence intervals. Asterisks indicate statistical significance: **, p<0.001. Numbers in parenthesis denote fold increase with respect to wt.

Taken all together, our data demonstrates that during the first cell cycles after the loss of Sic1, cells spontaneously suffer from a paucity of initiation events in both early efficient and late/dormant origins that, together, caused elevated rates of chromosomal instability. Thus, instead of a simple paucity of origin numbers, our findings are more consistent with the genomic instability in *sic1* cells resulting from the fail of origins to be redundant locally and deficient to compensate adjacent origins loss. Also, it is possible that the lack of functional origin redundancy of early and late/dormant origins may

result in replication completion problems according to the origin redundancy model (Hyrien et al., 2003; Rhind, 2006).

2. Sic1 is critical for timely completion of DNA synthesis specifically at regions of deficient origin activity

We found that the limited pools of active origins in *sic1* cells cause chromosomal instability. But what is the molecular mechanism by which the paucity of replication initiation events ultimately causes genomic instability in *sic1* cells? Different studies have found that S phase is disturbed in cells lacking Sic1: S phase entry occurs prematurely, DNA replication initiates from fewer origins causing larger inter-origin distances and completion of S phase is prolonged (Lengronne and Schwob, 2002; Nugroho and Mendenhall, 1994; Schwob et al., 1994). Based on this observations, a model was proposed to explain the *sic1*'s instability including chromosomal regions replicating abnormally late in S phase due to less active origins and enter mitosis with still on-going replication so that attempts to segregate unresolved sister chromatids could lead to chromosome breaks during anaphase, ultimately causing genomic instability (Lengronne and Schwob, 2002). However, this model lacks of experimental support. Our findings of origin redundancy failure in *sic1* cells suggest that the loss of origin efficiency and redundancy might delay replication completion at genomic regions of high instability. To test this hypothesis at the molecular level, we analysed the DNA replication dynamics in *sic1* cells at several genomic regions, including the left arm of chromosome V, and compared it with the same analysis in control cells.

2.1 Completion of bulk DNA synthesis is delayed at the left end of chromosome V in *sic1* cells

Our strategy was to synchronise cultures of wt and *sic1* cells and follow the DNA synthesis along S phase to study the replication defects of cells lacking Sic1. Classically, to study S phase, cells are synchronised in the G1 phase by alpha-factor block-and-release. However, we found that this approach artificially lengthens the G1 phase and suppress origin-firing defects in *sic1* cells (data not shown), invalidating the strategy. As an alternative, we introduced the *cdc15-2* thermo sensitive mutation in W303-1a wt and *sic1* strains (see Material and Methods for construction details). The Cdc15 protein kinase of the mitotic exit network is required for efficient activation of the Cdc14 phosphatase, in turn required for complete CDK inactivation necessary for mitosis exit and entrance in the G1 phase. At the restrictive temperature (37 ºC), *cdc15-2* mutant cells arrest uniformly in late anaphase/telophase with a dumbbell morphology, large anaphase spindles and high activity of M-CDK, immediately before

the initiation of the G1 phase and the origin-licensing period. When switched to the permissive temperature (23 ºC), cells exit mitosis synchronously and perform a synchronous S phase (Futcher, 1999; Yeong et al., 2000).

We examined the phenotype of wt and *sic1* cells carrying the *cdc15-2* mutation (hereinafter referred as "control" and "*sic1"*, respectively). We confirmed that the viability was unaffected at the permissive temperature, regarding the parental strains, (Figure 18A, plates at 25 ºC) and, as expected, all clones carrying the *cdc15-2*^{ts} mutation fail to grow at the restrictive temperature (Figure 18A, plate at 32 ºC)

We designed synchronous *cdc15-2* block-and-release cultures of control and *sic1*, and refined the experiment so that we can study the dynamics of DNA synthesis in the first cycle after Sic1 depletion (Figure 19B). Basically, log phase cultures of control and *sic1* cells grown in raffinose-galactose media were arrested in G2/M with Noc for 3.5 hours at 25 ºC, shifted to glucose media in the presence of Noc for 90 additional minutes to deplete Sic1 in *sic1* cells, and then released from Noc at 37 ºC for 3.5 hours to block cells at the *cdc15-2* arrest point. Cells were then released at 23ºC and samples for 2D-Gel analysis of control and *sic1* cells were collected at six time points (20, 40, 55, 70, 85 and 100 minutes) covering G1 and S phase. Additional samples were taken at specific time points to monitor cell synchrony by tubulin immunofluorescence microscopy and Sic1 protein levels (Figure 18B-D).

The kinetics of release from the *cdc15-2* arrest was followed in control and *sic1* cells by tubulin staining and scored for anaphase spindles at different time points (Figure 18C). Consistent with the spindle dynamics, we observed that Sic1p accumulated at 20-, 30- and 40-min in the control (Figure 18E), indicative of cells being in G1 phase and disappeared in the subsequent time points, agreeing with cells entering synchronically into S phase in agreement with Sic1 stability (Nash et al., 2001). In *sic1* cells, Sic1p was detected in log phase raffinose-galactose-grown cells (Figure 18E, As.), as expected for cells overexpressing *SIC1*. After shifted to glucose-media, Sic1p remained undetectable in *sic1* cells (Figure 18E, Noc and the remaining of the experiment), as expected, indicating that Sic1p was largely depleted from *sic1* cells during the experiment.

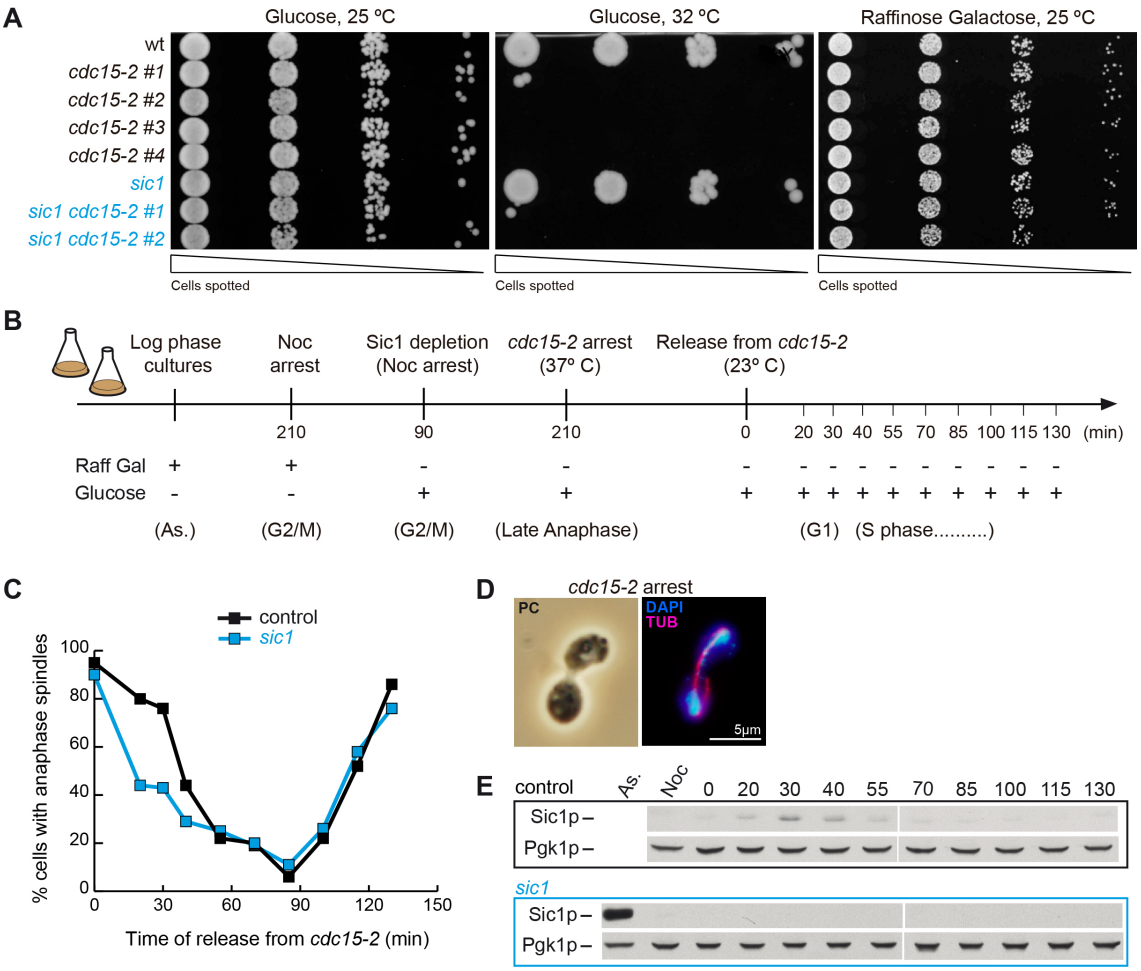

Figure 18: Synchronous S phase of control and sic1 cells by sequential nocodazole-and-cdc15-2 block-and-release. (A) Dilution spotting assay. Phenotype of several clones of W303-1a control (*cdc15-2* #1-4) and *sic1* (*sic1 cdc15-2* #1-2) carrying the *cdc15-2* mutation. **(B)** Outline of the experiment (see Material and Methods for details). Numbers represent the time of arrest at each block (in minutes) and time points at which control (YAC1104) and sic1 (YAC1107) were harvested and analysed after released from the cdc15-2 arrest. (+) and (-) indicate the presence of absence of raffinose-galactose (Raff Gal) or glucose in the growing media, during the experiment. **(C)** The release from the cdc15-2 arrest was monitored by microscopic examination of tubulin immunofluorescence on fixed cells at the time points indicated in A. The percentage of cells with long spindles (>4 μm, late-anaphase/telophase), indicative of the cdc15-2 arrest, was determined by scoring 100 cells per time point. **(D)** Phase contrast (PC), tubulin immunofluorescence (TUB) and nuclear staining (DAPI) show the late-telophase arrest characteristic of cdc15-2 cells. **(E)** Protein levels of Sic1 were examined by Western blotting analysis, harvesting asynchronous log phase cells in Raff-Gal media (As.), noc-arrested cells in glucose media (Noc Glu) and at the indicated time points after the released from the cdc15-2 arrest. Pgk1 was used as loading control.

The analysis of DNA replication dynamics on the left arm of chromosome V allows studying the relationship between completion of bulk DNA synthesis and the stability of the region. We used 2D gels to follow the progression of DNA synthesis during S phase along the first 100 kb of chromosome V, and paid attention to the timing of origin firing, the rate of fork progression, the time profile of bulk DNA-synthesis completion, and the activity of early-efficient and late/dormant origins. For this analysis, RI of control and *sic1* cells were isolated, resolved in 2D gels, transferred

to membranes and sequentially hybridized in parallel against six fragments covering the left arm of chromosome V, from the early *ARS508* origin up to the chromosome end (Figure 19 for control cells and Figure 20 for *sic1* cells).

In control cells, at 20-min, no RIs were detected above background, denoting absence of replication, consistent with cells undergoing G1 phase as confirmed by Sic1p levels (Figure 19B). At 40-min, bubble-arcs were detected at *ARS507* and *ARS508* denoting initiation of active replication and S phase. Since very faint passive Y-arcs were detected at these origins and no forks are visible at short distance (20 kb, *SOM1* fragment), this cell population is very early in S phase. We conclude that replication of the 100 kb of chromosome V left arm initiates efficiently at *ARS508* and *ARS507*, agreeing with previous studies that have identified those origins as the earliest within the whole chromosome V (Raghuraman et al., 2001).

Analysing the replication of the *ARS508* fragment, the maximum bubble-arcs signals were observed at 40- and 50-min, while at 85- and 100-min, RI were practically absent consistent with a synchronous replication in these conditions, and with bulk DNA synthesis being completed by 100 minutes (see quantification in Figure 21).

The replication of the *ARS507* fragment mimics the replication dynamics of *ARS508*. However, differences in the firing timing of both origins were observed. Bubble-arcs in the *ARS507* fragment appear at 40-min although the maximum signal was detected at 55-min, while for *ARS508*, the maximum signal was observed at 40-min (Figure 20B), indicating that the overall firing timing of ARS507 is about 15 minutes later than ARS508, consistent with *ARS508* being earlier in firing than *ARS507* as published (Raghuraman et al., 2001) and validating our replication kinetics.

The analysis of the *SOM1* fragment (Figure 19B) allowed the detection of progressing replication forks from *ARS507* or *ARS508* moving to the telomere. Contrary to *ARS507* and *ARS508* fragments, only Y-arcs were detected in the *SOM1* fragment, indicating passive replication, an expected result since no origin was identified within this fragment. The maximum Y-arc signals were observed at 70-min and, by 100-min, bulk replication is completed (Figure 21, control).

The replication of the subtelomeric region (*ARS503-504*, *ARS504.2* and *ARS506*) was very similar to the replication timing of the *SOM1* fragment, and most replication occurs by 70-min and by 100-min, bulk DNA synthesis of this region was largely replicated (Figure 19C and Figure 21, control). Consistent with *ARS504.2* and *ARS506* being late origins, overexposed blots revealed weak bubble-arc signals by 70-min (Figure 19C) and agreeing with control cells relying on these origins to assist early-efficient origins in completing replication of the late-replicating subtelomeric region as part of the replication program.

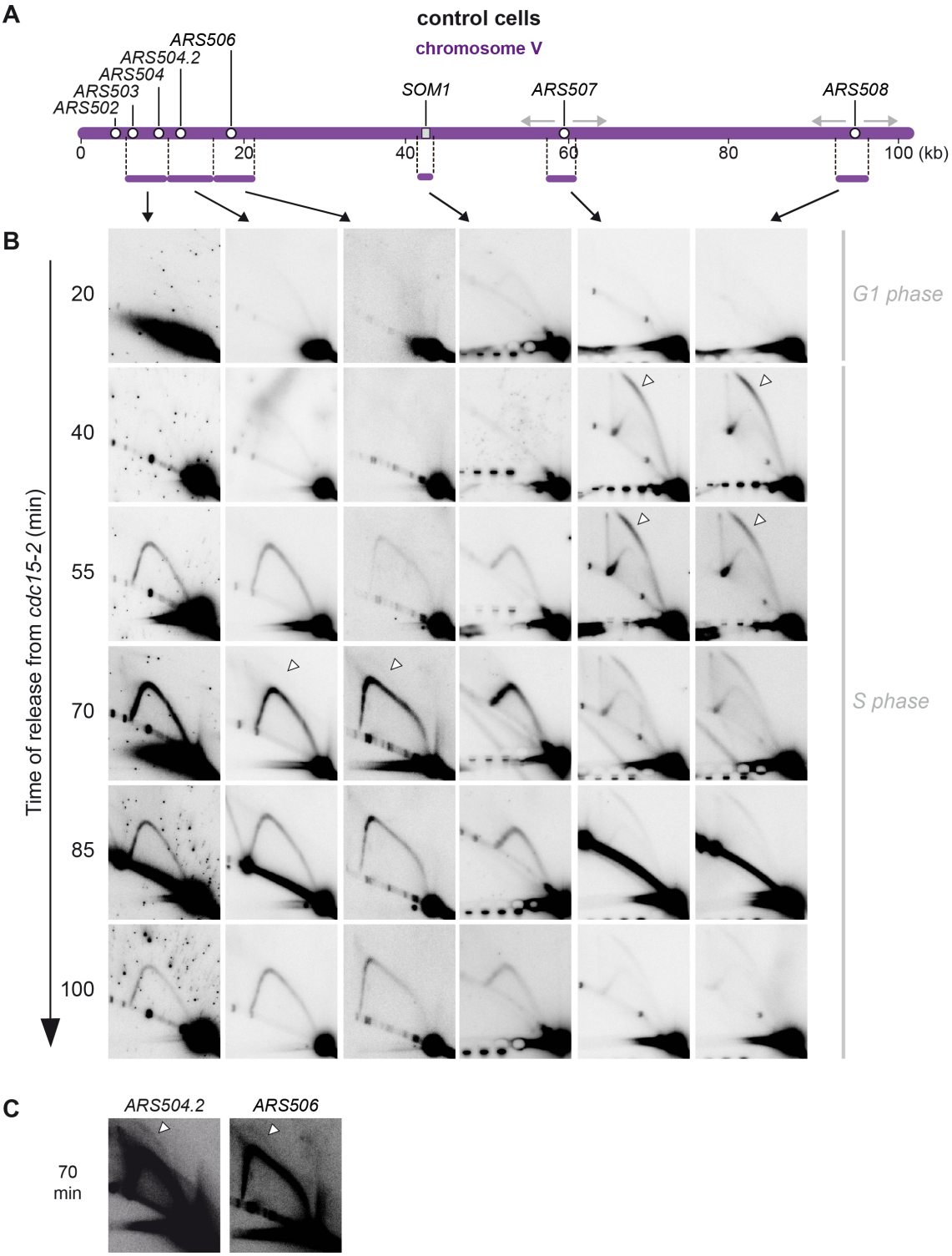

Figure 19: Dynamics of DNA replication of the left arm of chromosome V in control cells. W303-1a control cells (YAC1104) were synchronously released from the cdc15-2 arrest into the cell cycle at 23 ºC. Cells were harvested at the indicated time points after the release and processed for 2D-gel analysis. **(A)** Schematic view of the first 100 kb of chromosome V left arm. All ARS elements mapped in the region are indicated (open circles). Grey arrows denote fork movement fired from the earliest origins in the region. Horizontal bars flanked by dashed lines represent the restriction fragments analysed. **(B)** 2D gel analysis of replication intermediates along the indicated fragments. Restriction enzyme digestions, fragments sizes and probes are described in Material and Methods. White arrowheads denote origin-firing activity. **(C)** Overexposed blots of ARS504.2 and ARS506 from B, at the indicated time point.

In *sic1* cells, we found differences in the replication dynamics of chromosome V left arm from control cells (Figure 20B). Bubble-arcs (active replication) were found at 40-min in *ARS507* and *ARS508* fragments, the maximum-active replication achieved by 55- or 40- to 55-min respectively, as in control cells, and no passive replication at the flanking *SOM1* fragment, indicating no delayed timing of origin firing and good replication synchrony in *sic1* cells. Strikingly, the replication dynamics of these early origins differed in respect to control. Y-arcs enriched differentially in *sic1* cells by 70-, 85- and 100-min blots, indicating that these loci were replicated passively and later than in control cells where Y-arcs were practically absent (compare with blots in Figure 19B). This result agrees with previous data showing inefficient firing at *ARS507* in cells lacking Sic1 (Ayuda-Duran et al., 2014) (Figure 11B), and is consistent with delayed replication dynamics of these loci by deficient origin firing. Also importantly, replication of the left subtelomeric region at chromosome V was abnormal in *sic1* cells. Although most replication of *ARS503-504*, *ARS504.2* and *ARS506* fragments occurred synchronously in *sic1* and control cells (70-min) (see quantification in Figure 21), a prevalence of replication intermediates was observed at later time-points (100-min) in *sic1* cells. These findings indicate that the chromosome end replicated asynchronously in the *sic1* cell population so that some *sic1* cells retain this region unreplicated in contrast to control cells. This defect is further contributed by deficient activity of the late *ARS504.2* and *ARS506* origins (Figure 20B) regarding control cells (see Figure 19B for comparison). Since the prevalence of replication intermediates at later time points is also observed at *SOM1* and *ARS507* fragments in *sic1* cells, although with less intensity, but not at the *ARS508* fragment, it shows that regions of delayed replication in *sic1* cells coincides spatially with areas of origins losing firing efficiency.

Finally, another difference observed with respect to control replication dynamics was the replication of the *SOM1* fragment that in *sic1* cells initiated earlier (at 55-min) than in Control cells (at 70-min) but, remarkably, the maximum replication intermediates signals were detected at 55- and 70-min, with equal intensity, while in Control cells the maximum signal was observed at a single time point (70-min). This result confirm that the replication of the *SOM1* fragment is not synchronic within the *sic1* cell population, probably because part of *sic1* cells fail to fire *ARS507* and, consequently, the *SOM1* fragment is replicated later by forks coming from *ARS508* that is located far more distant (~50 kb), compared to *ARS507* (~20 kb).

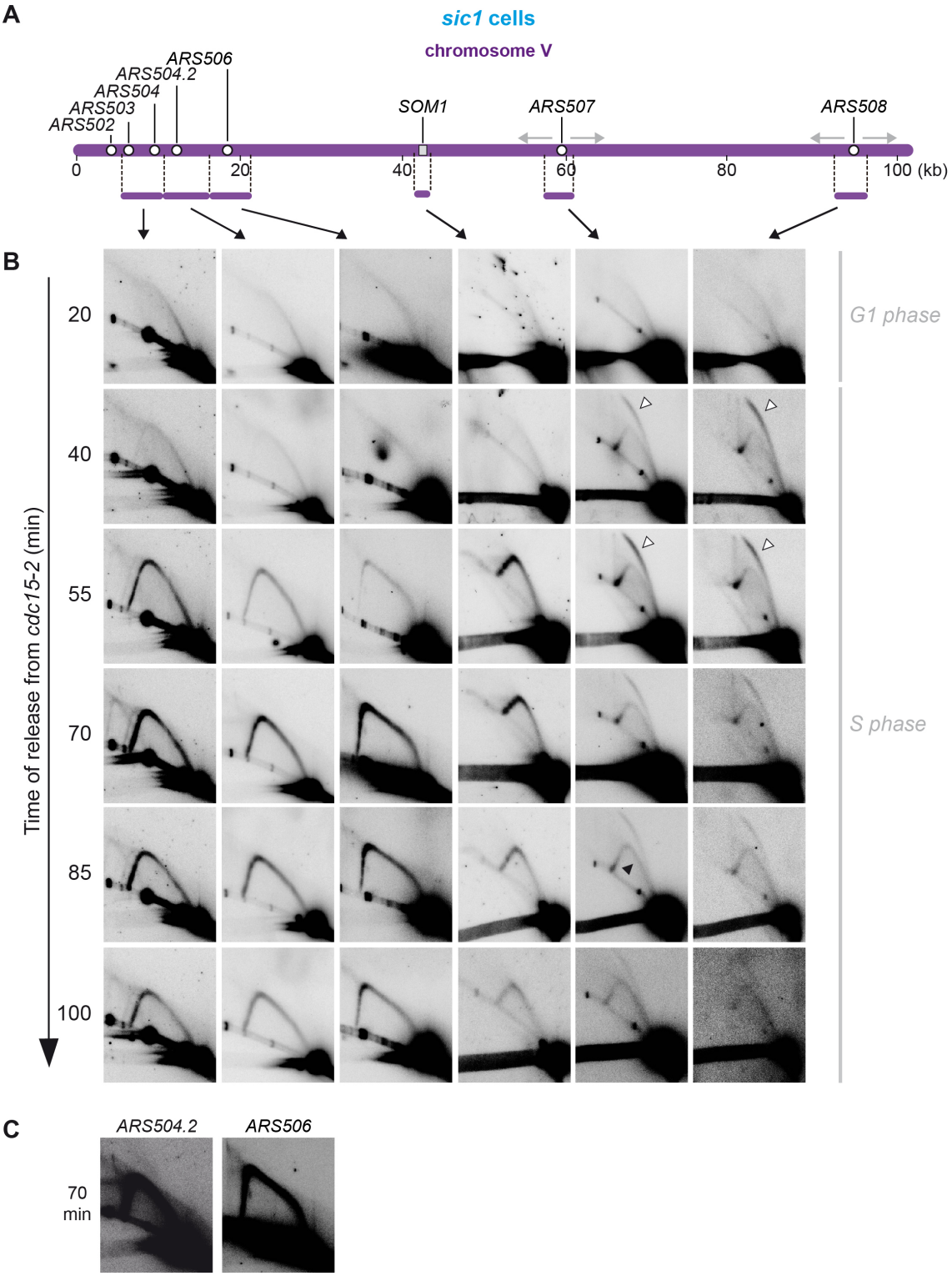

Figure 20: Dynamics of DNA replication of the left arm of chromosome V in sic1 cells. W303-1a sic1 cells (YAC1107) were synchronously released from the *cdc15-2* arrest into the cell cycle at 23 ºC. Cells were harvested at the indicated time points after the release and processed for 2D-gel analysis. **(A)** Schematic view of the first 100 kb of chromosome V left arm. All ARS elements mapped in the region are indicated (open circles). Grey arrows denote fork movement fired from the earliest origins in the region. Horizontal bars flanked by dashed lines represent the restriction fragments analysed. **(B)** 2D gel analysis of replication intermediates along the indicated fragments. Restriction enzyme digestions, fragments sizes and probes are described in Material and Methods. White arrowheads denote origin-firing activity. **(C)** Overexposed blots of *ARS504.2* and *ARS506* from B, at the indicated time point.

Finally, fork progression is normal during the first steps of S phase and forks reach the chromosome end with similar timing in control and *sic1* cells (Figure 21).

Overall, these results confirm that in *sic1* cells the programme of DNA synthesis at the left arm of chromosome V is normal in the timing of origin firing and fork progression rates, but delayed in completion as an outcome of the inefficient use of dormant origins and the loss of efficiency of the early-firing origin *ARS507*.

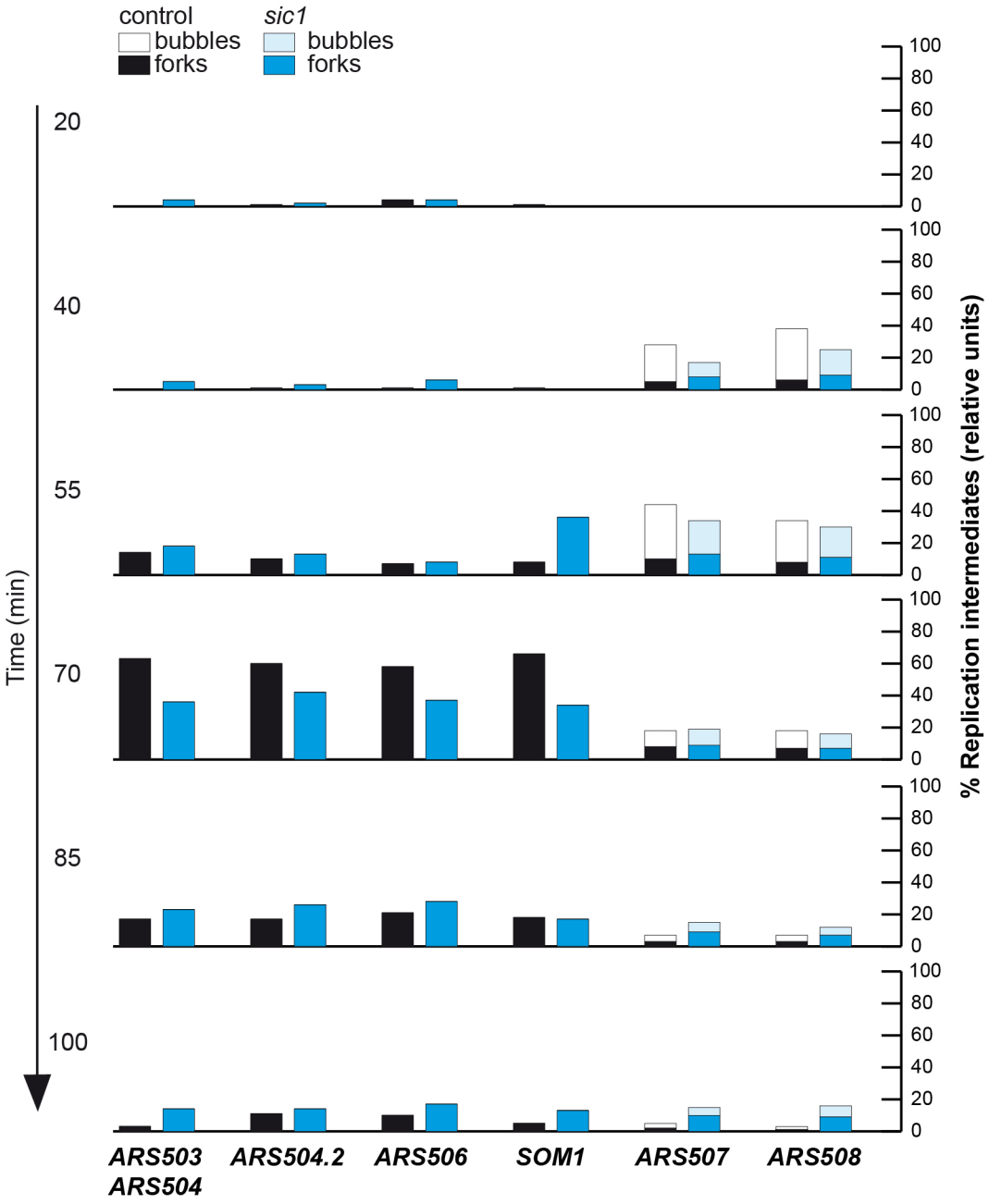

Figure 21: Delayed replication completion enrich specifically at regions of deficient origin firing in chromosome V. Histograms show the quantification of replication intermediates signals on 2D-gel membranes (bubble- and Y-arcs) in **Figure 19** and **Figure 20**, at the indicated time points (calculated as described in Material and Methods).

2.2 Normal timing of DNA synthesis at the left subtelomeric region of chromosome III in *sic1* cells

To confirm if the delay in DNA synthesis completion in *sic1* cells is specific of chromosome regions of deficient origin firing, a general feature to all chromosomes, or alternatively a particularity of chromosome V, we analysed the dynamics of DNA synthesis on the left arm of chromosome III were the efficiency of *ARS305* and *ARS306* is known in these cells (Ayuda-Duran et al., 2014).

Analogously to chromosome V, the first 100 kb of chromosome III contain several dormant origins distributed within the telomeric and subtelomeric region (*ARS300*, *ARS301*, *ARS302*, *ARS320*, *ARS304*) and two very early origins, one of them nearly resistant to CDK deregulation (*ARS305*) and the other very sensitive to CDK deregulation (*ARS306*) (Figure 24B) (Ayuda-Duran et al., 2014). Notably, in this region the origin that looses efficiency in *sic1* cells (*ARS306*) is localised proximal to the centromere, the opposite situation of chromosome V where the inefficient origin *ARS507* is localized next to the subtelomeric region. It is also important to note that the left arm of Chromosome III contains a defined replication slow zone (RSZ) *ARS306*-proximal between kilobases 80 and 95 previously identified in *mec1* mutant cells (Cha and Kleckner, 2002). This region was described in the S288C background, and its full sequence is available in the reference *S. cerevisiae* S288C genome of the SGD (www.yeastgenome.com). Hence, we were interested in analysing the dynamics of DNA synthesis from *TEL03L* up to the RSZ. To confirm the integrity of the RSZ in our W303-1a strains, we analysed the size of this locus containing one transposable element (*YCLWTy2-1*), two tRNAs (*tE(UUC)C* and *tL(CAA)C*) and several LTRs (Figure 22A-C) by Southern blot analysis. DNA from S288C and W303-1a wild type cells was digested with different restriction enzymes resolved in a pulsed-field gel electrophoresis, transferred to a membrane and hybridized sequentially with probes detecting *YCL021W-A* or *LEU2*. The size of the DNA bands in the Southern blots was equal between strains and matches the expected size of the fragments generated after each restriction enzyme digestion (Figure 22D-E), consistent with this RSZ being conserved intact on chromosome III in W303-1a strains.

After this confirmation, the same 2D-Gel membranes used to study the replication dynamics on chromosome V were stripped and reprobed sequentially against five different fragments within the first 90 kb of chromosome III left arm in control (Figure 24) and *sic1* cells (Figure 25). The analysed fragments included the left side of the RSZ (*YCL021W*), two very early origins (*ARS305* and *ARS306*), the *HML* ARS cluster (*HML* locus, *ARS302, ARS303*, *ARS320*) and the telomere containing *ARS300* and one retrotransposon (*YCLWTy5-1*).

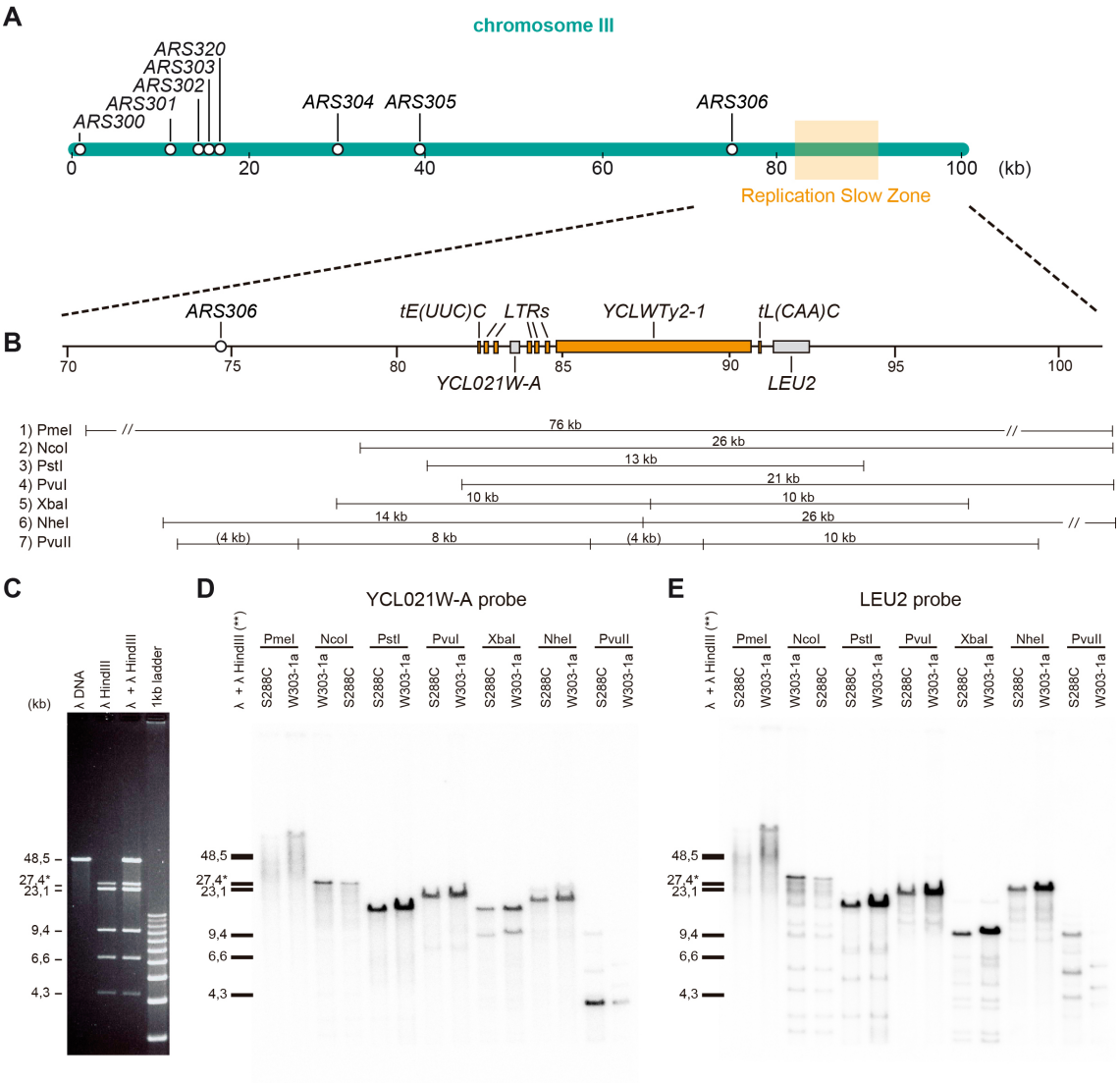

Figure 22: Analysis of the replication slow zone on chromosome III in S288C and W303-1a strains. (A) Schematic view of the first 100 kb of chromosome III, including the localization of all ARS elements mapped in the region (open circles) and the previously described replication slow zone (RSZ) highlighted in orange. **(B)** Zoom of the RSZ containing two tRNAs (*tE(UUC)C* and *tL(CAA)C*), one retrotransposon (*YCLWTy2-1*), several long terminal repeats (*LTRs*) and the genes *YCL021W-A* and *LEU2* (grey squares), located at ~10 kb from origin *ARS306*. Numbers represent chromosome coordinates according to the SGD. Below chromosome III it is represented the expected restriction map of the intact region. The numbers over each line indicate fragment sizes. **(C)** Ethidium bromide (EtBr)-stained PFGE allowing the visualization of DNA from phage λ (λ DNA), phage λ digested with HindIII (λHindIII), a mix of both (λ + λ HindIII) and 1 kb ladder. **(D)** Southern blot analysis of the region hybridized with a probe of *YCL021W-A*. **(E)** The membrane in D after stripping and reprobing with a *LEU2* probe. (**) A mix of λ DNA and λ HindIII markers (λ + λ HindIII ladder) was labelled radioactively and included in the gel to estimate the size of the digested DNA bands. Because the hybridization signal of the λ + λ HindIII ladder was too low, the membrane in D and E was overexposed and the visualized ladder bands were included in the figure as an additional lane. Numbers indicate the molecular weight of DNA bands in kb.

As described for chromosome V, at 40-min we observed RI at ARS305 and ARS306 fragments (Figure 24B), indicating that these origins initiated replication very early consistent with *ARS305* and *ARS306* being the earliest origins within the region (Raghuraman et al., 2001). Flanking *YCL021W-A* and *HML-ARS* cluster fragments initiated replication 15-min after *ARS306* and *ARS305*, with maximum RI signals observed at 70-min, and bulk DNA synthesis completed by 100-min (see quantification in Figure 25). Although the *YCL021W-A* fragment is included in the RSZ, we do not observed a significant delay in replication in control cells, possibly because the analysed fragment is *ARS306*-proximal (~10 kb). Analysis of *ARS306*-distal replication of the RSZ would be necessary to confirm this result.

The *ARS306* fragment replicated actively (bubble-arcs) in the majority of cell population at 40- and 55-min and by 85-min, RI were absent indicating completion of bulk DNA synthesis. Although *ARS305* is a very efficient origin, the position of the ARS at the extremity of the fragment generates very small bubbles and limiting the resolution of a bubble-arc. Nevertheless, the replication dynamics of the *ARS305* fragment is similar of that on the *ARS306* fragment, and both replicated synchronously. Note that probably forks in *ARS305* initiated from this origin, instead of *ARS306*, considering that no forks reach *YCL021W* that is much more closer to *ARS306* (~10 kb) than *ARS305* (~35 kb).

At the HML ARS cluster, bubble-arcs were detected at 55-, 70- and 85-min, indicating that one of the origins within the fragment (ARS302, ARS303 or ARS320) fire significantly within the cell population (Figure 24B-C). A pausing-spot were observed at this fragment as previously described (Wang et al., 2001).

The subtelomeric *ARS300-YCLWTy5-1* fragment replicated very late in S phase, initiating replication 30 min after the *ARS305* fragment, and maximum RI signals were detected at 85-min (Figure 24). Because this fragment is adjacent to the *HML ARS* cluster, the replication delay could be a consequence of delayed fork progression by prolonged pausing at the replication fork barrier present at the *HML* locus (denoted as "P" in Figure 24B-C), and/or contributed by delayed replication of the *YCLWTy5-1* retrotransposon present within the fragment, also known to difficult fork progression. Supporting this idea, a bubble-arc of active replication was detected in this fragment, indicating *ARS300* firing in part of the cell population (Figure 24C), even when *ARS300* is located within the telomere, a heterochromatin region of limited access to the replication machinery. Consistently, bulk DNA synthesis completion of the telomere and the *HML-ARS* region is delayed regarding the inner-chromosome *ARS305* region (Figure 24B).

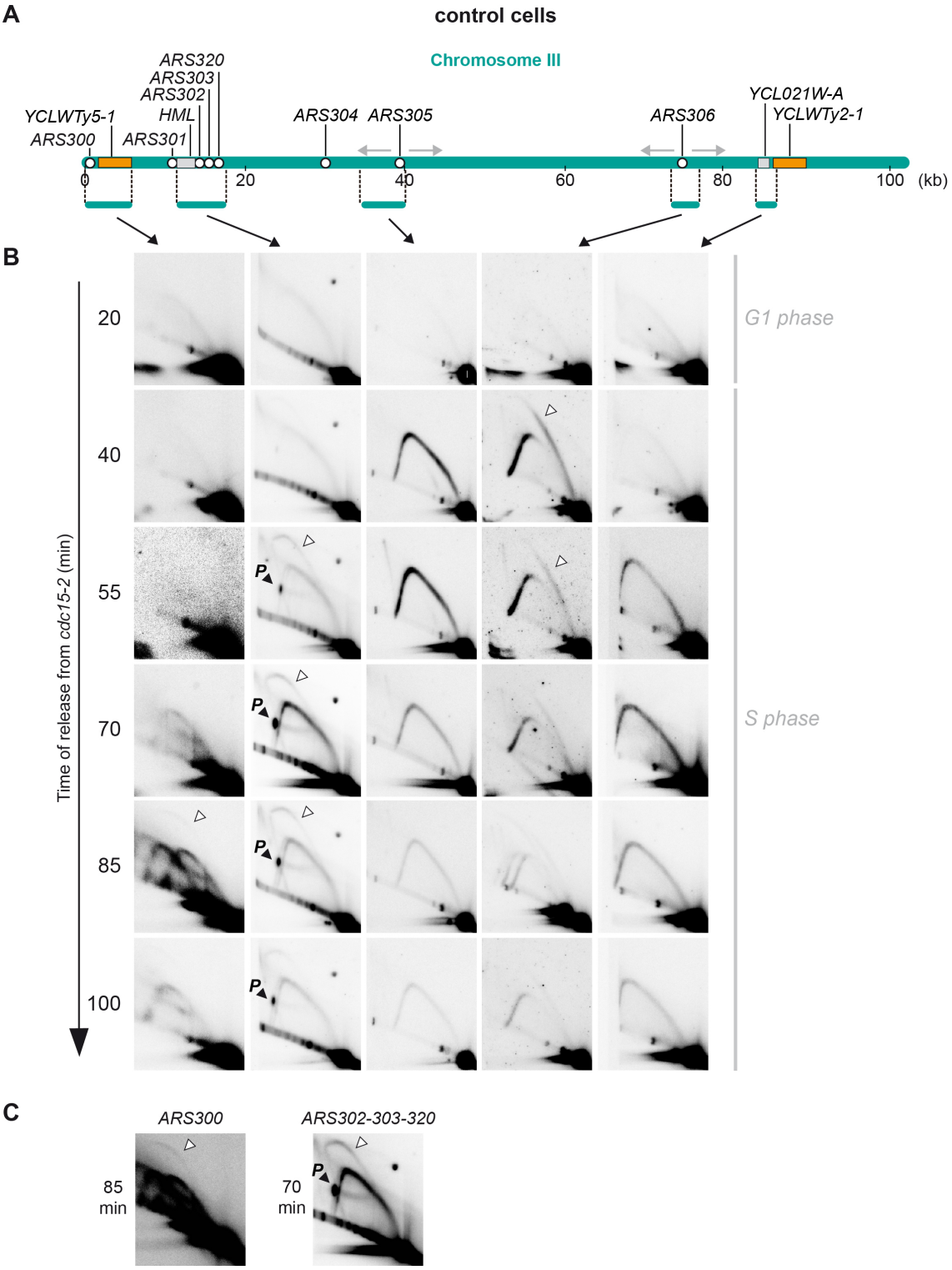

Figure 23: Dynamics of DNA synthesis of the left arm of chromosome III in control cells. **(A)** Schematic view of the first 100 kb of chromosome III left arm. All ARS elements mapped in the region are indicated (open circles) and also retrotransposons (orange squares), the *HML* locus and the *YCL021W-A* gene (grey squares). Grey arrows denote forks movement from the earliest origins in the region. Horizontal bars flanked by dashed lines indicate the restriction fragment analysed. **(B)** 2D-gels of replication intermediates along the indicated fragments. Restriction enzyme digestions, fragments sizes and probes are described in Material and Methods. White arrowheads denote origin-firing activity. '*P*' points to pausing-spots. **(C)** Overexposed blots of *ARS300* and *ARS302-303-320* from B, at the indicated time point.

All together, these results show that the replication of *ARS305* and *ARS306* fragments in chromosome III is very early and synchronous in control cells, as for *ARS507* and *ARS508* in chromosome V. However, the left end of chromosome III that contains a pausing site (*HML*) and a retrotransposon (*Ty5-a*) is replicated very late so that late origins fire (*ARS300* and *ARS302-ARS303-ARS320*), to help completing replication.

The dynamics of DNA synthesis was analysed in *sic1* cells as for control cells (Figure 25). Replication initiated at 40-min in *ARS305* and *ARS306* similarly in time and space to control cells. However, as for chromosome V, differences were found between control and *sic1* cells for replication completion of the *ARS306*. Hence, we observed accumulated passive replicating Ys at *ARS306* at later time points (70-, 85- and 100-min) that were absent in control cells, consistent with the observed inefficiency of *ARS306* in *sic1* cells (Ayuda-Duran et al., 2014). As a consequence, part of *sic1* cell population replicated the *ARS306* fragment abnormally late in S phase (see quantification in Figure 25). Significantly, the replication profile of *YCL021W-A* occurred slightly earlier than in control cells, with the maximum RI signals observed at 55-min, as previously observed at *SOM1* in chromosome V. No further delay in replication completion is observed at *YCL021W*-A. Since *ARS305* is resistant to CDK deregulation but not 100% efficient, Y-arcs within this fragment could in part correspond to forks coming mostly from flanking *ARS304*, *ARS306* or even from other distant origins. However, only weak accumulation of forks remains in this fragment at 100-min in *sic1* cells regarding control cells (Figure 24B and Figure 25B).

Regarding the subtelomeric region of chromosome III, we found that the replication profile of this region was quite similar in timing and completion between control and *sic1* cells (Figure 24B and Figure 25B). Importantly, there is not an accumulation in RI at later time points in *sic1* cells, in contrast to the left subtelomeric region on chromosome V, even when the same 2D blots are used. This result indicates that irregular replication completion problems arise in *sic1* cells among specific chromosome regions. Mechanistically, these differences could rely on differential origin usage, and significantly bubble-arcs were detected at the *HML-ARS* cluster and at *ARS300* in *sic1* cells, indicating that all or some of *ARS300* and *ARS302-303-320* fire in part of the *sic1* cell population, and that all or some are tolerant to the loss of Sic1 (Figure 25C). No difference in firing efficiency was apparent between control and *sic1* for the firing of these origins (compare Figure 24C and Figure 25C).

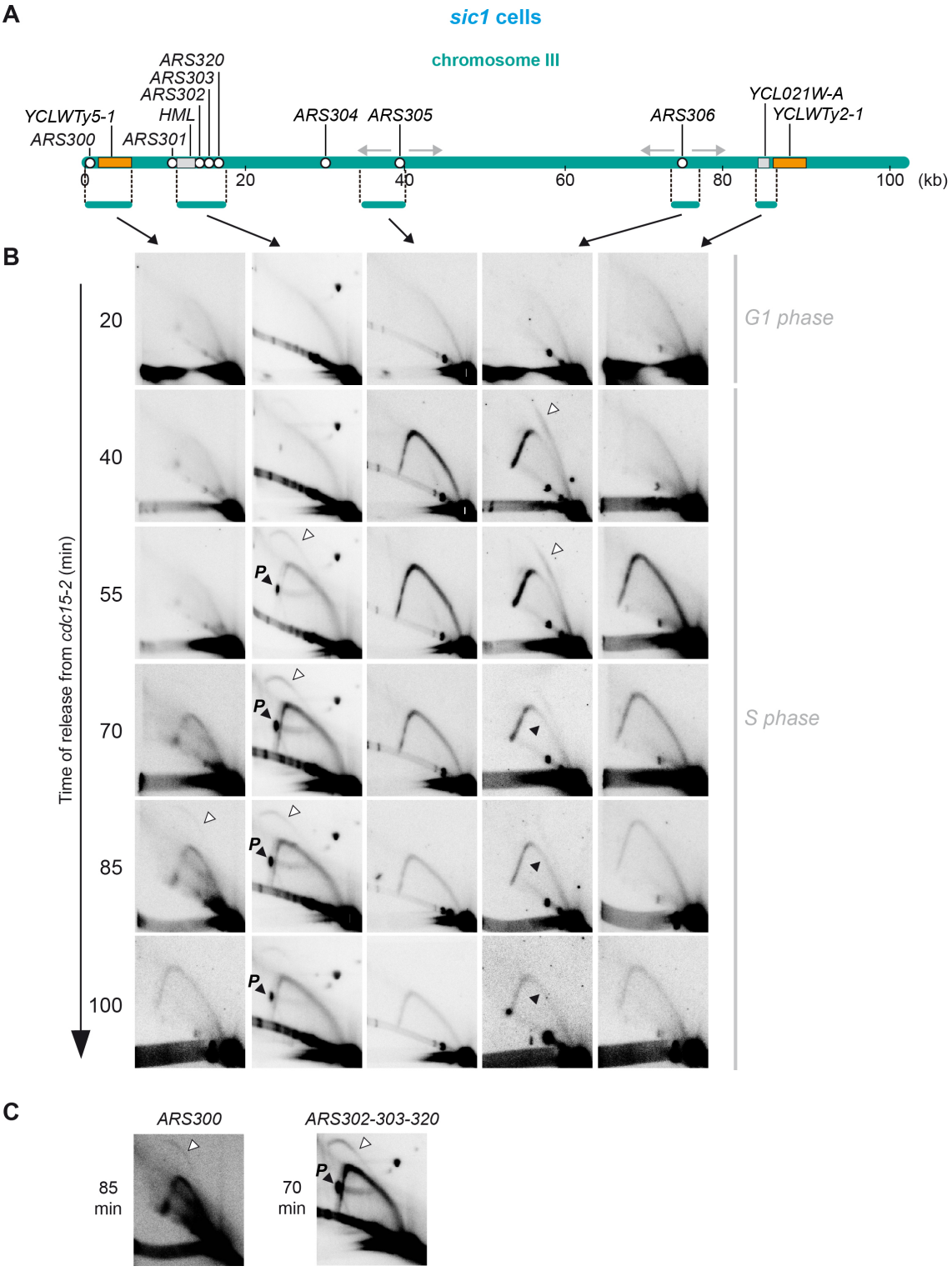

Figure 24: Dynamics of DNA synthesis of the left arm of chromosome III in *sic1* cells. (A) Schematic view of the first 100 kb of chromosome III left arm. All ARS elements mapped in the region are indicated (open circles) and also retrotransposons (orange squares), the *HML* locus and the *YCL021W-A* gene (grey squares). Grey arrows denote forks movement from the earliest origins in the region. Horizontal bars flanked by dashed lines indicate the restriction fragment analysed. **(B)** 2D gel analysis of replication intermediates along the indicated fragments. Restriction enzyme digestions, fragments sizes and probes are described in Material and Methods. White arrowheads denote origin-firing activity. '*P*' points to pausing-spots. **(C)** Overexposed blots of *ARS300* and *ARS302-303-320* from B, at the indicated time point.

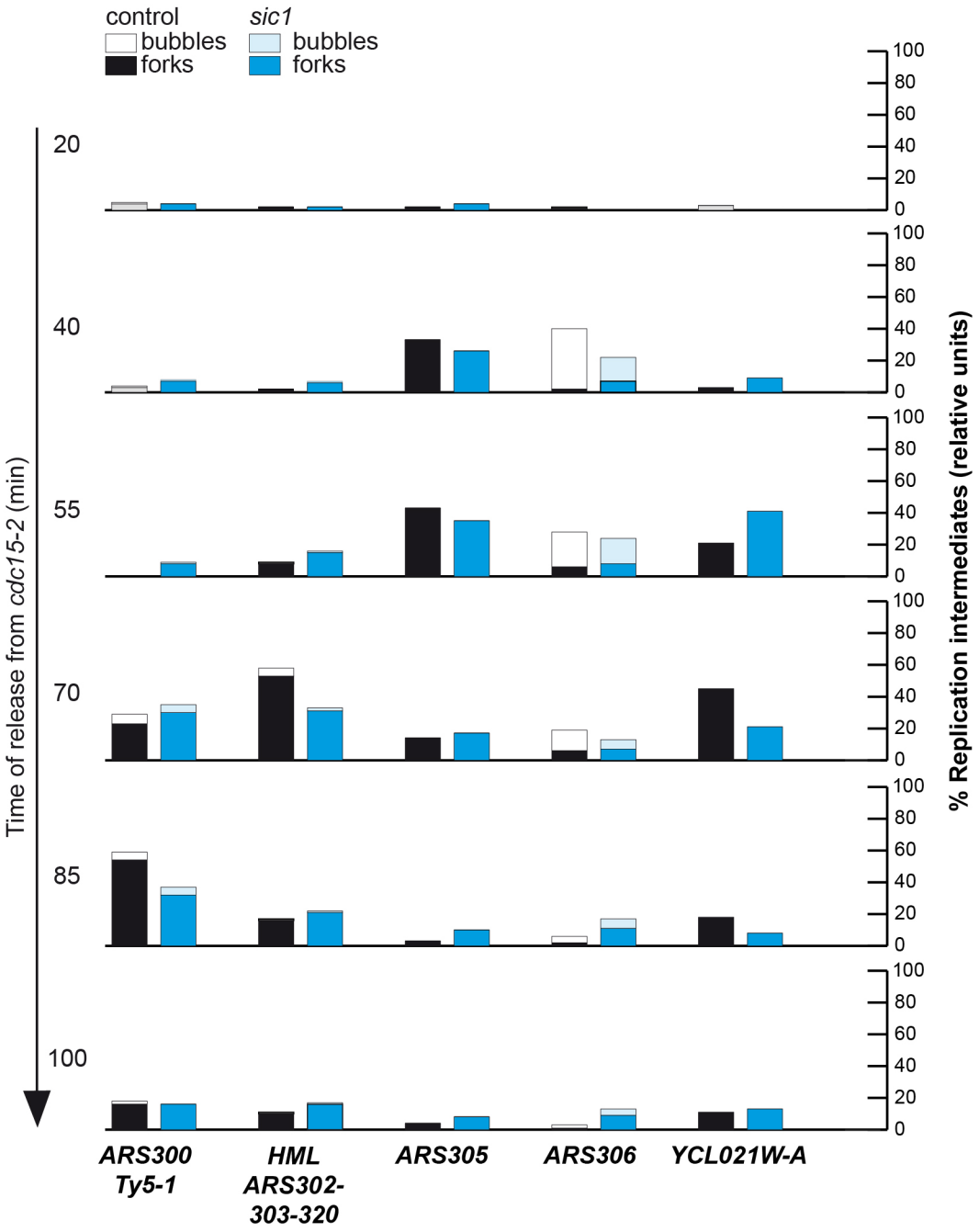

Figure 25: Absence of DNA synthesis completion delays at the left chromosome end of chromosome V. Histograms show the quantification of replication intermediates signals on 2D-gels (bubble- and Y-arcs) from Figure 24 and Figure 25, at the indicated time points (calculated as described in Material and Methods).

Altogether, this analysis of chromosome V and III points out the idea that regions replicating later than usual in *sic1* cells irregularly concentrate at chromosomal regions containing origins that have lost firing efficiency, and support that regions of higher paucity of initiation events by concentrating more Sic1-sensitive origins would suffer higher replication completion delays.

2.3 Delayed completion of bulk DNA synthesis at the *rDNA* locus in *sic1* cells

Previous observations of G1-phase deregulated mutants in budding yeast show that chromosome XII suffer elevated instability (Ayuda-Duran et al., 2014), and delayed replication of this chromosome is also observed in mitosis associated to fork-progression pausing in mutants associated to resolution of X-shaped molecules (Torres-Rosell et al., 2007c). To get further inside into DNA synthesis dynamics of chromosome XII in *sic1* cells, we analysed the rDNA region on this chromosome. The rDNA is formed by 9.1-kb repeating units, each of them containing coding (35S and 5S *rRNA* genes) and noncoding elements (replication origin, replication fork barrier, among others). In *S. cerevisiae*, approximately 150 copies of rDNA occupy 60% of chromosome XII, although the actual number in a cell can differ as rDNA repeating units can be deleted or expanded. For this reason, the rDNA is the most unstable region of the genome (Ganley and Kobayashi, 2011) and has been linked to lifespan and aging in budding yeast, as extrachromosomal circles (ERCs) excised from the rDNA array was observed to accumulate in cells suffering from genomic instability (Ganley et al., 2009). The 2D blots used to study the replication dynamics of chromosome V and III were stripped and reprobed against a specific probe of the rDNA locus.

As for chromosomes III and V, no defect in the timing of origin firing was found in *sic1* cells, which initiates at 40-min in both strains (Figure 27A). Most replication and firing timing occurs by 70-min, indicating that the replication origin fires in mid S phase in most control and *sic1* cells of the population. Consistent with similar efficiencies in fork pausing at the RFB in both cell types in asynchronous cultures, but inefficient firing of the *rDNA-ARS,* both higher RFB-paused forks and accumulated Y-arcs occurs by 55-, 70- and 85-min in *sic1* cells. Most remarkably, in 100-min blots, more than 90% of replication occurred by 100-min in control cells but not in *sic1* cells (see quantification in Figure 27B), indicating that the synthesis of the rDNA is delayed in completion in the *sic1* cell population, although origin efficiencies of the total of ARS at rDNA repeat units is similar between control and *sic1* cells (Figure 27C).

In conclusion, these results further support the view from data on the dynamics of DNA synthesis on chromosome V and III, revealing irregular delays in completion of bulk DNA synthesis among specific chromosome regions in cells lacking Sic1.

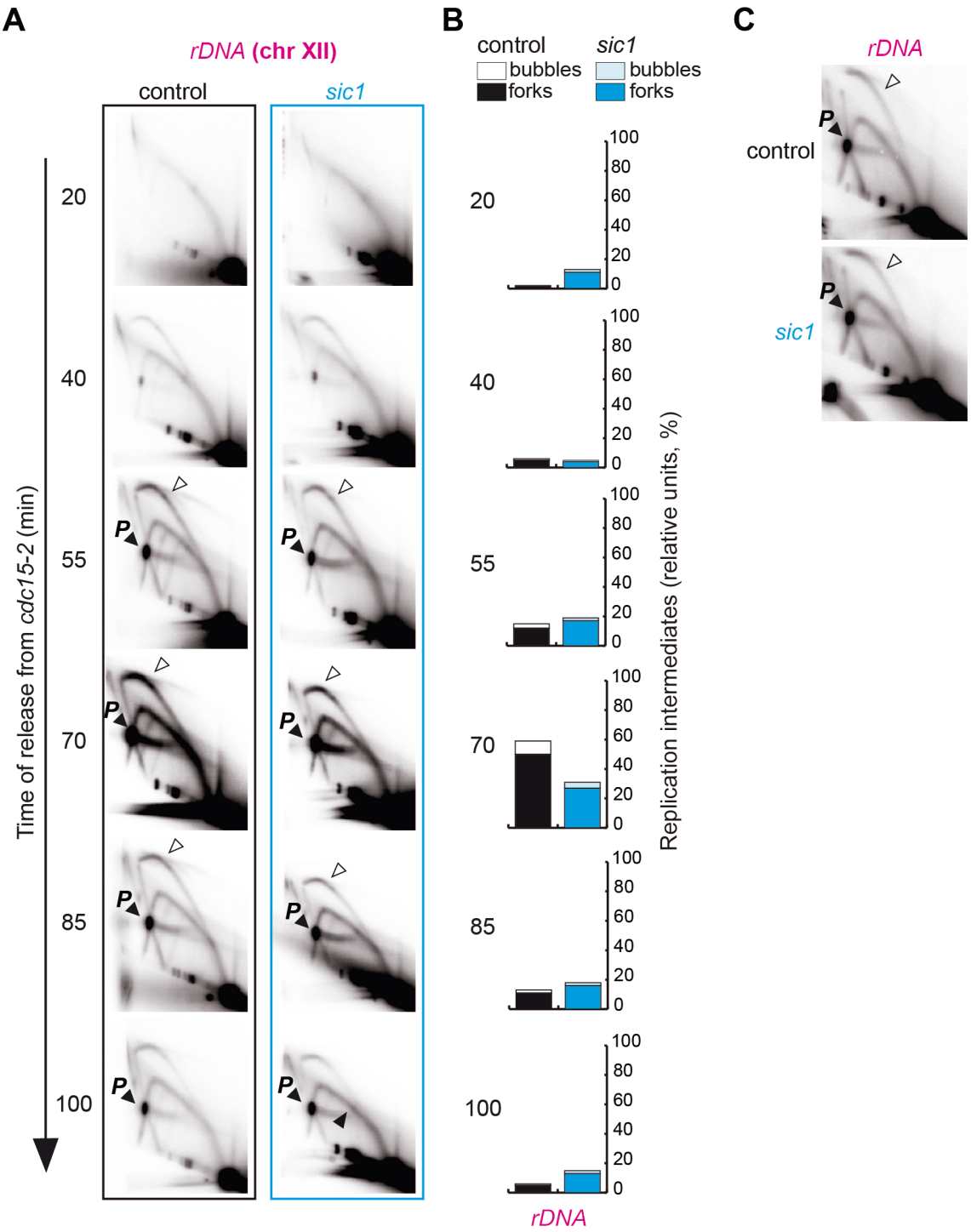

Figure 26: Dynamics of DNA synthesis of the rDNA locus on chromosome XII in control and *sic1* cells. (A) 2D gel analysis of replication intermediates along the rDNA. The same membranes used in the 2D Gels of Chr V and III were stripped and probed against the Chr XII to identify the *rDNA* locus. White arrowheads indicate origin-firing activity and black arrowheads denote prevalence of Y-arc structures. '*P*' points to the pausing-spots. **(B)** Histograms show the quantification of replication intermediate signals on 2D gels (bubble- and Y-arcs) from A. **(C)** Origin firing efficiency of ARS from the *rDNA* locus in asynchronous control and *sic1* cells. White arrowheads denote origin firing. '*P*' points to forks paused at the RFB from the *rDNA* locus (pausing-spot).

3. Loss of origin redundancy sensitises DNA replication in *sic1* cells to replication fork barriers, towards genomic instability.

Common fragile sites identified along human chromosomes frequently express in cancer cells upon DNA replication progression problems, as in the presence of aphidicolin (Durkin and Glover, 2007). At the molecular level, from defects in fork stability, to deficient fork progression along sequences of difficult structure were proposed to mechanistically account for the expression of fragile sites. Recently, a clear correlation was found between a paucity of initiation events and CFS fragility, through the delays of replication dynamics at CFS-containing chromosome regions (Letessier et al., 2011b). The fork-stalling model of CFS expression was proposed to explain how specific loci in the human genome characterized by deficient initiation events are more susceptible to replication elongation perturbations when cells are under replication stress, frequently leading to chromosome breaks during metaphase (Debatisse et al., 2012). Those regions that commit cells to fragility are well described in yeast and a common factor with human cells is that impedes fork progression (Cha and Kleckner, 2002; Lemoine et al., 2005). We hypothesised that our data on delayed replication dynamics in *sic1* cells specifically at regions losing origin firing efficiency, in strong correlation with increased instability of chromosome V fully matches the mechanism of fragile sites in G1-phase deregulated cell cycles. Considering that the molecular causes and mechanism of fragile site expression in cancer cells lacks experimental evidences, we wondered if spontaneous loss of origin redundancy as found in *sic1* cells could exacerbate chromosomal instability specifically at regions prone to delayed replication.

To check this hypothesis, we artificially created a fork progression impediment at a specific chromosome region losing origin redundancy in *sic1* cells but not in control cells, and chose the left arm of chromosome V where the chromosomal instability can be measured by the GCR assay. As a fork-delaying element, we chose to introduce a the RFB fork barrier from the *rDNA*, whose minimal sequence with ability to pause forks outside the nucleolus was previously defined and was demonstrated to work for this purpose (Calzada et al., 2005). The *RFB* is a directional DNA sequence present on each *rDNA* tandem repeat unit that temporarily pause forks coming in opposite direction to transcription (Figure 27A). Importantly, the *RFB* sequence is not inherently difficult to replicate, but instead, depends on the binding of the protein, Fob1, to transiently arrest forks (Ward et al., 2000). Given the directionality of the *RFB* in pausing forks, we oriented the *RFB* on chromosome V to temporarily arrest forks moving from the inner chromosome (from early firing origins) towards the left telomere (right to left in Figure 30A). Prior to this strategy we confirmed by 2D-gels analysis that

cells lacking Sic1 were proficient in fork pausing at DNA-protein replication fork barriers by analysing the efficiency of fork pausing at the *RFB* on the *rDNA* and at *ARS501* in log phase control and *sic1* cells (Figure 27B-C).

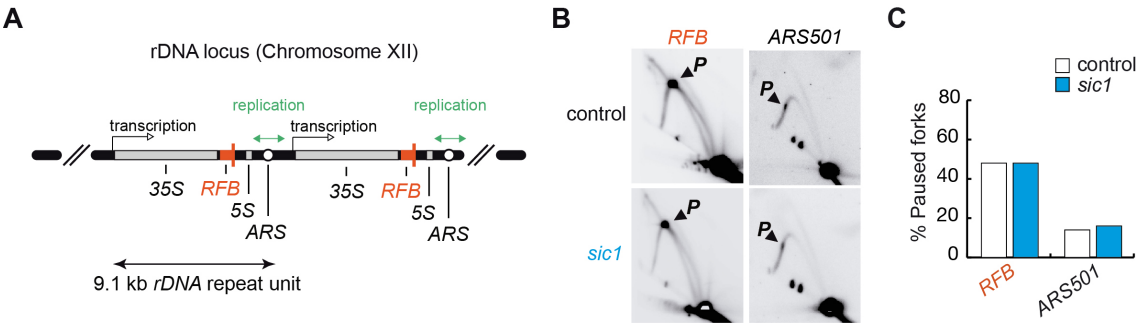

Figure 27: Fork pausing efficiency at DNA-protein fork barriers is normal in *sic1* cells. (A) Schematic of two rDNA repeat units of 9.1 kb on chromosome XII budding yeast. The location of the RFB, replication origin (*ARS1200-1, ARS1200-2*), 35S rDNA (35S) and 5S rDNA (5S) genes is indicated, according to the SGD. **(B)** 2D gel analysis of replication intermediates at the *RFB* on the *rDNA* locus and *ARS501* in log phase W303-1a control (YAC188) and *sic1* cells (YAC198). '*P*' points to paused forks (pausing-spot). **(C)** Quantification of the percentage of forks paused at the barriers in B, estimated from the ratio between intermediates in the pausing-spot and intermediates along the total Y-arc.

3.1 Completion of DNA replication is delayed at all chromosomes in cells lacking Sic1

To test if replication elongation is compromised in control and *sic1* cells carrying the RFB element on chromosome V, we analysed and compared the replication timing of chromosomes in synchronous cells populations. To synchronize cells, we introduced the *cdc15-2* mutation in W303-1a *RFB-chrV* and *sic1 RFB-chrV* cells, due to the impossibility of constructing S288C *cdc15-2* cells by backcross (S288C cells are defective in conjugation). We first inserted the *LEU2-RFB* cassette (Calzada et al., 2005) on chromosome V (*RFB-chrV*) in the intergenic region between *PRB1* and *SOM1* (Figure 31A) in W303-1a control and *sic1* cells (see Material and Methods for construction details) and confirmed that the insertion did not affect cells viability (Figure 29A). Then, the *cdc15-2* mutation was introduced on both strains (see Material and Methods for details) to perform synchronic experiments. The phenotype of the resulted strains, control *cdc15-2 RFB-chrV* and *sic1 cdc15-2 RFB-chrV*, was confirmed using the spotting assay. We observed that all *cdc15-2* mutant cells behave as temperature sensitive conditional mutants as they all grew well onto plates incubated at 25º C (*cdc15-2* permissive temperature) comparable to the respective parental strain, but did not grew at 32º C (*cdc15-2* restrictive temperature), as expected for cells arrested at late anaphase/telophase (Figure 28A).

To test whether replication completion was compromised in *sic1 cdc15-2 RFB-chrV* cells, we synchronized in parallel control *cdc15-2 RFB-chrV* and *sic1 cdc15-2 RFB-chrV* cells and analysed the timing of replication completion of all chromosomes by PFGE analysis. Synchronous cultures were obtained by *cdc15-2* block-and-release by shifting cells from YPARG at 25 ºC to YPAD at 37 ºC to simultaneously arrest cells at *cdc15-2* and deplete Sic1 from *sic1 RFB-chrV cdc15-2* cells, and then cells were shifted to fresh YPAD at 23 ºC to release them into the cell cycle (Figure 28B). Samples were collected after the release from *cdc15-2* and processed for PFGE analysis in conditions preserving intact chromosomes (see Material and Methods for details). Additional samples were taken at specific time points to monitor cell synchrony by FACS analysis and protein levels of Sic1 by Western blotting (Figure 29C and D).

Both cultures were efficiently arrested at *cdc15-2*, then released synchronously into the cell cycle, progressed through S phase, reached mitosis and initiated a new cycle between 130 and 160 min (Figure29 C-D). Noteworthy, *sic1* cells display the known delay in completing bulk DNA synthesis (Figure 29C, time-points 70 and 85), and delayed mitotic exit (Figure 29C, time-point 190) (Lengronne and Schwob, 2002).

The first plot in Figure 29C represents the cell cycle distribution of asynchronously raffinose galactose-grown cells. In *sic1 RFB cdc15-2* cells, there is an excess of cells with 1C DNA content comparing to the control (Figure 28C, As), indicating an excess of cells in G1, as expected for cells moderately overexpressing *SIC1*. At the time-point 0 (i.e., *cdc15-2* arrest), the entire population accumulates at the 2C peak, indicating that both cells population were uniformly arrested at late anaphase/telophase. In the control, the 2C peak remained fixed between 20-, 30- and 40-min (Figure 28C, control *RFB-chrV cdc15-2*) and Sic1p was detected in that same time points in the control (Figure 28D, control *RFB-chrV cdc15-2*), consistent with cells passing through G1 phase. As both time course proceeds, we observed a 2C to 4C shift in the DNA content between 50-, 70, 85- and 100-min (Figure 28C) and Sic1p levels dropped to undetectable levels in Control cells (Figure 28D), consistent with cells being replicating its DNA (S phase). In *sic1 RFB-chrV cdc15-2*cells, levels of Sic1p were undetectable during all time points (Figure 29D, except As), confirming that the depletion of Sic1 in these cells was accomplished during the experiment.

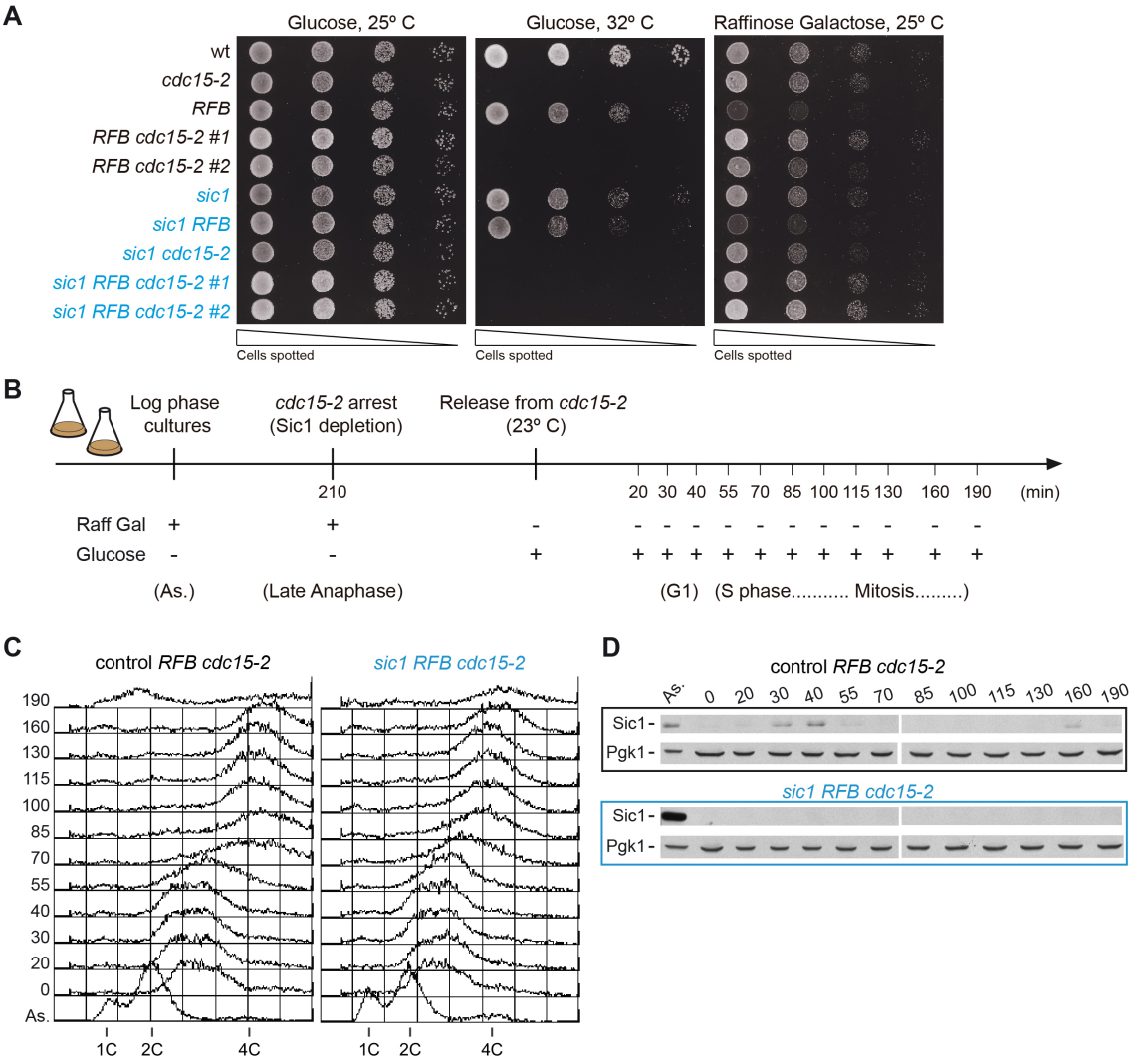

Figure 28: Synchronous S phase of control *RFB* and *sic1 RFB* cells by block-and-release from *cdc15-2*. (A) Dilution spotting assay. Phenotype of W303-1a wt (YAC188), *cdc15-2* (YAC1104), *RFB* (YAC1164), *cdc15-2 RFB* (YAC1358), *sic1* (YAC198), *sic1 RFB* (YAC1190), *sic1 cdc15-2* (YAC1107) and *sic1 cdc15-2 RFB* (YAC1362) cells. Plates were incubated 2 days at 25º or 32º C and photographed. *GAL1,10p-SIC1* strains (in blue) deplete or overexpress Sic1 onto YPAD (left and mid panels) or YPARG (right panel) plates, respectively. (B) Outline of the experiment. Control *RFB* and *sic1 RFB* were block-and-release from *cdc15-2* (see Material and Methods for details). (+) and (-) are indicative of raffinose-galactose- or glucose-grown cells, during the experiment. (C) FACS profiles of *control RFB* and *sic1 RFB* in asynchronous (As.), *cdc15-2* arrested (time point 0) and at the indicated time points after the release from the *cdc15-2* arrest. because cells released from a *cdc15-2* block are delayed in cytokinesis, replicating cells (S phase) results in a 2C to 4C shift in the DNA content (Cheng and Hardy, 1998) **.** (D) Protein levels of Sic1 in the same strains and time points in C. Pgk1 was used as loading control.

PFGE analysis was used to follow replication timing of chromosomes in control *RFB-chrV cdc15-2* and *sic1 RFB-chrV cdc15-2* cells. Chromosomes containing bubbles (i.e., replicating chromosomes) get stuck in the well, while fully replicated chromosomes enter the gel and migrate according to their size (Mesner and Hamlin, 2006). Figure 29A shows ethidium-bromide stained gels of control *RFB-chrV cdc15-2* and *sic1 RFB-chrV cdc15-2* cells, allowing the visualization of 12 bands corresponding

to the 16 W303-1a budding yeast chromosomes (chromosome XII and IV, XV and VII, XIII and XVI, V and VIII co-migrate). Consistent with the Sic1-accumulation at 30- and 40-min, and with the FACS profile in the control (Figure 29C-D, control *RFB-chrV cdc15-2*), chromosomes were largely gel-depleted and well-enriched between 55- and 85-min after the release from the *cdc15-2* arrest, and re-entering the gel by 85-min (Figure 29A). These results are consistent with chromosomes being replicated between 55- and 85-min and completing bulk replication by 85-min in the control.

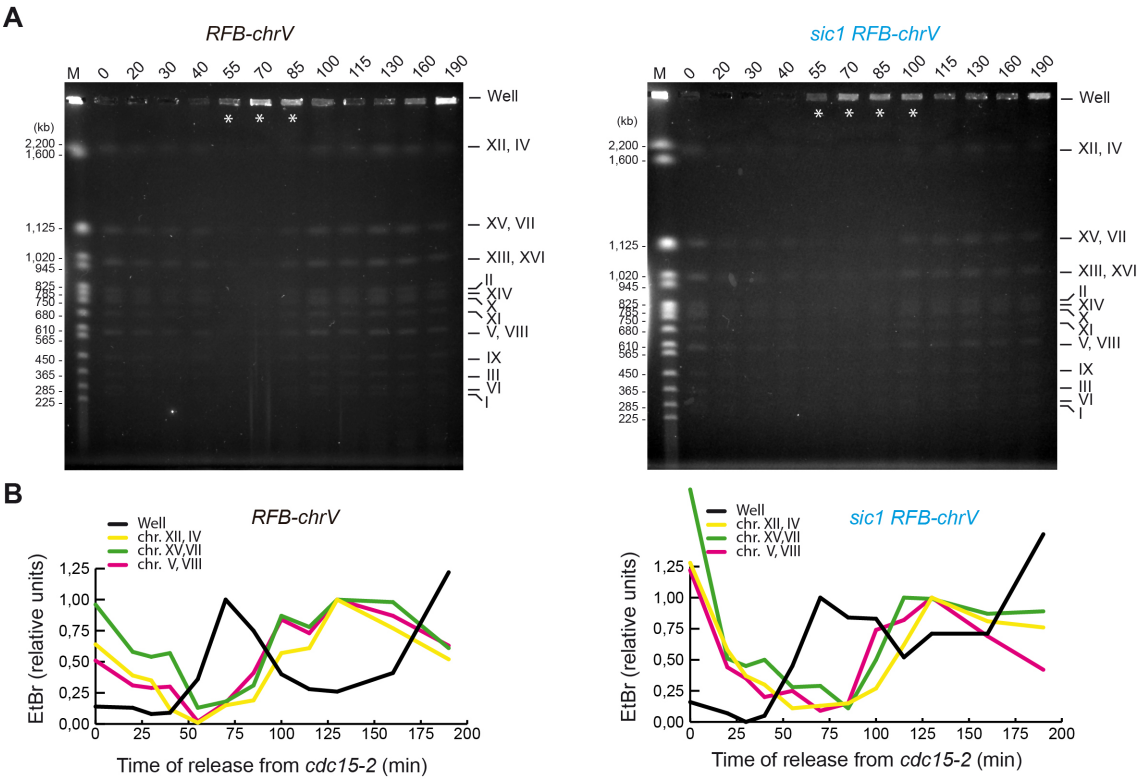

Figure 29: DNA replication completion is delayed at all *sic1's* chromosomes. Control *RFB* (YAC1358) and *sic1 RFB* (YAC1362) cells were synchronously released from the *cdc15-2* arrest and replication of chromosomes was followed by PFGE analysis. **(A)** EtBr-stained PFGE allowing the visualization of 12 bands corresponding to intact chromosomes. Numbers above the gel indicate time points after release from the *cdc15-2* arrest. The first lane contains a commercial yeast chromosomal DNA size marker (M). Chromosome sizes (left) and chromosome numbers (right) are indicated. Asterisk denotes the accumulation of replication intermediates trapped in the well. **(B)** Quantification of EtBr-signals from chromosome bands and wells from A.

In *sic1 RFB-chrV cdc15-2* cells, chromosomal bands disappeared at 55-min after the release from the *cdc15-2* arrest (Figure 30B), as in the control (Figure 30A). However, in contrast to the control, chromosomes remained in the well up to 100-min and re-entered the gel around 15 minutes later, compared to the control. Thus, we conclude that replication of all chromosomes is delayed by ~15 minutes in *sic1 RFB-chrV cdc15-2* cells. To confirm that the replication completion delay in *sic1 RFB-chrV cdc15-2* cells was not chromosome-specific, the intensity of three randomly chosen

chromosomal bands (chromosomes XII/IV, XV/VII and V/VIII), and also the well, were quantified and normalized measures are represented in Figure 29C-D. In the control, we observed that replication timing of chromosomes followed a very similar kinetics: all chromosomal bands intensities dropped at approximately the same rate from 0- until 55-min, remained low at 55-, 70- and 85-min, while maximum within the well, and increased after 85-min (Figure 30C). In *sic1 RFB cdc15-2* cells, chromosomes followed the same kinetics, as all chromosomal bands intensities declined at about the same rate from 0- until 55-min, remained low between 55- and 100-min, while enriched within the well, and increased after 100-min (Figure 30C), indicating that virtually all *sic1's* chromosomes are delayed in fully completing replication.

3.2 Loss of origin redundancy sensitises chromosome stability to replication fork barriers

We inserted the *LEU2-RFB* cassette on chromosome V (*RFB*-chrV) in S288C wild type and *sic1* cells at the same locus as in in W303-1a (Figure 30A) (see Material and Methods for construction details). By dilution spotting we confirmed that the insertion (*RFB-chrV*) did not affect the viability of control or *sic1* cells (hereinafter referred to as *RFB-chrV* and *sic1 RFB-chrV* cells, respectively) (Figure 30B). Next, we confirmed that the chromosome end is not lost due to *RFB*-paused forks, by analysing the size of chromosome V in log phase glucose-grown *RFB-chrV* and *sic1 RFB-chrV* cells (and respective parental strains) in a PFGE followed by southern analysis, as smaller chromosomes migrate faster in a gel than full-length chromosomes. As a control of full-length intact chromosomes, we used no replicating cells, that is, wt cells blocked in G1 phase with α-factor (wt α-F). The cell cycle distribution of wt α-F cells and log phase glucose-grown wt, *sic1*, *RFB-chrV* and *sic1 RFB-chrV* cells was analysed by flow citometric analysis on propidium iodide-stained cells (Figure 30C). In the wt α-F histogram, the entire population accumulated at the 1C peak, indicating that cells were efficiently arrested at G1 phase (Figure 30C). In the cell cycle distribution of *sic1* and *sic1 RFB-chrV* cells, a lower percentage of cells with 1C DNA content is observed, when compared to wt and *RFB-chrV* cells (Figure 30C), indicating a shorter G1 length in these cells, as expected for cells lacking Sic1.

To analyse the size of chromosome V in the same cultures, full-length chromosomes of all strains were resolved in a PFGE (not shown), transferred to a membrane and southern hybridized with the ARS508 probe (Table 6) to visualize the chromosome V. We observed the appearance of one band corresponding to the full-length chromosome V with similar size in all strains, including the control wt α-F (Figure 30D), indicating that the chromosome V has the same size in all analysed strains. This

result suggest that the end of chromosome V is not lost in *sic1 RFB-chrV* cells or, if it is lost, it occurs at a low frequency and is undetected on asynchronous cells using the PFGE technique.

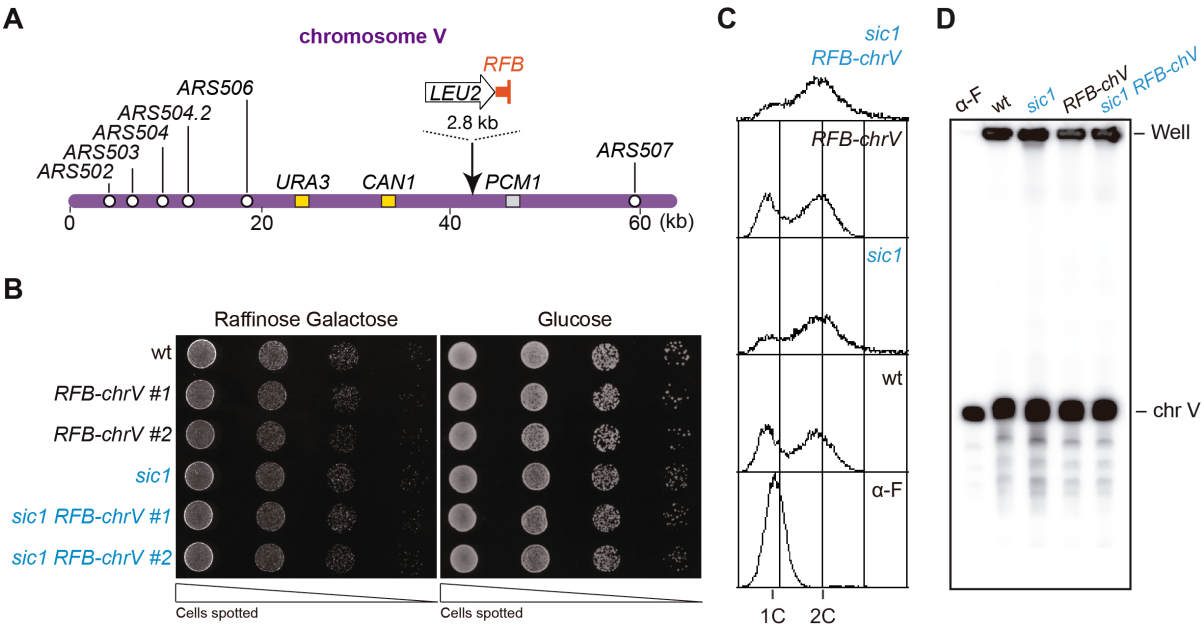

Figure 30: The insertion of the *RFB* element in chromosome V does not compromise cells viability or the stability of the chromosome end in S288C strains. (A) Schematic view of the first 100 kb of chromosome V left arm. The *LEU2-RFB* cassette was inserted at the indicated position (see Material and Methods for details). The orientation of the RFB transiently arrests forks moving from right to the left. **(B)** Dilution spotting assay. S288C wt (YAC177), *RFB-chrV* (YAC1296 and YAC1297), *sic1* (YAC217) and *sic1 RFB-chrV* (YAC1299 and YAC1300) are compared for growth abilities in the indicated conditions. *GAL1,10p-SIC1* strains (in blue) deplete or moderately overexpress Sic1 onto YPAD (left) or YPARG (right) plates, respectively. **(C)** FACS profiles of α-factor-blocked wt cells (α-F) and log phase glucose-grown wt (YAC177), *sic1* (YAC217), *RFB-chrV* (YAC1296) and *sic1 RFB-chrV* (YAC1299) cells. **(D)** Full-length chromosomes of strains from C were resolved in a PFGE, transferred to a membrane and southern hybridized with a probe of chromosome V (*ARS508*).

Then we studied the activity of origins within the left arm of chromosome V by 2D-Gel analysis, on log phase glucose-grown *RFB-chrV* and *sic1 RFB-chrV* cells. Agreeing with the origin redundancy model, bubble-arcs are detected in *ARS504.2* and *ARS506*, indicating that dormant origins located telomere-distal to the *RFB* are activated in the control (Figure 32B, *RFB-chrV*) in response to RFB-mediated fork progression delay. Also, *ARS507* shows normal firing efficiency, consistent with functional origin redundancy (Figure 26B, and C). A strong pausing-spot at the *RFB* fragment is detected with similar intensity in *RFB-chrV* and *sic1 RFB-chrV* cells (Figure 31B) consistent with the unaffected fork pausing at DNA-protein fork barriers in *sic1* cells (Figure 28B-C). The quantification of the pausing-site with respect to the Y-arc showed that ~70% of forks paused at the *RFB,* indicating that forks are arrested at the *RFB* very efficiently. Importantly, *sic1 RFB-chrV* cells show deficient *ARS507* activity,

and late/dormant *ARS504.2* and *ARS506* remain largely dormant, demonstrating loss of origin redundancy (Figure 31B, *sic1 RFB-chrV*).

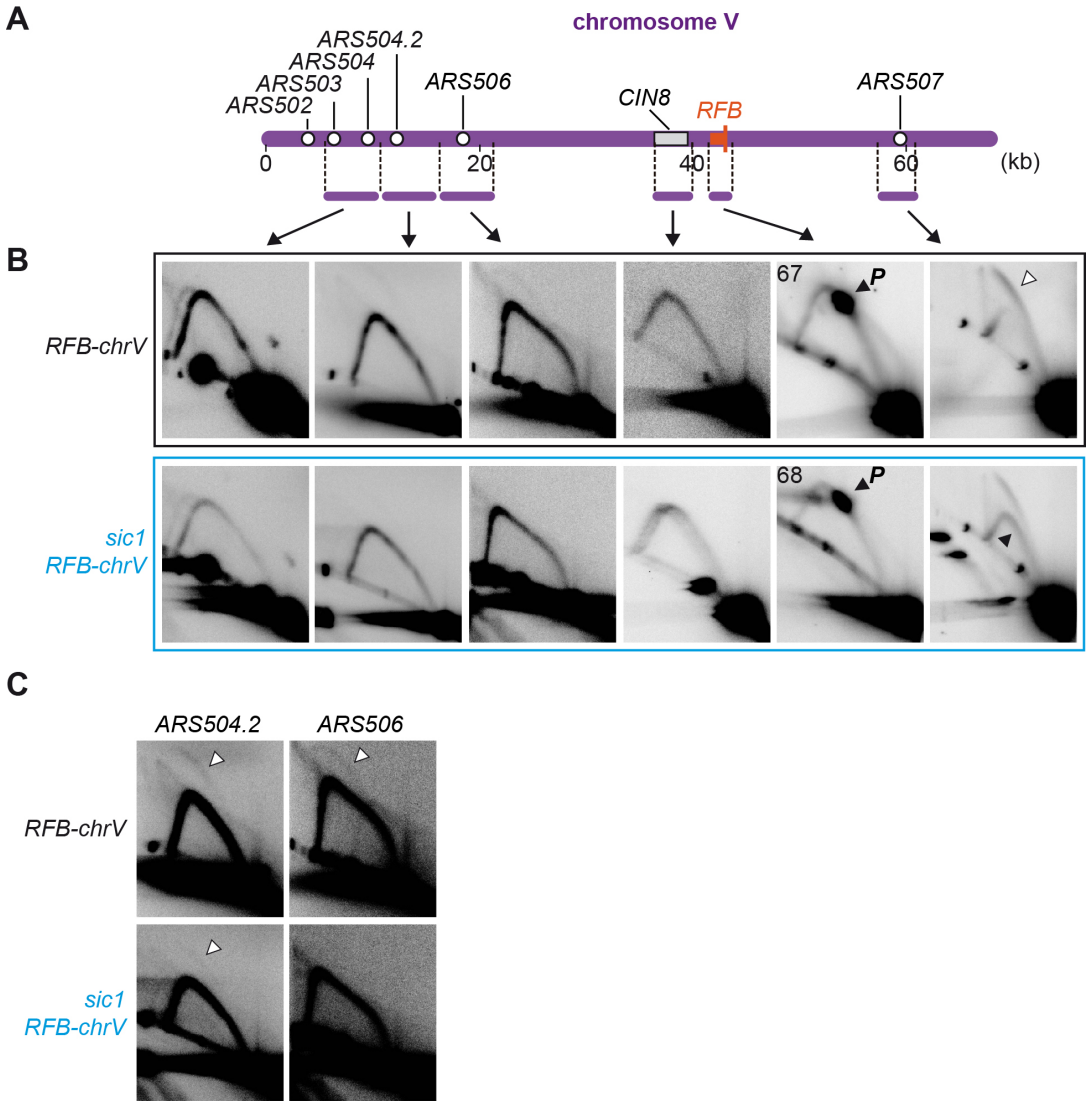

Figure 31: Cells lacking Sic1 fail in dormant-origin firing in response to a transiently pause of forks at the RFB. (A) Schematic view of the first 100 kb of chromosome V left arm. The position of the *RFB* element is indicated (red). Horizontal bars flanked by dashed lines represent the restriction fragments analysed. **(B)** 2D gel analysis of replication intermediates along the indicated fragments. Restriction enzyme digestions, fragments sizes and probes are described in Material and Methods. White arrowheads denote origin-firing and black arrowheads indicate loss of origin-firing efficiency. '*P*' points to forks paused at the RFB (pausing-spot). The percentage of paused forks at the RFB was estimated from the ratio between intermediates in the pausing-spot and intermediates along the Y-arc, and is indicated in the upper left corner of the respective 2D blot. **(C)** Overexposed blots of *ARS504.2* and *ARS506* fragments from B.

Noteworthy, less Y-arcs were repetitively found at *ARS503-504*, *ARS504.2* and *ARS506* fragments in *sic1 RFB-chrV* cells, regarding the control, and were even detected after reprobing the same 2D blots employed to study *ARS507*, ruling out technical artefacts concerning that forks (Y-arcs) were depleted only at the chromosome end. Because RI signals were likely depleted at the chromosome end, telomere-distal to the RFB, but not centromere-proximal to the RFB (*ARS507*) we hypothesized if RFB-arrested forks never released the pause, although it is was quite unexpected. To test this hypothesis, we analysed the *CIN8* fragment located downstream to the RFB, immediately adjacent to the *RFB* fragment. We found that RI within the *CIN8* fragment were not depleted, as expected, indicating that forks released from the RFB pause and progressed through the *CIN8* fragment. Although further analysis would be necessary to clarify this finding, these observations are consistent with forks being strongly delayed in progressing from *CIN8* to the chromosome end, meaning that the chromosome V left end in *sic1 RFB-chrV* cells is likely fragile.

We reasoned that genomic instability would significantly arise in the region reflecting the paucity of initiation events in *sic1* cells if fork progression delaying elements are a significant source of regional instability. To this end, we performed the GCR assay on *RFB-chrV* and *sic1 RFB-chrV* cells, and respective isogenic parental strains (Figure 32).

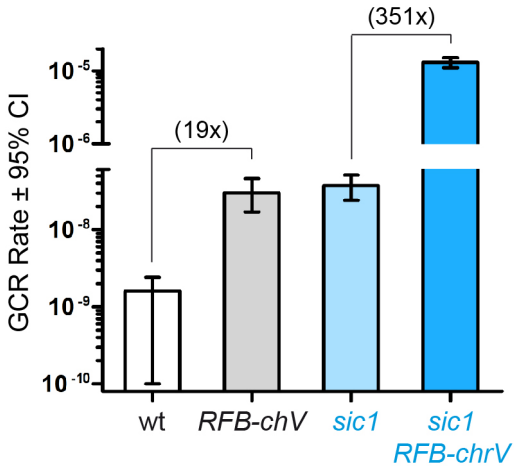

Figure 32: The *RFB* element induces high rates of GCR in cells lacking Sic1. Bar chart with 95% confidence intervals of the indicated strains. Numbers above the bars indicate fold increase with respect to control cells. GCR rates are per cell division. Asterisks indicate statistical significance: **, p<0.001.

In *RFB-chrV* cells, the GCR rate moderately increased by one order of magnitude (19-fold) regarding wild type cells, showing that this strong pausing is deleterious in a region of mostly unidirectional replication (see Figure 16), even under the firing of

dormant origins. This is consistent with natural dormant origins being rate-limiting to compensate strong delays in fork progression. Remarkably, in *sic1 RFB-chrV* cells, the rate of GCR highly increased by two-orders of magnitude (351-fold) with respect to *sic1* cells. This result demonstrates that the *RFB* element significantly compromises the stability of chromosome V in *sic1* cells, and strongly suggests that impediments to fork progression are significantly poorly tolerable in terms of genomic instability by cells lacking Sic1.

3.3 Extra dormant origin activity reverts chromosomal instability of *sic1* cells carrying a RFB element

We tested whether the molecular cause of chromosomal instability in *sic1 RFB-chrV* cells is the loss of backup firing from dormant origins. To this end, extra origin activity was inserted at the subtelomeric region of chromosome V in *sic1 RFB-chrV* cells and the possible reversion on their high instability was tested by the GCR assay. Following the same strategy as in Section 1.2, we integrated a pRS303 plasmid containing a tandem of seven *ARSH4* (*pRS303-7xARSH4*) at the *SIT1* gene in *RFB-chrV* and *sic1 RFB-chrV* cells (hereinafter referred to as control *RFB 7xARSH4* and *sic1 RFB 7xARSH4*, respectively), or the same plasmid without origins (*pRS303-empty)* as a control (hereinafter referred to as control *RFB empty* and *sic1 RFB empty*, respectively) (Figure 33B). By dilution spotting we confirmed that the integration of the *pRS303-7xARSH4* or *pRS303-empty* at *SIT1* do not affected cell viability (Figure 34A).

Then, to confirm that the seven copies of *ARSH4* were competent for replication initiation, we analysed the origin activity at the *pRS303-7xARSH4* or *pRS303-empty* loci by 2D gels in respective strains (Figure 34B). We found that some weak *7xARSH4* firing occurs in the control (Figure 29B, control *RFB 7xARSH4*), consistent with the activation of natural late/dormant origins being insufficient to compensate fork pausing at the RFB. Significantly, higher *7xARSH4* firing efficiency was found in the *sic1* (Figure 29B, *sic1 RFB 7xARSH4*), consistent with the deficiency of the natural dormant *ARS504.2* and *ARS506*.

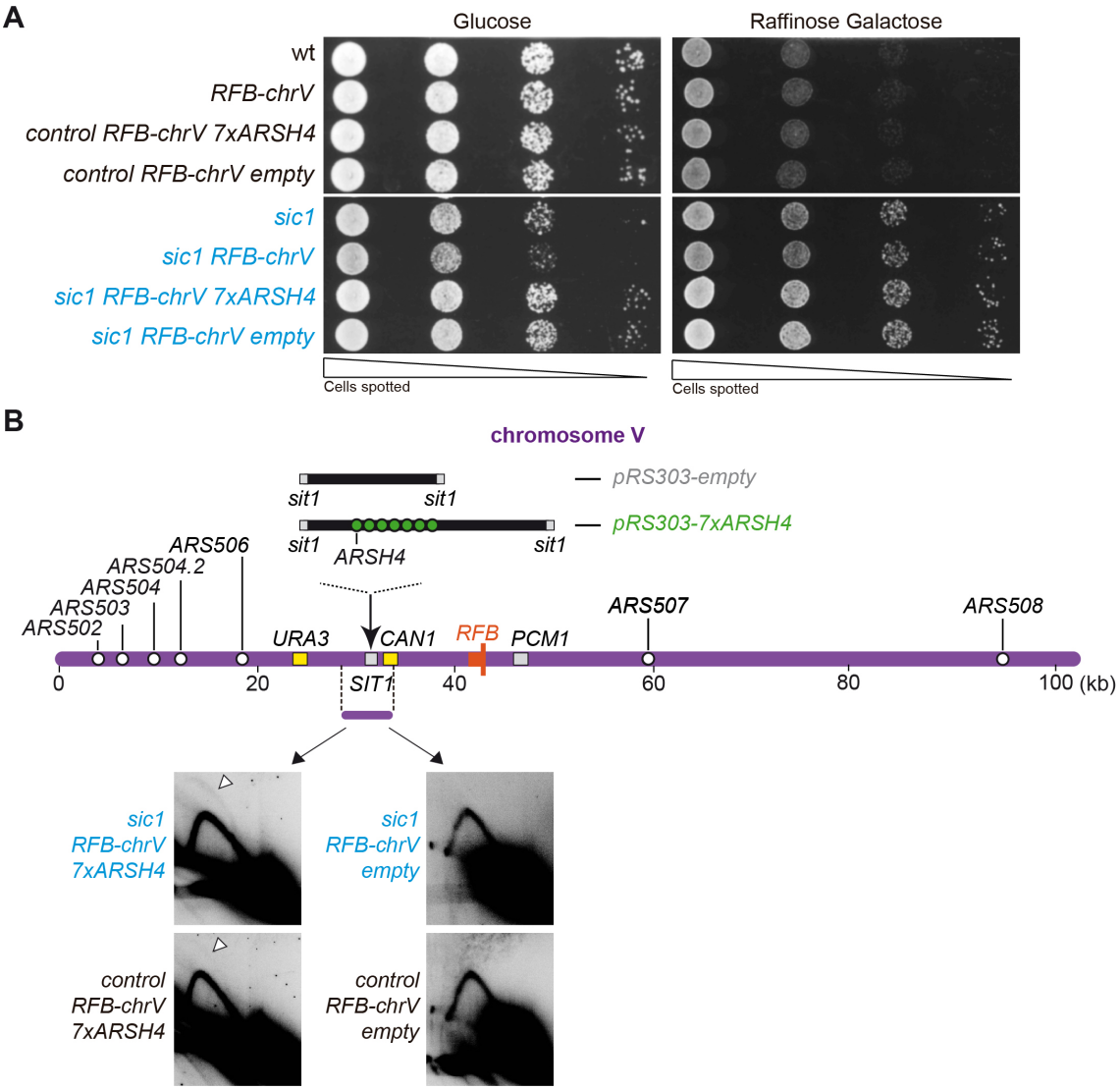

Figure 33: Extra origins downstream the *RFB* behave as dormant origins in *sic1* cells. (A) Dilution spotting assay of the indicated strains. *GAL1,10p-SIC1* strains (in blue) deplete or moderately overexpress Sic1 onto YPAD (left) or YPARG (right) plates, respectively. **(B)** 2D gels of the activity of a tandem of *7xARSH4* in control (in black) and *sic1* cells (in blue), and respective empty plasmid controls.

Finally, we tested whether the extra dormant origin activity affected the chromosomal instability of control *RFB 7xARSH4* and *sic1 RFB 7xARSH4* cells, and the respective empty plasmids controls (*RFB empty* and *sic1 RFB empty*). Figure 35 shows that the GCR rates of *7xARSH4* caused a statistically significant reduction in the GCR rates of both strains, decreasing to 97-fold in the *sic1* (Figure 35, *sic1 RFB 7xARSH4*) and to 7-fold in the control (Figure 35, *RFB 7xARSH4*), while no reduction was obtained in empty plasmid controls (Figure 35, *RFB empty* and *sic1 RFB empty)*. We interpret the partial rescue of genomic instability, as the tandem array of origins being inserted at a single locus, in contrast to the control, although the implication of other additional causes cannot be discarded. We conclude that coincident origin redundancy losses and replication fork barriers enrich chromosome instability at

specific chromosome regions. And these data strongly suggest that chromosome regions naturally late-replicating or suffering replication delays by any reason would be specially unstable in G1-phase deregulated cell cycles when colocalising with spontaneous losses of origin redundancy.

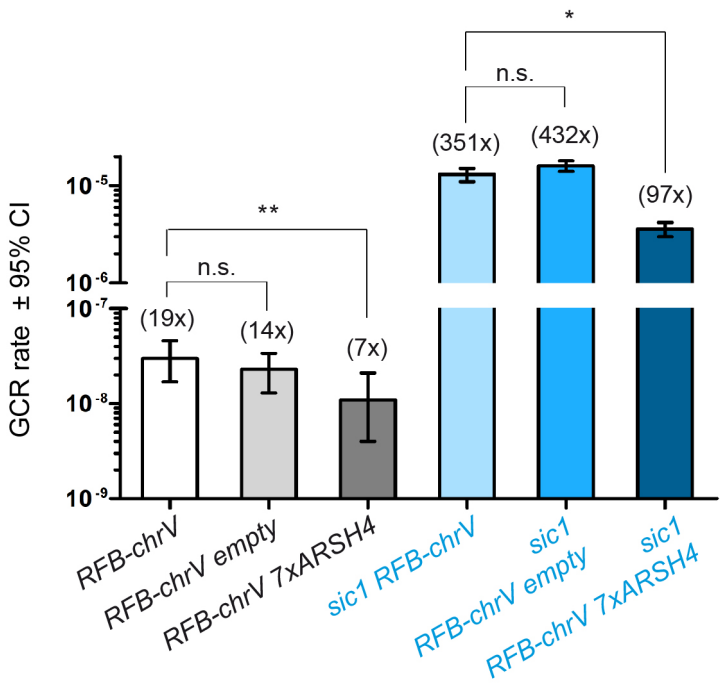

Figure 34: Chromosomal instability by *RFB*-chrV is partially reverted by multiple origins placed upstream the fork barrier. Bar charts with 95% confidence intervals of GCR rates of Control (A) and *sic1* cells (B). Numbers above the bars indicate fold increase with respect to control *RFB-chrV* (left) or control *sic1 RFB-chrV* (right). GCR rates are per cell division. Asterisks indicate statistical significance: **, p<0.001.

4. The anaphase defects and chromosomal instability of *sic1* cells can be reverted by delaying mitosis entry

G1-phase deregulated mutations, including mammalian oncogenic cell-cycle mutations, very frequently share abnormal anaphases with chromosome segregation aberrancies and genomic instability. Previous studies showed that *sic1* mutant cells are delayed in early anaphase and present high frequency of Ddc1 foci (suggesting DNA damage) dependent on anaphase entry (Lengronne and Schwob, 2002). Anaphase defects were suggested to be a consequence of incomplete DNA replication at specific loci. Subsequent failure, during anaphase, to segregate unreplicated chromosomes that are still interconnected would lead to chromosome breakage and rearrangements leading to genomic instability. However, experimental support for this model is lacking, as is whether premature entry into mitosis is a necessary step for G1-phase cells to acquire genomic instability. Thus, we asked if delaying the mitosis entry in *sic1* cells

might provide extra time and, therefore, suppress the anaphase delays and chromosomal instability in *sic1* cells.

4.1 *clb2*Δ delays the mitosis entry and suppress the accumulation in anaphase and genomic instability in *sic1* cells

To test if premature entry into anaphase is a necessary step for genomic instability in *sic1* cells, we delayed anaphase entry in *sic1* cells without alleviating G1-phase and origin firing defects and measured the rates of GCR in *sic1* cells. We chose deleting *CLB2* in *sic1* cells. Clb2 is a M-phase specific cyclin, expressed during G2 and necessary to activate sufficient Cdk1/Clb1,2 complexes for cells to entry the mitotic phase an reach metaphase. Cells lacking *CLB2* are viable, show slight slow growth, and delayed mitosis entry (Surana et al., 1991).We constructed *clb2*Δ *and sic1 clb2*Δ cells by replacing a 1476-bp DNA fragment containing *CLB2* with the *HIS3* marker (see Material and Methods for construction details) and confirmed no variation in the viability of newly constructed strains using the dilution spotting assay (Figure 35A). As a control, we show that *GAL-SIC1 clb2*Δ cells barely grew, confirming that the deletion of *CLB2* in cells overexpressing Sic1 is synthetic lethal (Figure 36A, *sic1* in raffinose galactose-plates). We studied the cell cycle distribution of asynchronously log phase control and *clb2*Δ cells by FACS analysis to check for not rescue of G1-phase length defects in *sic1* cells (Figure 36C). As expected, *clb2*Δ and *sic1 clb2*Δ cells showed a higher proportion of cells with a 2C DNA content, comparing to WT cells (Figure 36C), confirming that the deletion of *CLB2* did not suppress the G1-length defect of *sic1* cells, as previously shown (Lengronne and Schwob, 2002).

To rule out the rescue of origin firing inefficiency in *sic1* cells by *clb2*Δ*,* we measured origin-firing inefficiency in *sic1 clb2*Δ, in parallel to *clb2*Δ cells. Importantly, we found that in contrast to *clb2*Δ, *clb2*Δ *sic1* cells maintained the inefficient firing activity at *ARS507* found in *sic1* cells (Figure 35B). Given the G2/M delay observed by FACS in the double mutant, to confirm if *sic1 clb2*Δ cells were specifically defective at a particular stage of mitosis, we determined the percentage of cells in metaphase and anaphase and compared to control and single mutant cells. Immunofluorescence of tubulin in asynchronous control, *clb2*Δ, *sic1* and *sic1 clb2*Δ to examine the length of mitotic spindles and DAPI to monitor nuclear morphology was performed. Cell counts of no spindles, short spindles (2 μm) with the nucleus positioned at the bud neck (metaphase), and elongated-spindles (>2 μm) with the nucleus moving to opposite directions (anaphase), were recorded (Figure 35D). In comparison to wt cells, *clb2*Δ cells accumulated in metaphase whereas the percentage of cells in anaphase was considerably lower (Figure 35D), as expected for a Clb2 requirement in mitosis entry.

In contrast, the percentage of *sic1* cells in anaphase was much higher comparing to control cells as previously observed (Lengronne and Schwob, 2002). When combined, *sic1 clb2*Δ double mutant cells accumulate the metaphase defect of single cells, while most remarkably, the percentage of cells at anaphase greatly decreased compared to *sic1* cells (Figure 36D). These findings indicate that the deletion of *CLB2* suppressed the anaphase delay of *sic1* cells.

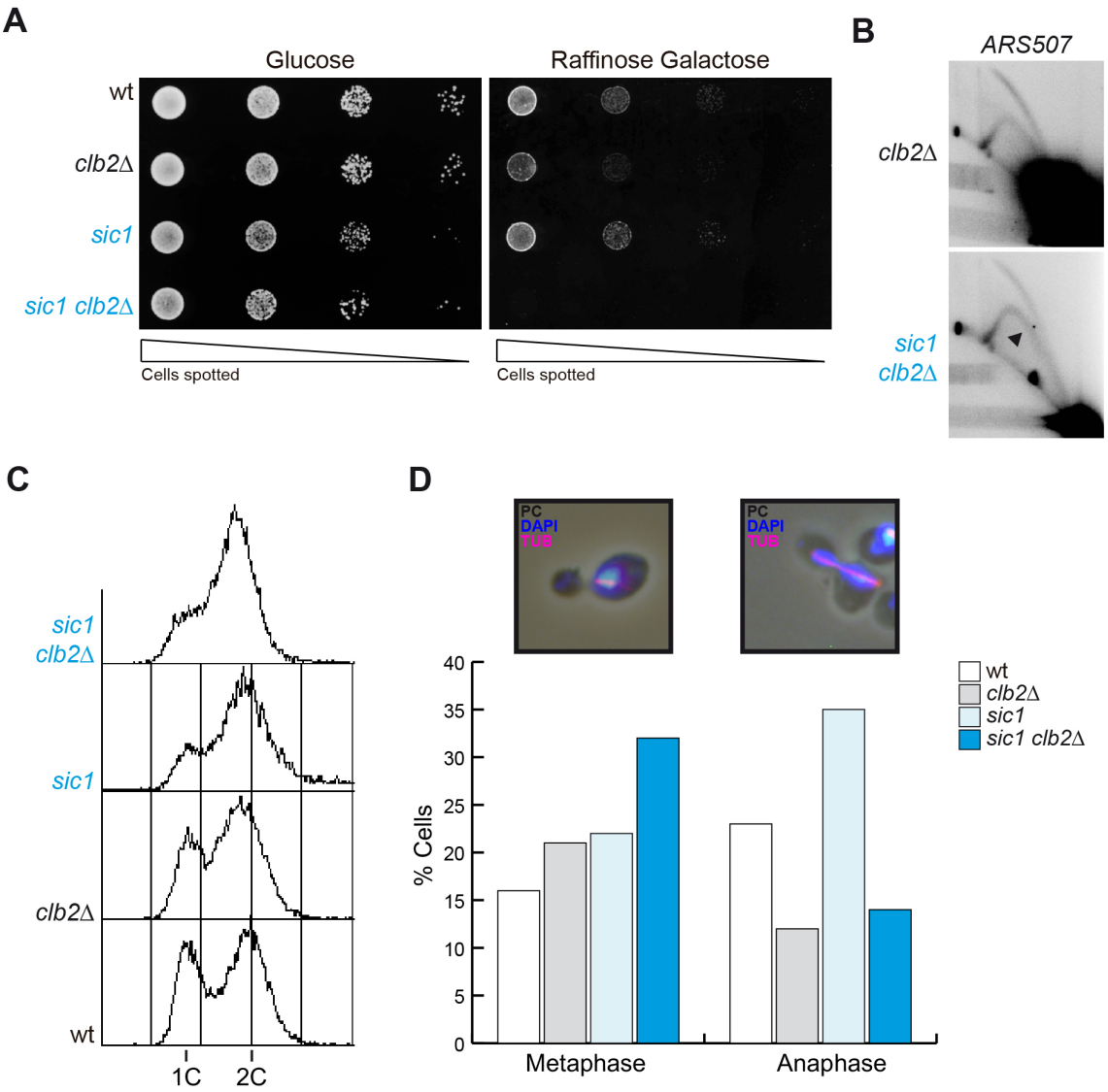

Figure 35: *clb2*Δ reverts the anaphase delay in *sic1* cells without alleviating their G1-phenotype defects. S288C wild type (YAC177), *clb2*Δ (YAC1424), *sic1* (YAC217) and *sic1 clb2*Δ (YAC1426) glucose-grown cells were analysed to determine their cell cycle distribution, nuclear morphology, spindles length, origin firing efficiency and chromosomal instability. **(A)** Dilution spotting assay. Plates were incubated 2 days at 25º C and photographed. *GAL1,10p-SIC1* strains (in blue) deplete or moderately overexpress Sic1 onto YPAD (left) or YPARG (right) plates, respectively. **(B)** Cell cycle distribution (FACS profiles) of asynchronous cells of the indicated phenotypes. **(C)** Firing efficiency of *ARS507* determined by 2D-gel analysis on asynchronous *clb2*Δ and *sic1 clb2*Δ cells. **(D)** The percentage of cells with short spindles (2 μm) with the nucleus positioned at the bud neck (metaphase) and elongated-spindles (>2 μm) with the nucleus moving to opposite directions (anaphase) was determined on tubulin- and DAPI-stained cells and represented in a graphic.

As genomic instability of *sic1* cells was suggested to be dependent on premature anaphase entry and segregation of sister chromatids still interconnected by incomplete DNA replication leading to chromosomal rearrangements, we tested whether *clb2*Δ suppressed the chromosomal instability of *sic1* cells. We performed a GCR assay on *clb2*Δ and *sic1 clb2*Δ cells, and compare the rates to the respective parental strains (Figure 37). The GCR rate of *clb2*Δ (0.4x) did not increased with respect to wild type cells (1.0x), however, *clb2*Δ caused a significant suppression of GCR rates in *sic1* cells (Figure 37, from 23-fold in *sic1* to 1.7-fold increase in *sic1 clb2*Δ). This result demonstrates that genomic instability in *sic1* cells depends on premature anaphase entry, and that artificial pre-anaphase delaying in cell cycle progression is sufficient to rescue instability even under inefficient origin usage (possibly with unreplicated chromosomes). And suggest that pre-mitosis could rescue incomplete DNA synthesis in *sic1* cells.

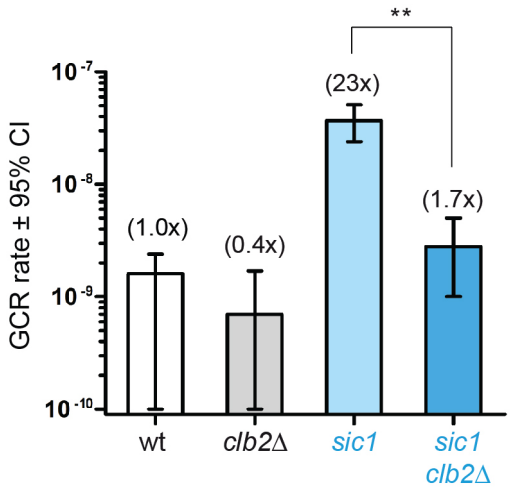

Figure 36: Chromosomal instability in *sic1* cells is greatly suppressed by *clb2*Δ. Bar charts with 95% confidence intervals of GCR rates of the same strains in Figure 36. Numbers above the bars indicate fold increase with respect to wt. GCR rates are per cell division. Asterisks indicate statistical significance: **, p<0.001.

4.2 G2/M arrest rescues incomplete DNA synthesis in *sic1* cells

If *sic1* cells enter mitosis with on-going DNA replication due to a paucity of initiation events and loss of origin redundancy, we tested whether providing extra time before mitotic entry, by arresting cells at G2/M with nocodazole, would provide enough time to *sic1* cells complete replication and resolve on-going forks. We incubated control and *sic1* cells with nocodazole for 3h to efficiently arrest cells at G_2/M and collected cells at this point for 2D-gel analysis (Figure 39).

To increase replication defects in *sic1* cells, cultures were grown at 37 ºC instead of 25 ºC (Figure 37A), a condition that aggravates origin inefficiency at origins (not shown). We monitored the cell cycle distribution of control and *sic1* cells by flow

cytometry (Figure 37B) and Sic1p levels by Western blotting of key time points (Figure 37C), so that asynchronous raff-gal grown *sic1* cells enrich with 1C content accumulated Sic1p, (Figure 37B-C, Raff Gal), in glucose *sic1* cells enrich in G2/M with undetectable Sic1p levels (Figure 37B-C, Glu 240), and in nocodazole of control and *sic1* cells block with 2C DNA content and absent Sic1p in *sic1* cells (Figure 37C, Noc 180). We noted a faint accumulation of Sic1p in nocodazole-arrested control cells that could derive from cells escaping the blockage and reaching G1 phase (Figure 37B).

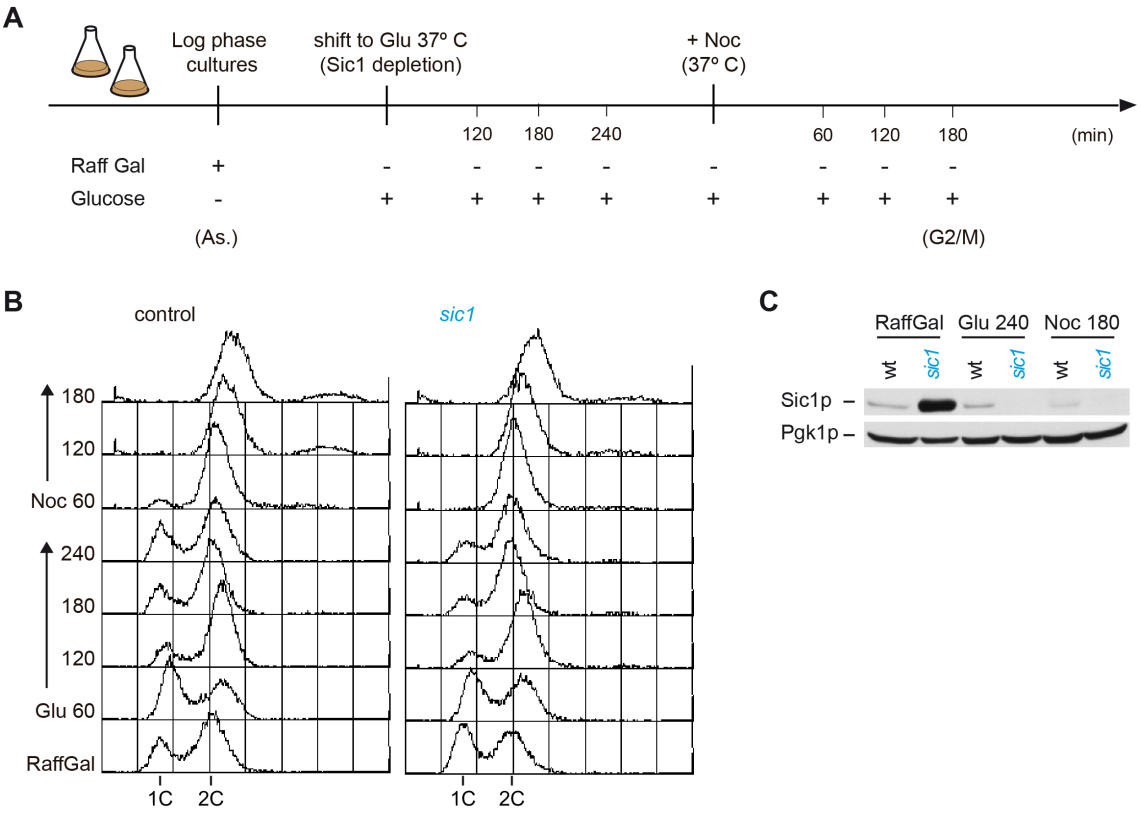

Figure 37: Control and *sic1* cells were efficiently arrested at G_2/M by nocodazole. (A) Outline of the experiment. (+) and (-) are indicative of YPARG (RaffGal)- or YPAD (Glucose)-grown cells, during the experiment. **(B)** Cell cycle distribution of control and *sic1* cells grown in raffinose-galactose media (RaffGal), shifted to glucose media (Glu), and incubated with nocodazole (Noc) monitored by FACS analysis during the experiment. (C) Protein levels of Sic1 in asynchronous raffinose-galactose-grown cells (RaffGal), after the Sic1 repression (Glu 240) and in nocodazole arrested (Noc 180) WT and *sic1* cells. Pgk1 was used as loading control.

The presence of progressing forks along the left arm of chromosome V was analysed in nocodazole-arrested control and *sic1* cells by 2D gels (Figure 39). Strikingly we found that no accumulation of RI were present in 2D blots from *sic1* cells at any region of the left arm or chromosome V, in comparison to control cells (Figure 39B), indicating that none of the regions were delayed in replication completion in nocodazole-arrested *sic1* cells. We conclude that a prolonged G2/M arrest is sufficient to compensate the delay in replication completion in cells lacking Sic1. Unexpectedly,

we detected persistent migrating signals above the Y-arc in a region proposed to contain X-shaped structures that might represent replication-termination or recombination structures. In agreement with "termination" structures, these signals specifically enrich at *HXT13-SOM1* region were termination was shown to occur more frequently in this chromosome region (Raghuraman et al., 2001).

Then, we asked whether the presence of RIs in mitosis might be more evident at the rDNA locus in *sic1* cells. The rDNA was previously found to delay in replication completion (Torres-Rosell et al., 2007c), chromosome XII displayed delayed replication completion (Figure 23), and is highly unstable in G1-phase deregulated cells (preliminary observations). 2D blots from Figure 38B were reprobed against the *rDNA* locus on chromosome XII (Figure 38C).

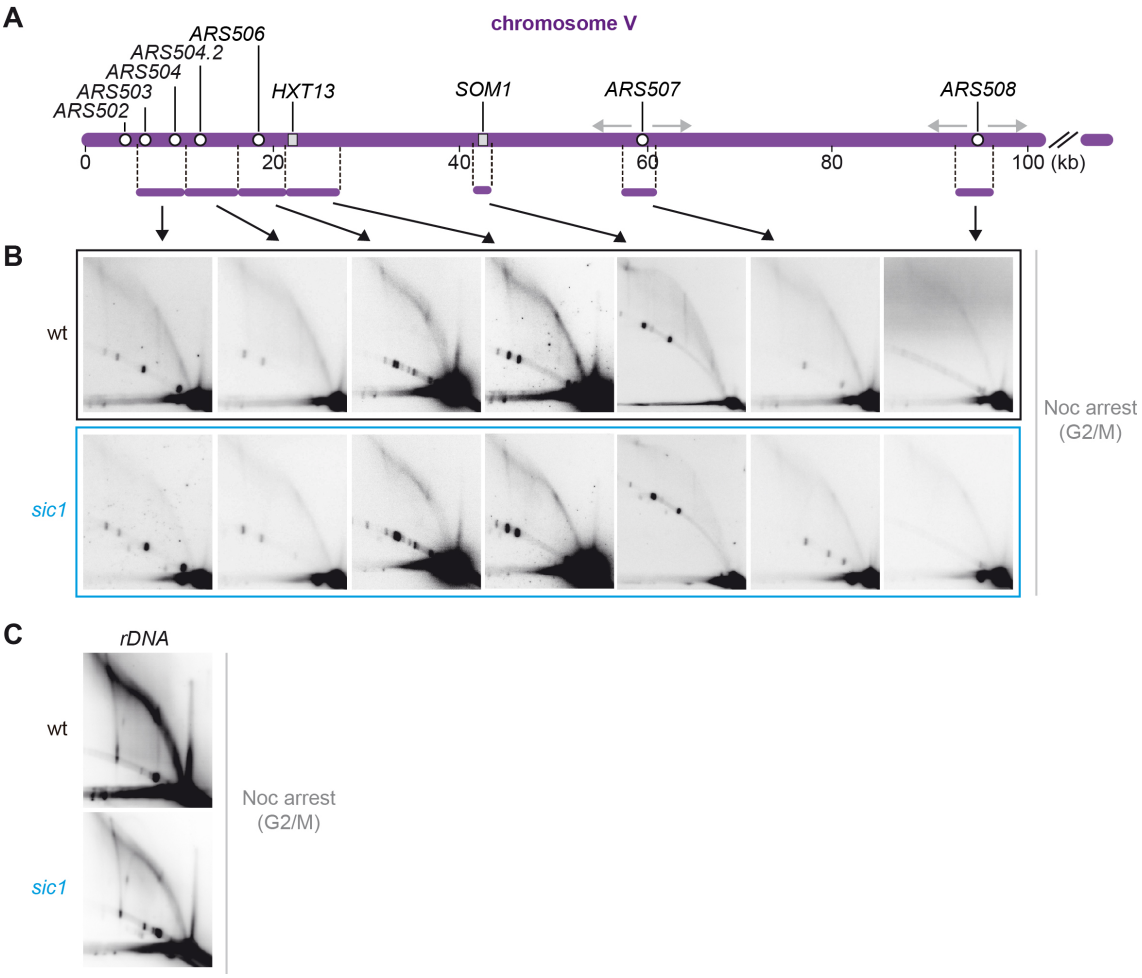

Figure 38: 2D gels of the left arm of chromosome V and the rDNA on chromosome XII in nocodazole-arrested cells. W303-1a control (YAC272) and *sic1* (YAC276) glucose-grown cells were arrested at G2/M by incubation with nocodazole (see Materials and Methods for details) and collected for 2D-gel analysis. **(A)** Schematic view of the first 100-kb of chromosome V. Horizontal bars flanked by dashed lines indicate the restriction fragment analysed. **(B)** 2D blots of the indicated fragments. **(C)** 2D blots of the rDNA locus. The same membranes from B were stripped and reprobed against the rDNA repeats.

As for chromosome V, no differential fork accumulation was detected in *sic1* cells, indicating that the delay in replication completion in *sic1* cells is compensated by delayed mitotic entry. And again, X-like arcs appeared evidencing that these structures were not specific artefacts from chromosome V. The disappearing of delayed forks in *sic1* cells by simply postponing mitosis entry is consistent with forks being not stalled, and instead functional in progressing replication. Furthermore, the absence of phosphorylated Rad53 (Supplemental Figure 2) denotes no checkpoint activation, consistent with no major replication stress present in these cells.

Overall, these results on the suppression of delayed DNA-synthesis completion and of genomic instability by delayed mitotic entry suggest that the premature initiation of chromosome segregation in the presence of unfinished DNA synthesis by on-going forks is a necessary step for cells to acquire genomic instability.

DISCUSSION

Genomic instability is a hallmark of cancer but the pathways by which it is induced during oncogenesis remain unknown. The regulators that control progression through the G1 phase of the cell cycle are frequently mutated in cancer and were proposed to be involved in the early stages of tumour development and cause genomic instability. We took advantage of budding cells lacking Sic1, the orthologous of $p27^{Kip1}$ in mammals, to identify the causes and molecular mechanism underlying the genomic instability present at G1/S deregulated cell cycles.

1. A correct G1/S transition is key to provide functional origin redundancy during S phase and prevent genomic instability

Most cancers present deregulated CDK activation during the G1 phase, which has been proposed to contribute to oncogenesis and also cause genomic instability (Ekholm and Reed, 2000; Ho and Dowdy, 2002; Malumbres and Barbacid, 2001; Rane et al., 2002; Sherr, 2000; Zhang et al., 2009). Indeed, in mammals, the overexpression of cyclin E lead to elevated levels of aneuploidy and polyploidy, consistent with a direct role in tumorigenesis (Spruck et al. 1999). Also, the ectopic overexpression of cyclin D resulting in G1/S deregulation increased genomic instability including gene amplification, which often occurs in cancer development (Zhou et al. 1996). But, what are the causes of genomic instability in tumour cells? A study using budding yeast cells shows that the overexpression of the G1 cyclin Cln2 contributes to genomic instability by inhibiting pre-RC assembly (i.e., origin licensing). Also, the authors show that the instability in these cells can be partially suppressed by integrating multiple origins, suggesting that the instability is caused by inefficient origin firing (Tanaka and Diffley, 2002). However, whether origin usage is actually inefficient, and what is abnormal in origin usage or how origin misuse could mechanistically cause genomic instability is still unknown.

The origin redundancy model proposes that a large excess of potential origins are licensed in a sufficiently regular distribution and, during S phase, only a subset is activated and fire with different activation times. In this way, if DNA gaps remain unreplicated later in S phase, late origins fire to ensure their timely replication completion (Hyrien et al., 2003). Indeed, inefficient licensing is found in mammalian oncogenic cell cycles deregulation upon misregulation of the G1/S transition (Ekholm and Reed, 2000). Also, origin firing is also inefficient in cells lacking G1-phase regulators (Ayuda-Duran et al., 2014; Lengronne and Schwob, 2002).

Here, using genetic cause-effect experiments on origin activities and genomic instability, we show that decreasing the firing activity of single origins does not affect cell viability but significantly increases chromosomal instability of cells lacking Sic1

(Figure 14 and 18) and that restoring firing efficiency at or near inefficient origins significantly suppresses instability. These results are the first demonstrating that deficient origin activity directly causes genomic instability when the G1/S transition is deregulated. Moreover, we importantly show that both early or late/dormant origin inefficiency contributes similarly to genomic instability in *sic1* cells. It is important to point that, each cell cycle, early origins are much more efficient than late/dormant origins, as for *ARS507* and *ARS504.2* (the last is weakly or never activated, Ayuda-Duran et al. (2014) and Figure 11) in *sic1* cells. This means that *ARS507* quantitatively contributes with more forks to replicate the chromosome V left arm than *ARS504.2*. Therefore, one might expect that the deletion of *ARS507* would be more harmful to the stability of the chromosomal arm than the deletion of *ARS504.2*. But then, why does *ars507*Δ and *ars504.2*Δ increased the GCR rates in *sic1* cells in a similar way (4.0x in *ars507*Δ vs. 3.0x in ars504.2Δ)? Remarkably, *ARS507* deletion lead to dormant origins activation in control cells (Figure 12C), hence counteracting delayed fork arrival to the subtelomeric region, and showing that control cells are proficient in origin redundancy. However, in *sic1* cells, dormant origins are scarcely activated when *ARS507* is deleted showing loss of origin redundancy (Figure 12C). Thus, we demonstrate that inefficiency of early origins plus loss of redundant firing by late/dormant origins together cause genomic instability in *sic1* cells (Figure 40). This strongly suggests that genomic instability arising from G1-deregulated cell cycles can be contributed by loss of dormant origins and reduced origin redundancy, as spontaneously occur in *sic1* cells (Ayuda-Duran et al. (2014), Figure 11B and Figure 18).

Notably, our data showing the spontaneous loss of dormant origin activity and origin redundancy validate suggestions posed by modelling studies on dormant origins keeping a first line of defence for the genome during S phase as if forks stall or their progression is impeded, dormant origins may be activated within these regions engaged in replication and promote the replication completion of the entire genome (Alver et al., 2014). Thus, we propose that genomic instability may not be simply due to inefficiency of few origins but mostly as a consequence of cells losing an important compensatory mechanism to respond to fork depletion with new origin firing (Figure 40). Hence, we predict that regions that stochastically concentrate less numbers of active origins due to simultaneous loss of early or dormant/late origins at nearby regions, and additionally containing fork progression impediments or being normally late-replicating, will be more prone to experience chromosomal rearrangements, ultimately suffering from genomic instability. In addiction to that, late replicating regions and fragile sites are regions prone to instability in G1-phase deregulated cells (Donley and Thayer, 2013).

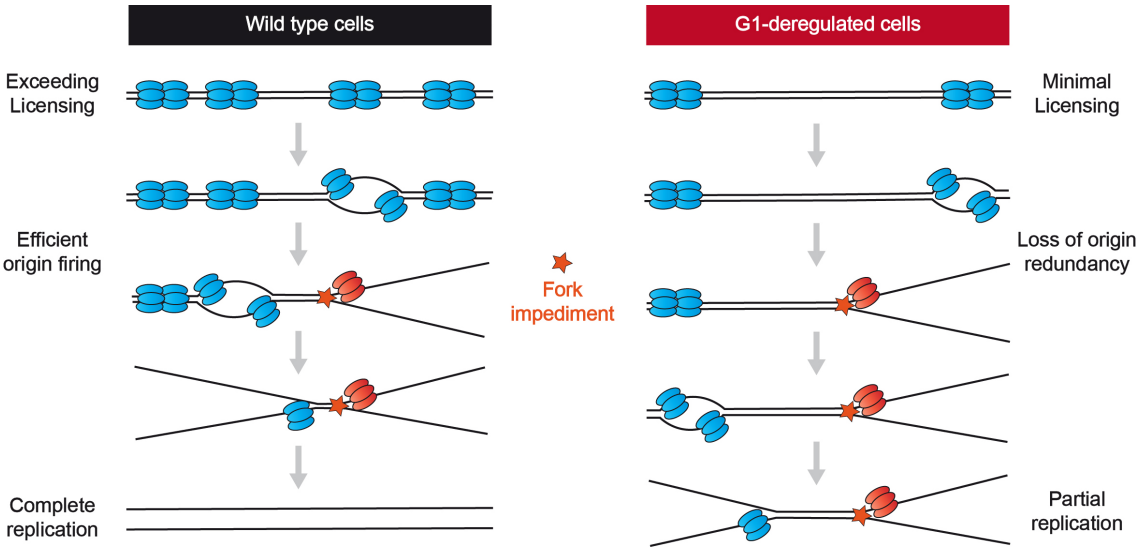

Figure 39: Model of G1-deregulated cells suffering from loss of origin redundancy to counteract natural fork pausing sites or stochastic impediments to fork progression leading to partial replicated chromosomes.

2. Loss of G1 control sensitizes chromosomal regions to fragility upon fork-delaying elements toward genomic instability

A significant association between fragile sites and chromosome aberrations in tumour cells has been demonstrated in different studies (Hecht and Glover 1984; Mangelsdorf et al. 1999; Yunis and Soreng, 1984). Indeed, most of all gross chromosomal rearrangements accumulating in solid tumours occur at fragile sites (Gorgoulis et al., 2005; Negrini et al., 2010). Different models propose that common fragile sites correspond to regions of the genome that replicate very slow as they contain secondary structures or pausing sites that may impair fork progression resulting in replication stress (Lucas et al., 2007; Rahat et al., 2007; Durkin and Glover, 2007). Apart from this possibility, a new concept proposed by Debatisses' group suggest a role for replication origin density in determining the fragility of CFS. The idea is based on a study showing that the region FRA3B is constitutively fragile in lymphoblastic cells but not in fibroblasts, and propose that its fragility is not due to fork slow or stalling but to a scarcity of replication initiation events that forces forks to travel longer distances to finish replication (Letessier et al., 2011b).

To simulate a fragile-like site without disturbing DNA replication with drugs, we create an impediment to fork progression by inserting a fork barrier element at the subtelomeric region of chromosome V that is flanked by low efficient origins. We show that a fork barrier element caused a dramatic increase in the genomic instability of *sic1* cells, when compared to control (Figure 33, 351x and 19x, respectively), suggesting a

strong correlation between impediments to fork progression at regions that lack of origin redundancy leading to extreme genomic instability. Indeed, the fold increase we obtained for the genome instability of *sic1* cells carrying the RFB element has a similar order of magnitude to those observed for S-phase checkpoint mutants treated with low doses of the alkylating agent methyl methane sulfonate (Kolodner et al. (2002), 12,000 to 14,000-fold increase). Importantly, the sensitivity to the RFB in *sic1* cells in correlation with dormant origins failure strongly suggests that they are mechanistically related. One might think that the increased instability in *sic1* cells is due to defective fork pausing at programmed pausing sites in *sic1* than in control cells. However, fork pausing is equally efficient in control and *sic1* cells (Figure 28B-C), discarding this possibility. Alternatively, we found that loss of redundant firing at dormant origins together with inefficient activity of early origins cause the elevated instability (Figure 14 and Figure 18).

In this thesis we demonstrate that origin redundancy is lost when cells enter prematurely in S phase, furthermore evidenced when forks face DNA replication delays by transient fork impediments due to replication fork barriers (Figure 32B). We believe that genomic instability caused by the fork barrier is due to deficient replication initiation events as the instability is greatly suppressed if origin firing is restored downstream to RFB-paused forks by inserting a plasmid carrying multiple origins *ARSH4* (Figure 35). Remarkably, it is interesting to note that *sic1* cells fire those origins *ARSH4* but not control cells (Figure 34B). One possibility is that activated dormant origins in control cells replicate *ARSH4* passively thereby inactivating them, whereas *sic1* cells that lack of functional origin redundancy, fail to activate dormant origins in most cells, relying on the activation of origins *ARSH4* to help complete replication. Altogether, these results show that a precise control of the G1/S transition by Sic1 is necessary to ensure functional origin redundancy during S phase which is crucial to counteract impediments to fork progression that may arise naturally during DNA replication like fork blocking elements, secondary structures on DNA or other impediments.

According with our data, we presume that more forks will be delayed in reaching the chromosome end that now relies on long-travel forks to replicate the telomere. Therefore, it is possible that the chromosome is not fully replicated by the end of S phase. A commonly proposed scenario of oncogenic G1-deregulated cell cycles is that cells undergo mitosis prematurely regarding replication completion, with surveillance mechanisms failing in detecting small amounts of on-going forks (Bielinsky, 2003; Magiera et al., 2014; Sidorova and Breeden, 2003; Teixeira et al., 2015). Importantly, our results fully support that origin firing inefficiency and reduced origin redundancy might coincide with regions of programmed or eventual fork progression impediments,

as fragile sites, to enhance their instability in G1-deregulated cell cycles, thus mechanistically explaining the higher expression of fragile sites in cancer cells. Our data in the light of human CFS instability in oncogenic cell cycles support that CFS expression is favoured in regions deprived of replication initiation events in addition to forks elongation defects, so that both contribute to fragility, rather than only by a scarcity of origins. Moreover, we propose that regions spontaneously losing origin activity upon CDK deregulation and spatially coincide with any impediment to fork progression will commit cells to fragility if they enter prematurely in mitosis with replication completion defects.

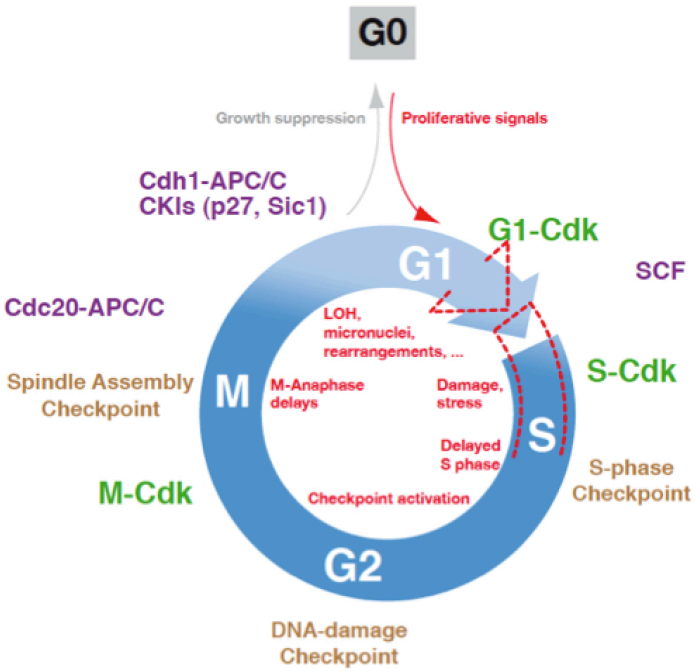

Figure 40: Schematic view of a G1-deregulated cell cycle. A premature G1/S transition will delay S phase completion due to less replication initiation events and compromise replication completion at regions concentrating more inactive origins. As a consequence, cells may escape surveillance mechanisms and enter mitosis with on-going replication resulting in DSBs during anaphase, which ultimately leads to genomic instability.

Finally, it has been suggested in the context of human CFS instability that long travelling forks emanating from an early domain may accidently disassembly the replisome before merging with forks from the late domain if fork progression is blocked either by accidental formation of secondary structures or programmed pause sites (Debatisse et al., 2012) that exist both in *S. cerevisiae* and human cells (Mirkin and Mirkin, 2007). Supporting this idea, we observe a depletion of RI at the left end of chromosomes V, suggesting a reduction of forks progressing through the subtelomeric and telomeric regions after being released from the fork barrier (Figure 36B, *ARS503*-

4, ARS504.2, ARS306 but not *CIN8*), with the same phenotype observed in another *S. cerevisiae* background in the same conditions (Supplemental Figure 1B, *sic1 RFB-chrV*). However, *sic1* cells do not show evidences of fork stalling at pausing sites (lack of X-like recombination intermediates in our 2D gels at pausing sites), nor fork-paused molecule accumulation at pausing sites (identical signal of pausing spots in our 2D gels), nor even signs of replication stress (absence of phospho-Rad53 or activated Rad53, phospho-H2A, or Rad52 requirements, Supplemental Figure 2) despite the hundreds of pausing sites widespread along the budding yeast genome, ruling out this possibility.

3. A premature entry into S phase alters the replication timing program at specific chromosomal regions to delay replication completion

G1 phase is the preparatory phase for DNA replication where origin licensing occurs, thus it is not surprising that interferences with G1 length (or regulation) frequently result in an impaired S phase with inefficient origin usage (Ekholm-Reed et al., 2004; Rizzardi and Cook, 2012; Sidorova and Breeden, 2003; Teixeira et al., 2015). Here, aside from revealing that inefficient origin firing cause genomic instability upon Sic1 depletion, we have identified the primary molecular mechanism by which the genomic instability arises in G1/S deregulated cell cycles. We show that during the first S phase after Sic1 loss, the replication timing of specific chromosomal regions (like the subtelomeric region of chromosome V) desynchronizes and the completion of DNA synthesis delays in the cell population (Figure 22). Importantly, this region displays loss of origin redundancy (Ayuda-Durán et al., 2014, 2D-gels of *ARS507*, *ARS504.2*). Two possibilities exist to explain the delayed replication completion observed in *sic1* cells. First, fork progression rates are reduced in the mutant such that forks delay in replicating the subtelomeric region. And second, not mutually exclusive with the first hypothesis, reduced origin activity and redundancy surrounding the subtemoleric region provoke that replication of the region rely on forks departing from distant origins that thus need to travel longer distances to reach the subtelomeric region and replicate the region late in S phase. Importantly, longer replicons at non specific regions accumulate in *sic1* cells (Lengronne and Schwob, 2002) consistent with this second possibility. Moreover, our data on the synchronic replication dynamics of *sic1* cells evidence that forks from early origins take about the same time (~30 minutes) to reach the telomere (Figure 21) than control cells (Figure 20), indicating no defects in fork progression rates in *sic1* cells. Finally, supporting the second possibility, replication of

the normally early region surrounding *ARS507* is delayed in replication completion in *sic1* cells due to *ARS507* inefficiency (Figure 26).

Replication dynamics is also delayed in chromosome XII (Figure 27 A-B). However, the efficiency of origins within the *rDNA* locus is not defective in *sic1* cells (Figure 27C), and hence it is difficult to relate delayed completion of chromosome XII synthesis with origin usage as for chromosome V, unless first, since all *rDNA ARS* are equal, 2D gels show the average efficiency of all origins, instead of the frequency of origin activation within each repeat unit. Or, second, origins efficiencies outside of the *rDNA* locus were not studied and incoming forks from nearby regions will surely influence the replication dynamics of the region. However, the rDNA is enriched in fork pausing sites that delay fork progression and lead this region to be late replicating. Indeed, recent results from the laboratory show that chromosome XII is unstable in *sic1* cells and show frequent variations in size (not shown).

Importantly, replication completion problems ensue irregularly along the genome in *sic1* cells. In contrast to chromosomes V and XII, DNA synthesis is not delayed at the left arm of chromosome III in *sic1* cells (Figure 26). Notably, this region do not suffer from a scarcity of active origin, as the timing and efficiency of origins within the chromosome III left arm is similar to control cells (Figure 24 and 25; Ayuda-Durán et al, 2014). Altogether, our findings are consistent with delayed completion of DNA synthesis arising at specific large chromosomal regions deprived of origin firing upon CDK deregulation, or enriched in fork progression impediments, rather than occurring randomly at all chromosomes or at particular domains as telomeres.

But what might be the biological consequences of delayed replication completion? The existence of aberrant replication timing in many genetic diseases, including cancer, suggest that preserving the correct timing of DNA synthesis is a vital cellular process. Actually, increasing evidences exist that replication timing contribute to the distribution of genomic changes that arises during cancer development (Donley and Thayer, 2013), suggesting that perturbations in DNA replication timing is linked with genome instability. An additional unstable feature of mammalian chromosomes is the presence of CFS that were found to coincide at regions of delayed replication completion. The mechanism of fragile site expression in cancer cells could be a paucity of initiation events, helped by delayed fork progression, leading to delays in replication completion, incomplete replication in mitosis, and chromosome breakage (Debatisse et al., 2012)

Having this in mind, our results provide evidences that changes in the replication timing program at specific regions of the genome by irregular losses of origin efficiency and distribution of fork progressing impediments characterize the first molecular events

leading to genomic instability when the G1 control is lost, which could be in fact a common feature of cancer cells. Hence we conclude that a correct G1/S transition promoted by G1 regulators is needed to avoid replication completion problems at chromosomal regions deficient in initiation events.

Our data sustain previous suggestions that, upon G1 phase deregulation as for overexpression of cyclin E in human cells, partial DNA synthesis enrich at particular regions by the end of S phase, like fragile sites, subtelomeric regions and others, leading to on-going replication during mitosis (Teixeira et al., 2015).

4. Genomic instability by precocious G1/S transition can be largely suppressed later in the cell cycle

Our data show an essential role for Sic1 in the timely completion of DNA synthesis before cells enter mitosis by promoting a functional origin redundancy during S phase, possibly through the licensing of a sufficient number of origins in late G1 as suggested by Lengronne and Schwob (Lengronne and Swchob, 2012). As a consequence of the lack of Sic1, cells accumulate at mid-anaphase with a high frequency of Ddc1 foci (denoting DNA damage) that are specific of mitosis and produced after cells undergo anaphase (Lengronne and Schwob, 2012). Importantly, the number of Ddc1 foci decreases when cells are incubated with nocodazole, consistent with the damage being posterior to anaphase. The authors hypothesized that the possible delay of S phase dynamics might hinder the normal chromosome segregation during anaphase and cause genomic instability. However, it was not addressed whether the defects that accumulate *sic1* cells in anaphase contributes to its genomic instability and can be reverted by non-G1 manipulation. Here we show that the instability of *sic1* cells is greatly suppressed when cells are delayed in mitotic entry by deleting *CLB2* (Figure 37). These results provide two important conclusions. First, that *sic1*'s instability depends on cells entering mitosis anaphase prematurely. And, second, that the defects occurring during G1 and S phase as a consequence of the lack of Sic1 can be compensated later in the cell cycle. Indeed, we show that the suppression of the instability occurs without alleviating the G1-phenotype defect of *sic1* cells, that is, its short G1 length (Figure 36C) or restoring origin efficiency defects (Figure 36B). According to the initial hypothesis, these evidences are consistent with and support the idea of DNA replication completion being uncoupled from mitosis entry. In further support of this view, we show a clear rescue of replication intermediates in nocodazole-arrested cells in *sic1*'s chromosomes V and XII (Figure 39), including the regions replicating later than usual in *sic1* cells (Figure 22 and Figure

27B), indicating that blocking mitosis entry upon Sic1 depletion compensate replication completion defects.)

In budding yeast, DNA damage or stalled DNA replication is sensed by checkpoints that prevent the anaphase onset by activating specific signal transduction pathways that converge on Mec1 and Rad53 kinases for biological responses (Lowndes and Murguia, 2000). Nevertheless, apart of this, the notion that cells may lack of a surveillance mechanism to prevent entering mitosis with small amounts of on-going replication during an unperturbed S phase (no checkpoint activation) has been proposed (Schwob, 2004; Torres-Rosell et al., 2007a; Torres-Rosell et al., 2007b). Consistent with this idea, *sic1* cells do not trigger the S/M checkpoint as signs of Rad53 hyperphosphorylation were not detected by Western blot or *in situ* kinase assay in asynchronous *sic1* cells (Supplemental Figure 3A). Indeed, *sic1* cells accumulate in anaphase, rather then metaphase, as expected for a checkpoint activation arrest dependent on *MEC1* and *RAD53* (Lengronne and Schwob, 2002). Moreover, mutations on *RAD9*, *MEC1* and *PDS1* (coding for checkpoint components involved in the metaphase arrest and prevention of the mitotic exit) did not rescue the mitosis defects of *sic1* cells, nor the disruption of *MAD1* and *BUB2* (coding for components of the SAC), suggesting that their mitotic delay is not dependent on known S/M or SAC checkpoints (Lengronne and Schwob, 2002). However, the partial separation of chromosome arms in *sic1* cells during anaphase suggests that sister chromatids are still interconnected, possibly at unreplicated regions (Lengronne and Schwob, 2002).

But why then the checkpoint is not activated if a subpopulation of *sic1* cells may still have on-going replication as they enter mitosis? It was proposed that in case of the checkpoint fail to be activated, cells might rely on other mechanisms to ensure replication completion before mitosis such as the reservoir of unlicensed origin or the absence of centromeres replication (Torres-Rosell et al, 2007; Magiera et al., 2014). For instance, in yeast cells lacking *CLB5* and *CLB6* and engineered in a way that S phase onset is postponed by 30 minutes without affecting its duration (*clb5,6*Δ cells), their delayed S phase was able to transiently restrain mitosis (Magiera et al., 2014). This mechanism involves the transient activation of the SAC (Mad2) when kinetochores detach from microtubules upon centromere replication that prevent mitosis while DNA replication is on-going. Notably, when *MEC1* was deleted in these cells, they now suffered from increased DSBs/Rad52 foci, possibly as a result of precocious spindle extension with on-going forks that are not signalled and cells undergo anaphase before having finished DNA synthesis, indicating a role for the S-phase checkpoint (Mec1) on holding mitosis when S phase is postponed (Magiera et al., 2014). Similar to *clb5.6*Δ cells, *sic1* cells also have an extended S phase and some

regions replicate later than usual, when compared to the control (Figure 22 and 27). However, because late-replicating loci likely represent a small percentage of the genome, fewer on-going forks may not be sufficient to activate anaphase-delaying mechanisms (checkpoints), likely behaving as *mec1*Δ cells. Additionally, one important difference exist between *clb5,6*Δ and *sic1* cells regarding their delayed S phase. While in *clb5,6*Δ cells S phase occurs later but takes about the same time than wild-type cells, *sic1* cells in contrast initiate S phase earlier than wild-type cells but it takes longer to be completed. Thus, It is tempting to speculate that because replication starts at the same time, if not earlier, than the control, then most *sic1*'s centromeres might replicate earlier in S phase, rather than being all lately replicating as in the case of *clb5,6*Δ cells. In this way, it is unlikely that the SAC may be holding the mitosis entry in *sic1* cells due to detached kinetochores upon delayed replication of centromeres, as we predict that it may not occur frequently or, if it does, it is restricted to a few cells with centromeres surrounded by low efficient orgins upon CDK deregulation. Alternatively, it is more likely that anaphase-delaying signals might fall below threshold detection in *sic1* cells after all kinetochores have been replicated and when the number of active forks drops, as suggested for other yeast mutants driving replication with fewer forks and entering anaphase with incompletely replicated chromosomes (Torres-Rosell et al., 2007; Dulev et al., 2009). In support of this, Rad52 (a recombinase involved in the repair of DNA DSBs) is not required for survival of *sic1* cells (Supplemental Figure 3B), indicating that the repair of the damage in *sic1* cells do not require Rad52, in disparity of what occurs in *clb5,6*Δ cells.

In conclusion, our results are consistent with forks still progressing and not stalled when *sic1* cells enter mitosis, as giving extra time to fork elongation by delaying the anaphase onset greatly suppresses its genomic instability and reverts replication completion defects. Thus, similar of what occurs in *sic1* cells, we propose that when G1/S transition is deregulated, genomic instability is triggered by a low reservoir of licensed origins to compensate for eventual replication fork failure during S phase. As a consequence, late-replicating regions may remain unreplicated by the end of S phase and because on-going forks are probably a few regarding all the genome, a risk exist that cells with replicated centromeres escape surveillance mechanisms and enter mitosis with still-on-going replication, possibly resulting in chromosome breaks upon attempts to segregate still interconnected sister chromatids and ultimately causing genomic instability.

5. Origin redundancy model of genomic instability in G1-deregulated cell cycles

Sic1 plays a pivotal role during the G1 phase by allowing cells to license a sufficient number of origins necessary for the timely completion of S phase before mitosis, and also by controlling the fine tuning of the Clb5,6/Cdc28 activity at the G1/S transition, important for the precise temporal activation of origins. When cells undergo G1 without the Sic1, complexes Clb5,6/Cdc28 are precociously activated as they fail to be inhibited by Sic1 and become available as soon as *CLB5* and *CLB6* are synthesize. As a consequence, the assembly of pre-RCs is blocked by the premature increasing levels of CDK activity, possibly impeding origin licensing in late G1. This result in a premature S phase entry and DNA replication driven from a reduced number of origins, such that inter-origin distances are longer and forks have to travel longer distances. If large regions of chromosomes lack active origins, it is possible that adjacent forks are unable to travel far enough, leaving unreplicated stretches of DNA in between. Additionally, long-travel forks are more prone to stall. Moreover, our analysis on replication dynamics of *sic1* cells show that particular chromosomal regions that accumulate more inactive origins, either early or late/dormant origins, are delayed in completing replication, possibly because forks take longer to meet and converge with other forks or reach the telomere. Importantly, the reservoir of origins is reduced in cells lacking Sic1 to counteract fork stalling or fork progression delays as we show that a functional origin redundancy is lost. Furthermore, long-travel forks encounter impediments to fork progression such as natural fork pausing sites or aberrant secondary structures on DNA, may delay the replication completion until very late in S phase or even remain unreplicated. Because a reduced number of on-going forks may fail bellow the threshold to trigger a checkpoint response, also because forks are not stalled but still on-going, cells may enter mitosis with still replicating chromosomes. Indeed, to date, no such mechanisms capable of preventing mitosis by directly detecting on-going forks when centromeres are already replicated were described. Therefore, cells undergoing anaphase prematurely before complete DNA synthesis may result on DSBs upon failure to spindle extension of still-interconnected chromatids at unreplicated DNA (Figure 42)

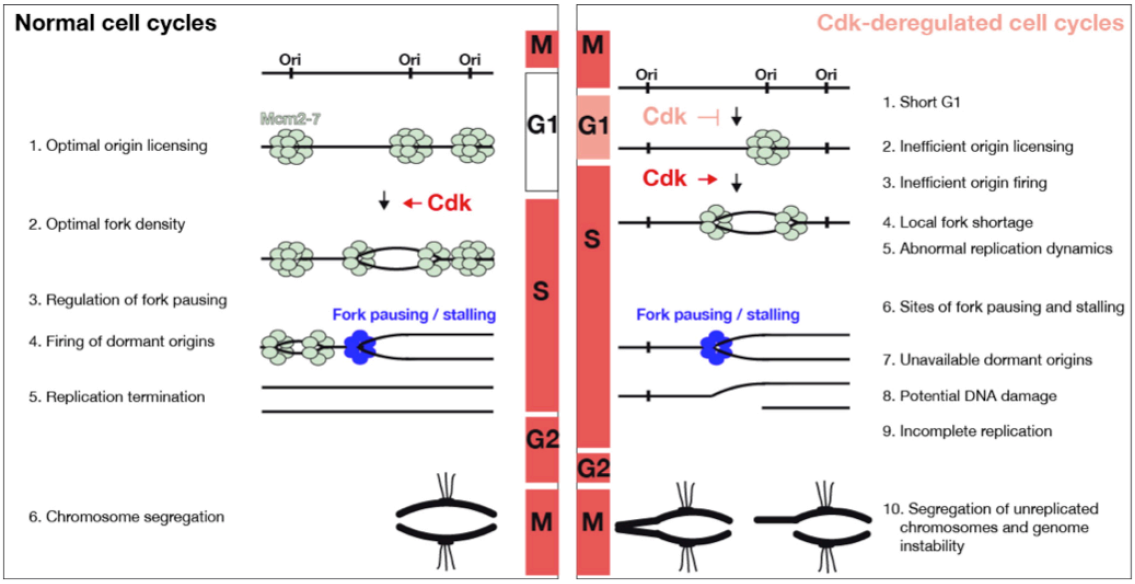

Figure 41: Model of CDK-deregulated cell cycles. A short G1, as in the case of cells lacking Sic1, result in less efficient origin firing which delays replication completion at particular regions of the genome that loss a higher number of active origins. As a consequence, because dormant origins are not available to counteract stalled forks or fork progression delays, chromosomes may enter prematurely in mitosis and attempts to segregate sister chromatids that are still interconnected may result in chromosome breaks and genomic instability.

6. G1 phase CKI as possible targets to prevent cancer

CDK misregulation is one of the most frequent alterations in human cancer. In contrast to *S. cerevisiae*, different CDK and not only one associate with different cyclins to form active complexes and regulate the mammalian cell cycle. For instance, CDK 4, 5 and 6 mainly associate with cyclin D family and function during the G0/G1 phases of the cycle, while CDK2 more commonly associates with cyclin A and E and functions during the G1 phase and also during the G1-S transition.

The frequent lost of G1 regulation is suggested to confer a proliferative advantage to cancer cells. Following this rationale, the targeting of cyclin-CDK complexes to block CDK activity are considered good strategies for anti-cancer therapy as the cell cycle arrest of cancer cells by CDK inhibition could induce apoptosis (Fukasawa 2012). Indeed, a high number of CDK inhibitors have been developed as anti-proliferation agents for the cell cycle arrest or apoptosis of aberrant cells, including purines (as Purvalanol or Roscovitine), pyrimidines (as CINK4), flavonoids (as Flavopiridol), natural products (as Hymenialdisine isolated form marine sponge or Butyrolactone I isolated from *Aspergillus*), among others (Singh et al 2012).

Based in the finding we achieve in this thesis, it is tempting to propose that the overexpression of the CKI $p27^{Kip1}$ may result in a good strategy to prevent cancer if, in similarity of what occur when Sic1 is overexpressed in yeast cells, a large enough G1 length result in an excessive licensing of origins. Actually, increasing the redundancy

mechanism of origin usage could be of a major value to counteract hindered forks during DNA replication, ultimately avoiding chromosomal breaks and rearrangements that are known to be a driving force of oncogenesis.

CONCLUSIONS

The conclusions obtained with this thesis were the following:

1. Cells lacking Sic1 loss origin redundancy by inefficiency of early and late/dormant origins at specific chromosomal regions.

2. Lack of functional origin redundancy causes chromosomal instability upon Sic1 loss.

3. Chromosomal instability at specific regions can be suppressed by increasing the number and distribution of functional dormant origins in cells lacking Sic1.

4. The loss of Sic1 delays the dynamics of replication completion at specific chromosome regions deficient in origin activity.

5. Replication fork barriers have deleterious effects on chromosome stability at regions that lost origin redundancy by the lack of Sic1.

6. A prolonged G2/M cell-cycle arrest rescues delayed replication completion in cells lacking Sic1.

7. Genomic instability in *sic1* cells depends on unscheduled mitotic entry and can be suppressed by retaining cells prior to anaphase.

Las conclusiones que se obtuvieron en esta tesis son:

1. Células sin Sic1 pierden redundancia de orígenes por ineficiencia de orígenes tempranos y tardíos/durmientes en regiones cromosómicas específicas.

2. La pérdida de redundancia funcional de orígenes causa inestabilidad cromosómica tras la pérdida de Sic1.

3. La inestabilidad cromosómica en regiones específicas se puede suprimir incrementando el número y distribudión de orígenes durmientes funcionales en células sin Sic1.

4. La pérdida de Sic1 retrasa la dinámica de finalización de la replicación en regiones cromosómicas específicas deficientes en actividad de orígenes.

5. Las barreras de horquillas de replicación tienen efectos deletéreos en la estabilidad cromosómica de regiones que pierden redundancia de orígenes por la pérdida de Sic1.

6. Una parada prolongada del ciclo celular en G2/M rescata los retrasos en finalización de la replicación en células carentes de Sic1.

7. La inestabilidad genómica en células sin Sic1 depende de una entrada prematura en mitosis y puede ser suprimida reteniendo las células antes de anafase.

BIBLIOGRAPHY

Aladjem, M.I., Rodewald, L.W., Lin, C.M., Bowman, S., Cimbora, D.M., Brody, L.L., Epner, E.M., Groudine, M., and Wahl, G.M. (2002). Replication initiation patterns in the beta-globin loci of totipotent and differentiated murine cells: evidence for multiple initiation regions. Mol Cell Biol *22*, 442-452.

Alver, R.C., Chadha, G.S., and Blow, J.J. (2014). The contribution of dormant origins to genome stability: from cell biology to human genetics. DNA Repair (Amst) *19*, 182-189.

Alvino, G.M., Collingwood, D., Murphy, J.M., Delrow, J., Brewer, B.J., and Raghuraman, M.K. (2007). Replication in hydroxyurea: it's a matter of time. Mol Cell Biol *27*, 6396-6406.

Amiel, A., Kirgner, I., Gaber, E., Manor, Y., Fejgin, M., and Lishner, M. (1999). Replication pattern in cancer: asynchronous replication in multiple myeloma and in monoclonal gammopathy. Cancer Genet Cytogenet *108*, 32-37.

Amiel, A., Litmanovitch, T., Lishner, M., Mor, A., Gaber, E., Tangi, I., Fejgin, M., and Avivi, L. (1998). Temporal differences in replication timing of homologous loci in malignant cells derived from CML and lymphoma patients. Genes Chromosomes Cancer *22*, 225-231.

Aparicio, J.G., Viggiani, C.J., Gibson, D.G., and Aparicio, O.M. (2004). The Rpd3-Sin3 histone deacetylase regulates replication timing and enables intra-S origin control in Saccharomyces cerevisiae. Mol Cell Biol *24*, 4769-4780.

Aparicio, O.M. (2013). Location, location, location: it's all in the timing for replication origins. Genes Dev *27*, 117-128.

Aparicio, O.M., Stout, A.M., and Bell, S.P. (1999). Differential assembly of Cdc45p and DNA polymerases at early and late origins of DNA replication. Proc Natl Acad Sci U S A *96*, 9130-9135.

Arlt, M.F., Durkin, S.G., Ragland, R.L., and Glover, T.W. (2006). Common fragile sites as targets for chromosome rearrangements. DNA Repair (Amst) *5*, 1126-1135.

Ayuda-Duran, P., Devesa, F., Gomes, F., Sequeira-Mendes, J., Avila-Zarza, C., Gomez, M., and Calzada, A. (2014). The CDK regulators Cdh1 and Sic1 promote efficient usage of DNA replication origins to prevent chromosomal instability at a chromosome arm. Nucleic Acids Res *42*, 7057-7068.

Baker, T.A., Sekimizu, K., Funnell, B.E., and Kornberg, A. (1986). Extensive unwinding of the plasmid template during staged enzymatic initiation of DNA replication from the origin of the Escherichia coli chromosome. Cell *45*, 53-64.

Barberis, M., De Gioia, L., Ruzzene, M., Sarno, S., Coccetti, P., Fantucci, P., Vanoni, M., and Alberghina, L. (2005). The yeast cyclin-dependent kinase inhibitor Sic1 and mammalian p27Kip1 are functional homologues with a structurally conserved inhibitory domain. Biochem J *387*, 639-647.

Barberis, M., Spiesser, T.W., and Klipp, E. (2010). Replication origins and timing of temporal replication in budding yeast: how to solve the conundrum? Curr Genomics *11*, 199-211.

Bartek, J., and Lukas, J. (2007). DNA damage checkpoints: from initiation to recovery or adaptation. Curr Opin Cell Biol *19*, 238-245.

Bartkova, J., Rezaei, N., Liontos, M., Karakaidos, P., Kletsas, D., Issaeva, N., Vassiliou, L.V., Kolettas, E., Niforou, K., Zoumpourlis, V.C*., et al.* (2006). Oncogene-induced senescence is part of the tumorigenesis barrier imposed by DNA damage checkpoints. Nature *444*, 633-637.

Bell, S.P., and Dutta, A. (2002). DNA replication in eukaryotic cells. Annu Rev Biochem *71*, 333-374.

Bell, S.P., and Stillman, B. (1992). ATP-dependent recognition of eukaryotic origins of DNA replication by a multiprotein complex. Nature *357*, 128-134.

Bensimon, A., Aebersold, R., and Shiloh, Y. (2011). Beyond ATM: the protein kinase landscape of the DNA damage response. FEBS Lett *585*, 1625-1639.

Berbenetz, N.M., Nislow, C., and Brown, G.W. (2010). Diversity of eukaryotic DNA replication origins revealed by genome-wide analysis of chromatin structure. PLoS Genet *6*, e1001092.

Bielinsky, A.K. (2003). Replication origins: why do we need so many? Cell Cycle *2*, 307-309.

Blow, J.J., and Dutta, A. (2005). Preventing re-replication of chromosomal DNA. Nat Rev Mol Cell Biol *6*, 476-486.

Blow, J.J., and Ge, X.Q. (2009). A model for DNA replication showing how dormant origins safeguard against replication fork failure. EMBO Rep *10*, 406-412.

Blow, J.J., Ge, X.Q., and Jackson, D.A. (2011). How dormant origins promote complete genome replication. Trends Biochem Sci *36*, 405-414.

Bras, A., Cotrim, C.Z., Vasconcelos, I., Mexia, J., Leonard, A., Sanzhar, I., Akhmatullina, N., and Rueff, J. (2008). Asynchronous DNA replication detected by fluorescence in situ hybridisation as a possible indicator of genetic damage in human lymphocytes. Oncol Rep *19*, 369-375.

Brewer, B.J., and Fangman, W.L. (1987). The localization of replication origins on ARS plasmids in S. cerevisiae. Cell *51*, 463-471.

Brewer, B.J., and Fangman, W.L. (1988). A replication fork barrier at the 3' end of yeast ribosomal RNA genes. Cell *55*, 637-643.

Brewer, B.J., and Fangman, W.L. (1991). Mapping replication origins in yeast chromosomes. Bioessays *13*, 317-322.

Brewer, B.J., and Fangman, W.L. (1993). Initiation at closely spaced replication origins in a yeast chromosome. Science *262*, 1728-1731.

Burgers, P.M. (2009). Polymerase dynamics at the eukaryotic DNA replication fork. J Biol Chem *284*, 4041-4045.

Calzada, A., Hodgson, B., Kanemaki, M., Bueno, A., and Labib, K. (2005). Molecular anatomy and regulation of a stable replisome at a paused eukaryotic DNA replication fork. Genes Dev *19*, 1905-1919.

Calzada, A., Sanchez, M., Sanchez, E., and Bueno, A. (2000). The stability of the Cdc6 protein is regulated by cyclin-dependent kinase/cyclin B complexes in Saccharomyces cerevisiae. J Biol Chem *275*, 9734-9741.

Cha, R.S., and Kleckner, N. (2002). ATR homolog Mec1 promotes fork progression, thus averting breaks in replication slow zones. Science *297*, 602-606.

Chen, C., and Kolodner, R.D. (1999). Gross chromosomal rearrangements in Saccharomyces cerevisiae replication and recombination defective mutants. Nat Genet *23*, 81-85.

Chen, C.L., Rappailles, A., Duquenne, L., Huvet, M., Guilbaud, G., Farinelli, L., Audit, B., d'Aubenton-Carafa, Y., Arneodo, A., Hyrien, O.*, et al.* (2010). Impact of replication timing on non-CpG and CpG substitution rates in mammalian genomes. Genome Res *20*, 447-457.

Chen, S., and Bell, S.P. (2011). CDK prevents Mcm2-7 helicase loading by inhibiting Cdt1 interaction with Orc6. Genes Dev *25*, 363-372.

Chen, S., de Vries, M.A., and Bell, S.P. (2007). Orc6 is required for dynamic recruitment of Cdt1 during repeated Mcm2-7 loading. Genes Dev *21*, 2897-2907.

Cheng, L., Collyer, T., and Hardy, C.F. (1999). Cell cycle regulation of DNA replication initiator factor Dbf4p. Mol Cell Biol *19*, 4270-4278.

Chesnokov, I.N. (2007). Multiple functions of the origin recognition complex. Int Rev Cytol *256*, 69-109.

Ciccia, A., and Elledge, S.J. (2010). The DNA damage response: making it safe to play with knives. Mol Cell *40*, 179-204.

Cornacchia, D., Dileep, V., Quivy, J.P., Foti, R., Tili, F., Santarella-Mellwig, R., Antony, C., Almouzni, G., Gilbert, D.M., and Buonomo, S.B. (2012). Mouse Rif1 is a key regulator of the replication-timing programme in mammalian cells. EMBO J *31*, 3678-3690.

Cosgrove, A.J., Nieduszynski, C.A., and Donaldson, A.D. (2002). Ku complex controls the replication time of DNA in telomere regions. Genes Dev *16*, 2485-2490.

Crampton, A., Chang, F., Pappas, D.L., Jr., Frisch, R.L., and Weinreich, M. (2008). An ARS element inhibits DNA replication through a SIR2-dependent mechanism. Mol Cell *30*, 156-166.

Cui, P., Ding, F., Lin, Q., Zhang, L., Li, A., Zhang, Z., Hu, S., and Yu, J. (2012). Distinct contributions of replication and transcription to mutation rate variation of human genomes. Genomics Proteomics Bioinformatics *10*, 4-10.

Czajkowsky, D.M., Liu, J., Hamlin, J.L., and Shao, Z. (2008). DNA combing reveals intrinsic temporal disorder in the replication of yeast chromosome VI. J Mol Biol *375*, 12-19.

Dahmann, C., and Futcher, B. (1995). Specialization of B-type cyclins for mitosis or meiosis in S. cerevisiae. Genetics *140*, 957-963.

Debatisse, M., El Achkar, E., and Dutrillaux, B. (2006). Common fragile sites nested at the interfaces of early and late-replicating chromosome bands: cis acting components of the G2/M checkpoint? Cell Cycle *5*, 578-581.

Debatisse, M., Le Tallec, B., Letessier, A., Dutrillaux, B., and Brison, O. (2012). Common fragile sites: mechanisms of instability revisited. Trends Genet *28*, 22-32.

DePamphilis, M.L. (1993). Eukaryotic DNA replication: anatomy of an origin. Annu Rev Biochem *62*, 29-63.

Dershowitz, A., and Newlon, C.S. (1993). The effect on chromosome stability of deleting replication origins. Mol Cell Biol *13*, 391-398.

Detweiler, C.S., and Li, J.J. (1998). Ectopic induction of Clb2 in early G1 phase is sufficient to block prereplicative complex formation in Saccharomyces cerevisiae. Proc Natl Acad Sci U S A *95*, 2384-2389.

Dewar, J.M., Budzowska, M., and Walter, J.C. (2015). The mechanism of DNA replication termination in vertebrates. Nature *525*, 345-350.

Di Micco, R., Fumagalli, M., Cicalese, A., Piccinin, S., Gasparini, P., Luise, C., Schurra, C., Garre, M., Nuciforo, P.G., Bensimon, A*., et al.* (2006). Oncogene-induced senescence is a DNA damage response triggered by DNA hyper-replication. Nature *444*, 638-642.

Di Rienzi, S.C., Collingwood, D., Raghuraman, M.K., and Brewer, B.J. (2009). Fragile genomic sites are associated with origins of replication. Genome Biol Evol *1*, 350-363.

Di Rienzi, S.C., Lindstrom, K.C., Mann, T., Noble, W.S., Raghuraman, M.K., and Brewer, B.J. (2012). Maintaining replication origins in the face of genomic change. Genome Res *22*, 1940-1952.

Diffley, J.F. (1996). Once and only once upon a time: specifying and regulating origins of DNA replication in eukaryotic cells. Genes Dev *10*, 2819-2830.

Diffley, J.F. (2004). Regulation of early events in chromosome replication. Curr Biol *14*, R778-786.

Diffley, J.F., and Cocker, J.H. (1992). Protein-DNA interactions at a yeast replication origin. Nature *357*, 169-172.

Diffley, J.F., Cocker, J.H., Dowell, S.J., and Rowley, A. (1994). Two steps in the assembly of complexes at yeast replication origins in vivo. Cell *78*, 303-316.

Dimitrova, D.S., and Gilbert, D.M. (1999). The spatial position and replication timing of chromosomal domains are both established in early G1 phase. Mol Cell *4*, 983-993.

Dirick, L., Bohm, T., and Nasmyth, K. (1995). Roles and regulation of Cln-Cdc28 kinases at the start of the cell cycle of Saccharomyces cerevisiae. EMBO J *14*, 4803-4813.

Donato, J.J., Chung, S.C., and Tye, B.K. (2006). Genome-wide hierarchy of replication origin usage in Saccharomyces cerevisiae. PLoS Genet *2*, e141.

Donley, N., and Thayer, M.J. (2013). DNA replication timing, genome stability and cancer: late and/or delayed DNA replication timing is associated with increased genomic instability. Semin Cancer Biol *23*, 80-89.

Donovan, J.D., Toyn, J.H., Johnson, A.L., and Johnston, L.H. (1994). P40SDB25, a putative CDK inhibitor, has a role in the M/G1 transition in Saccharomyces cerevisiae. Genes Dev *8*, 1640-1653.

Douglas, M.E., and Diffley, J.F. (2012). Replication timing: the early bird catches the worm. Curr Biol *22*, R81-82.

Drury, L.S., Perkins, G., and Diffley, J.F. (1997). The Cdc4/34/53 pathway targets Cdc6p for proteolysis in budding yeast. EMBO J *16*, 5966-5976.

Dubey, D.D., Davis, L.R., Greenfeder, S.A., Ong, L.Y., Zhu, J.G., Broach, J.R., Newlon, C.S., and Huberman, J.A. (1991). Evidence suggesting that the ARS elements associated with silencers of the yeast mating-type locus HML do not function as chromosomal DNA replication origins. Mol Cell Biol *11*, 5346-5355.

Dulev, S., de Renty, C., Mehta, R., Minkov, I., Schwob, E., and Strunnikov, A. (2009). Essential global role of CDC14 in DNA synthesis revealed by chromosome underreplication unrecognized by checkpoints in cdc14 mutants. Proc Natl Acad Sci U S A *106*, 14466-14471.

Durkin, S.G., and Glover, T.W. (2007). Chromosome fragile sites. Annu Rev Genet *41*, 169-192.

Eaton, M.L., Galani, K., Kang, S., Bell, S.P., and MacAlpine, D.M. (2010). Conserved nucleosome positioning defines replication origins. Genes Dev *24*, 748-753.

Edenberg, H.J., and Huberman, J.A. (1975). Eukaryotic chromosome replication. Annu Rev Genet *9*, 245-284.

Ekholm, S.V., and Reed, S.I. (2000). Regulation of G(1) cyclin-dependent kinases in the mammalian cell cycle. Curr Opin Cell Biol *12*, 676-684.

Ekholm-Reed, S., Mendez, J., Tedesco, D., Zetterberg, A., Stillman, B., and Reed, S.I. (2004). Deregulation of cyclin E in human cells interferes with prereplication complex assembly. J Cell Biol *165*, 789-800.

Elsasser, S., Chi, Y., Yang, P., and Campbell, J.L. (1999). Phosphorylation controls timing of Cdc6p destruction: A biochemical analysis. Mol Biol Cell *10*, 3263-3277.

Evrin, C., Clarke, P., Zech, J., Lurz, R., Sun, J., Uhle, S., Li, H., Stillman, B., and Speck, C. (2009). A double-hexameric MCM2-7 complex is loaded onto origin DNA during licensing of eukaryotic DNA replication. Proc Natl Acad Sci U S A *106*, 20240-20245.

Fachinetti, D., Bermejo, R., Cocito, A., Minardi, S., Katou, Y., Kanoh, Y., Shirahige, K., Azvolinsky, A., Zakian, V.A., and Foiani, M. (2010). Replication termination at eukaryotic chromosomes is mediated by Top2 and occurs at genomic loci containing pausing elements. Mol Cell *39*, 595-605.

Fangman, W.L., and Brewer, B.J. (1992). A question of time: replication origins of eukaryotic chromosomes. Cell *71*, 363-366.

Farkash-Amar, S., Lipson, D., Polten, A., Goren, A., Helmstetter, C., Yakhini, Z., and Simon, I. (2008). Global organization of replication time zones of the mouse genome. Genome Res *18*, 1562-1570.

Feldman, R.M., Correll, C.C., Kaplan, K.B., and Deshaies, R.J. (1997). A complex of Cdc4p, Skp1p, and Cdc53p/cullin catalyzes ubiquitination of the phosphorylated CDK inhibitor Sic1p. Cell *91*, 221-230.

Feng, W., Collingwood, D., Boeck, M.E., Fox, L.A., Alvino, G.M., Fangman, W.L., Raghuraman, M.K., and Brewer, B.J. (2006). Genomic mapping of single-stranded DNA in hydroxyurea-challenged yeasts identifies origins of replication. Nat Cell Biol *8*, 148-155.

Ferguson, B.M., Brewer, B.J., Reynolds, A.E., and Fangman, W.L. (1991). A yeast origin of replication is activated late in S phase. Cell *65*, 507-515.

Ferguson, B.M., and Fangman, W.L. (1992). A position effect on the time of replication origin activation in yeast. Cell *68*, 333-339.

Ferreira, M.F., Santocanale, C., Drury, L.S., and Diffley, J.F. (2000). Dbf4p, an essential S phase-promoting factor, is targeted for degradation by the anaphase-promoting complex. Mol Cell Biol *20*, 242-248.

Fitch, I., Dahmann, C., Surana, U., Amon, A., Nasmyth, K., Goetsch, L., Byers, B., and Futcher, B. (1992). Characterization of four B-type cyclin genes of the budding yeast Saccharomyces cerevisiae. Mol Biol Cell *3*, 805-818.

Foster, P.L. (2006). Methods for determining spontaneous mutation rates. Methods Enzymol *409*, 195-213.

Fragkos, M., Ganier, O., Coulombe, P., and Mechali, M. (2015). DNA replication origin activation in space and time. Nat Rev Mol Cell Biol *16*, 360-374.

Freudenreich, C.H. (2007). Chromosome fragility: molecular mechanisms and cellular consequences. Front Biosci *12*, 4911-4924.

Friedman, K.L., and Brewer, B.J. (1995). Analysis of replication intermediates by two-dimensional agarose gel electrophoresis. Methods Enzymol *262*, 613-627.

Friedman, K.L., Brewer, B.J., and Fangman, W.L. (1997). Replication profile of Saccharomyces cerevisiae chromosome VI. Genes Cells *2*, 667-678.

Friedman, K.L., Diller, J.D., Ferguson, B.M., Nyland, S.V., Brewer, B.J., and Fangman, W.L. (1996). Multiple determinants controlling activation of yeast replication origins late in S phase. Genes Dev *10*, 1595-1607.

Fu, Y.V., Yardimci, H., Long, D.T., Ho, T.V., Guainazzi, A., Bermudez, V.P., Hurwitz, J., van Oijen, A., Scharer, O.D., and Walter, J.C. (2011). Selective bypass of a lagging strand roadblock by the eukaryotic replicative DNA helicase. Cell *146*, 931-941.

Fuller, R.S., Funnell, B.E., and Kornberg, A. (1984). The dnaA protein complex with the E. coli chromosomal replication origin (oriC) and other DNA sites. Cell *38*, 889-900.

Futcher, B. (1999). Cell cycle synchronization. Methods Cell Sci *21*, 79-86.

Gambus, A., Jones, R.C., Sanchez-Diaz, A., Kanemaki, M., van Deursen, F., Edmondson, R.D., and Labib, K. (2006). GINS maintains association of Cdc45 with MCM in replisome progression complexes at eukaryotic DNA replication forks. Nat Cell Biol *8*, 358-366.

Ganapathi, M., Palumbo, M.J., Ansari, S.A., He, Q., Tsui, K., Nislow, C., and Morse, R.H. (2011). Extensive role of the general regulatory factors, Abf1 and Rap1, in determining genome-wide chromatin structure in budding yeast. Nucleic Acids Res *39*, 2032-2044.

Ganley, A.R., Ide, S., Saka, K., and Kobayashi, T. (2009). The effect of replication initiation on gene amplification in the rDNA and its relationship to aging. Mol Cell *35*, 683-693.

Ganley, A.R., and Kobayashi, T. (2011). Monitoring the rate and dynamics of concerted evolution in the ribosomal DNA repeats of Saccharomyces cerevisiae using experimental evolution. Mol Biol Evol *28*, 2883-2891.

Gao, F., and Zhang, C.T. (2007). DoriC: a database of oriC regions in bacterial genomes. Bioinformatics *23*, 1866-1867.

Ghiara, J.B., Richardson, H.E., Sugimoto, K., Henze, M., Lew, D.J., Wittenberg, C., and Reed, S.I. (1991). A cyclin B homolog in S. cerevisiae: chronic activation of the Cdc28 protein kinase by cyclin prevents exit from mitosis. Cell *65*, 163-174.

Gomez, M. (2008). Controlled rereplication at DNA replication origins. Cell Cycle *7*, 1313-1314.

Gorgoulis, V.G., Vassiliou, L.V., Karakaidos, P., Zacharatos, P., Kotsinas, A., Liloglou, T., Venere, M., Ditullio, R.A., Jr., Kastrinakis, N.G., Levy, B.*, et al.* (2005). Activation of the DNA damage checkpoint and genomic instability in human precancerous lesions. Nature *434*, 907-913.

Green, B.M., Finn, K.J., and Li, J.J. (2010). Loss of DNA replication control is a potent inducer of gene amplification. Science *329*, 943-946.

Halazonetis, T.D., Gorgoulis, V.G., and Bartek, J. (2008). An oncogene-induced DNA damage model for cancer development. Science *319*, 1352-1355.

Hall, B.M., Ma, C.X., Liang, P., and Singh, K.K. (2009). Fluctuation analysis CalculatOR: a web tool for the determination of mutation rate using Luria-Delbruck fluctuation analysis. Bioinformatics *25*, 1564-1565.

Hanahan, D., and Weinberg, R.A. (2011). Hallmarks of cancer: the next generation. Cell *144*, 646-674.

Hardy, C.F. (1997). Identification of Cdc45p, an essential factor required for DNA replication. Gene *187*, 239-246.

Hartwell, L.H., and Weinert, T.A. (1989). Checkpoints: controls that ensure the order of cell cycle events. Science *246*, 629-634.

Hayano, M., Kanoh, Y., Matsumoto, S., Renard-Guillet, C., Shirahige, K., and Masai, H. (2012). Rif1 is a global regulator of timing of replication origin firing in fission yeast. Genes Dev *26*, 137-150.

Heller, R.C., Kang, S., Lam, W.M., Chen, S., Chan, C.S., and Bell, S.P. (2011). Eukaryotic origin-dependent DNA replication in vitro reveals sequential action of DDK and S-CDK kinases. Cell *146*, 80-91.

Hellmann, I., Prufer, K., Ji, H., Zody, M.C., Paabo, S., and Ptak, S.E. (2005). Why do human diversity levels vary at a megabase scale? Genome Res *15*, 1222-1231.

Heun, P., Laroche, T., Raghuraman, M.K., and Gasser, S.M. (2001). The positioning and dynamics of origins of replication in the budding yeast nucleus. J Cell Biol *152*, 385-400.

Hill, T.M., and Marians, K.J. (1990). Escherichia coli Tus protein acts to arrest the progression of DNA replication forks in vitro. Proc Natl Acad Sci U S A *87*, 2481-2485.

Hiraga, S., Robertson, E.D., and Donaldson, A.D. (2006). The Ctf18 RFC-like complex positions yeast telomeres but does not specify their replication time. EMBO J *25*, 1505-1514.

Hiratani, I., and Gilbert, D.M. (2009). Replication timing as an epigenetic mark. Epigenetics *4*, 93-97.

Hiratani, I., Ryba, T., Itoh, M., Yokochi, T., Schwaiger, M., Chang, C.W., Lyou, Y., Townes, T.M., Schubeler, D., and Gilbert, D.M. (2008). Global reorganization of replication domains during embryonic stem cell differentiation. PLoS Biol *6*, e245.

Ho, A., and Dowdy, S.F. (2002). Regulation of G(1) cell-cycle progression by oncogenes and tumor suppressor genes. Curr Opin Genet Dev *12*, 47-52.

Hogan, E., and Koshland, D. (1992). Addition of extra origins of replication to a minichromosome suppresses its mitotic loss in cdc6 and cdc14 mutants of Saccharomyces cerevisiae. Proc Natl Acad Sci U S A *89*, 3098-3102.

Hoggard, T., Shor, E., Muller, C.A., Nieduszynski, C.A., and Fox, C.A. (2013). A Link between ORC-origin binding mechanisms and origin activation time revealed in budding yeast. PLoS Genet *9*, e1003798.

Hu, Y.F., Hao, Z.L., and Li, R. (1999). Chromatin remodeling and activation of chromosomal DNA replication by an acidic transcriptional activation domain from BRCA1. Genes Dev *13*, 637-642.

Huang, R.Y., and Kowalski, D. (1996). Multiple DNA elements in ARS305 determine replication origin activity in a yeast chromosome. Nucleic Acids Res *24*, 816-823.

Huberman, J.A. (1997). Mapping replication origins, pause sites, and termini by neutral/alkaline two-dimensional gel electrophoresis. Methods *13*, 247-257.

Huberman, J.A., Zhu, J.G., Davis, L.R., and Newlon, C.S. (1988). Close association of a DNA replication origin and an ARS element on chromosome III of the yeast, Saccharomyces cerevisiae. Nucleic Acids Res *16*, 6373-6384.

Hyrien, O., Marheineke, K., and Goldar, A. (2003). Paradoxes of eukaryotic DNA replication: MCM proteins and the random completion problem. Bioessays *25*, 116-125.

Inoue, H., Nojima, H., and Okayama, H. (1990). High efficiency transformation of Escherichia coli with plasmids. Gene *96*, 23-28.

Ivessa, A.S., and Zakian, V.A. (2002). To fire or not to fire: origin activation in Saccharomyces cerevisiae ribosomal DNA. Genes Dev *16*, 2459-2464.

Jacob, F., Brenner, S., and Cuzin, F. (1963). On the Regulation of DNA Replication in Bacteria. Cold Spring Harbor Symp Quant Biol *28*, 329-348.

Jaspersen, S.L., Charles, J.F., Tinker-Kulberg, R.L., and Morgan, D.O. (1998). A late mitotic regulatory network controlling cyclin destruction in Saccharomyces cerevisiae. Mol Biol Cell *9*, 2803-2817.

Johnson, A., and Skotheim, J.M. (2013). Start and the restriction point. Curr Opin Cell Biol *25*, 717-723.

Kamimura, Y., Tak, Y.S., Sugino, A., and Araki, H. (2001). Sld3, which interacts with Cdc45 (Sld4), functions for chromosomal DNA replication in Saccharomyces cerevisiae. EMBO J *20*, 2097-2107.

Kanemaki, M., and Labib, K. (2006). Distinct roles for Sld3 and GINS during establishment and progression of eukaryotic DNA replication forks. EMBO J *25*, 1753-1763.

Kaplan, N., Moore, I.K., Fondufe-Mittendorf, Y., Gossett, A.J., Tillo, D., Field, Y., LeProust, E.M., Hughes, T.R., Lieb, J.D., Widom, J.*, et al.* (2009). The DNA-encoded nucleosome organization of a eukaryotic genome. Nature *458*, 362-366.

Kawakami, H., and Katayama, T. (2010). DnaA, ORC, and Cdc6: similarity beyond the domains of life and diversity. Biochem Cell Biol *88*, 49-62.

Kelly, T.J., Martin, G.S., Forsburg, S.L., Stephen, R.J., Russo, A., and Nurse, P. (1993). The fission yeast cdc18+ gene product couples S phase to START and mitosis. Cell *74*, 371-382.

Knott, S.R., Viggiani, C.J., Tavare, S., and Aparicio, O.M. (2009). Genome-wide replication profiles indicate an expansive role for Rpd3L in regulating replication initiation timing or efficiency, and reveal genomic loci of Rpd3 function in Saccharomyces cerevisiae. Genes Dev *23*, 1077-1090.

Koch, C., Schleiffer, A., Ammerer, G., and Nasmyth, K. (1996). Switching transcription on and off during the yeast cell cycle: Cln/Cdc28 kinases activate bound transcription factor SBF (Swi4/Swi6) at start, whereas Clb/Cdc28 kinases displace it from the promoter in G2. Genes Dev *10*, 129-141.

Koivomagi, M., Valk, E., Venta, R., Iofik, A., Lepiku, M., Balog, E.R., Rubin, S.M., Morgan, D.O., and Loog, M. (2011). Cascades of multisite phosphorylation control Sic1 destruction at the onset of S phase. Nature *480*, 128-131.

Kolodner, R.D., Putnam, C.D., and Myung, K. (2002). Maintenance of genome stability in Saccharomyces cerevisiae. Science *297*, 552-557.

Kramer, K.M., Fesquet, D., Johnson, A.L., and Johnston, L.H. (1998). Budding yeast RSI1/APC2, a novel gene necessary for initiation of anaphase, encodes an APC subunit. EMBO J *17*, 498-506.

Labib, K., and De Piccoli, G. (2011). Surviving chromosome replication: the many roles of the S-phase checkpoint pathway. Philos Trans R Soc Lond B Biol Sci *366*, 3554-3561.

Labib, K., Diffley, J.F., and Kearsey, S.E. (1999). G1-phase and B-type cyclins exclude the DNA-replication factor Mcm4 from the nucleus. Nat Cell Biol *1*, 415-422.

Lang, G.I., and Murray, A.W. (2011). Mutation rates across budding yeast chromosome VI are correlated with replication timing. Genome Biol Evol *3*, 799-811.

Lemoine, F.J., Degtyareva, N.P., Lobachev, K., and Petes, T.D. (2005). Chromosomal translocations in yeast induced by low levels of DNA polymerase a model for chromosome fragile sites. Cell *120*, 587-598.

Lengauer, C., Kinzler, K.W., and Vogelstein, B. (1998). Genetic instabilities in human cancers. Nature *396*, 643-649.

Lengronne, A., and Schwob, E. (2002). The yeast CDK inhibitor Sic1 prevents genomic instability by promoting replication origin licensing in late G(1). Mol Cell *9*, 1067-1078.

Leonard, A.C., and Mechali, M. (2013). DNA replication origins. Cold Spring Harb Perspect Biol *5*, a010116.

Letessier, A., Birnbaum, D., Debatisse, M., and Chaffanet, M. (2011a). [Genome: does a paucity of initiation events lead to fragility?]. Med Sci (Paris) *27*, 707-709.

Letessier, A., Millot, G.A., Koundrioukoff, S., Lachages, A.M., Vogt, N., Hansen, R.S., Malfoy, B., Brison, O., and Debatisse, M. (2011b). Cell-type-specific replication initiation programs set fragility of the FRA3B fragile site. Nature *470*, 120-123.

Li, A., and Blow, J.J. (2005). Cdt1 downregulation by proteolysis and geminin inhibition prevents DNA re-replication in Xenopus. EMBO J *24*, 395-404.

Li, J.J., and Deshaies, R.J. (1993). Exercising self-restraint: discouraging illicit acts of S and M in eukaryotes. Cell *74*, 223-226.

Liachko, I., Bhaskar, A., Lee, C., Chung, S.C., Tye, B.K., and Keich, U. (2010). A comprehensive genome-wide map of autonomously replicating sequences in a naive genome. PLoS Genet *6*, e1000946.

Lian, H.Y., Robertson, E.D., Hiraga, S., Alvino, G.M., Collingwood, D., McCune, H.J., Sridhar, A., Brewer, B.J., Raghuraman, M.K., and Donaldson, A.D. (2011). The effect of Ku on telomere replication time is mediated by telomere length but is independent of histone tail acetylation. Mol Biol Cell *22*, 1753-1765.

Liku, M.E., Nguyen, V.Q., Rosales, A.W., Irie, K., and Li, J.J. (2005). CDK phosphorylation of a novel NLS-NES module distributed between two subunits of the Mcm2-7 complex prevents chromosomal rereplication. Mol Biol Cell *16*, 5026-5039.

Linskens, M.H., and Huberman, J.A. (1988). Organization of replication of ribosomal DNA in Saccharomyces cerevisiae. Mol Cell Biol *8*, 4927-4935.

Lipford, J.R., and Bell, S.P. (2001). Nucleosomes positioned by ORC facilitate the initiation of DNA replication. Mol Cell *7*, 21-30.

Lopes, M., Cotta-Ramusino, C., Pellicioli, A., Liberi, G., Plevani, P., Muzi-Falconi, M., Newlon, C.S., and Foiani, M. (2001). The DNA replication checkpoint response stabilizes stalled replication forks. Nature *412*, 557-561.

Lowndes, N.F., and Murguia, J.R. (2000). Sensing and responding to DNA damage. Curr Opin Genet Dev *10*, 17-25.

Luria, S.E., and Delbrück, M. (1943). Mutations of bacteria from virus sensitivity to virus resistance. Genetics *28*, 491-511.

Magiera, M.M., Gueydon, E., and Schwob, E. (2014). DNA replication and spindle checkpoints cooperate during S phase to delay mitosis and preserve genome integrity. J Cell Biol *204*, 165-175.

Malumbres, M., and Barbacid, M. (2001). To cycle or not to cycle: a critical decision in cancer. Nat Rev Cancer *1*, 222-231.

Malumbres, M., and Barbacid, M. (2009). Cell cycle, CDKs and cancer: a changing paradigm. Nat Rev Cancer *9*, 153-166.

Mantiero, D., Mackenzie, A., Donaldson, A., and Zegerman, P. (2011). Limiting replication initiation factors execute the temporal programme of origin firing in budding yeast. EMBO J *30*, 4805-4814.

Marahrens, Y., and Stillman, B. (1992). A yeast chromosomal origin of DNA replication defined by multiple functional elements. Science *255*, 817-823.

Masumoto, H., Muramatsu, S., Kamimura, Y., and Araki, H. (2002). S-Cdk-dependent phosphorylation of Sld2 essential for chromosomal DNA replication in budding yeast. Nature *415*, 651-655.

McCarroll, R.M., and Fangman, W.L. (1988). Time of replication of yeast centromeres and telomeres. Cell *54*, 505-513.

McCune, H.J., Danielson, L.S., Alvino, G.M., Collingwood, D., Delrow, J.J., Fangman, W.L., Brewer, B.J., and Raghuraman, M.K. (2008). The temporal program of chromosome replication: genomewide replication in clb5{Delta} Saccharomyces cerevisiae. Genetics *180*, 1833-1847.

McGuffee, S.R., Smith, D.J., and Whitehouse, I. (2013). Quantitative, genome-wide analysis of eukaryotic replication initiation and termination. Mol Cell *50*, 123-135.

Mead, D.A., Szczesna-Skorupa, E., and Kemper, B. (1986). Single-stranded DNA 'blue' T7 promoter plasmids: a versatile tandem promoter system for cloning and protein engineering. Protein Eng *1*, 67-74.

Mechali, M. (2010). Eukaryotic DNA replication origins: many choices for appropriate answers. Nat Rev Mol Cell Biol *11*, 728-738.

Melixetian, M., Ballabeni, A., Masiero, L., Gasparini, P., Zamponi, R., Bartek, J., Lukas, J., and Helin, K. (2004). Loss of Geminin induces rereplication in the presence of functional p53. J Cell Biol *165*, 473-482.

Mendenhall, M.D. (1993). An inhibitor of p34CDC28 protein kinase activity from Saccharomyces cerevisiae. Science *259*, 216-219.

Mendez, J., and Stillman, B. (2003). Perpetuating the double helix: molecular machines at eukaryotic DNA replication origins. Bioessays *25*, 1158-1167.

Messer, W., Meijer, M., Bergmans, H.E., Hansen, F.G., von Meyenburg, K., Beck, E., and Schaller, H. (1979). Origin of replication, oriC, of the Escherichia coli K12 chromosome: nucleotide sequence. Cold Spring Harb Symp Quant Biol *43 Pt 1*, 139-145.

Mihaylov, I.S., Kondo, T., Jones, L., Ryzhikov, S., Tanaka, J., Zheng, J., Higa, L.A., Minamino, N., Cooley, L., and Zhang, H. (2002). Control of DNA replication and chromosome ploidy by geminin and cyclin A. Mol Cell Biol *22*, 1868-1880.

Miller, C.A., Umek, R.M., and Kowalski, D. (1999). The inefficient replication origin from yeast ribosomal DNA is naturally impaired in the ARS consensus sequence and in DNA unwinding. Nucleic Acids Res *27*, 3921-3930.

Mirkin, E.V., and Mirkin, S.M. (2007). Replication fork stalling at natural impediments. Microbiol Mol Biol Rev *71*, 13-35.

Miyake, T., Loch, C.M., and Li, R. (2002). Identification of a multifunctional domain in autonomously replicating sequence-binding factor 1 required for transcriptional activation, DNA replication, and gene silencing. Mol Cell Biol *22*, 505-516.

Moyer, S.E., Lewis, P.W., and Botchan, M.R. (2006). Isolation of the Cdc45/Mcm2-7/GINS (CMG) complex, a candidate for the eukaryotic DNA replication fork helicase. Proc Natl Acad Sci U S A *103*, 10236-10241.

Muller, C.A., and Nieduszynski, C.A. (2012). Conservation of replication timing reveals global and local regulation of replication origin activity. Genome Res *22*, 1953-1962.

Muramatsu, S., Hirai, K., Tak, Y.S., Kamimura, Y., and Araki, H. (2010). CDK-dependent complex formation between replication proteins Dpb11, Sld2, Pol (epsilon}, and GINS in budding yeast. Genes Dev *24*, 602-612.

Muzi-Falconi, M., Brown, G.W., and Kelly, T.J. (1996). Controlling initiation during the cell cycle. DNA replication. Curr Biol *6*, 229-233.

Nash, P., Tang, X., Orlicky, S., Chen, Q., Gertler, F.B., Mendenhall, M.D., Sicheri, F., Pawson, T., and Tyers, M. (2001). Multisite phosphorylation of a CDK inhibitor sets a threshold for the onset of DNA replication. Nature *414*, 514-521.

Nasmyth, K. (1993). Control of the yeast cell cycle by the Cdc28 protein kinase. Curr Opin Cell Biol *5*, 166-179.

Natsume, T., Muller, C.A., Katou, Y., Retkute, R., Gierlinski, M., Araki, H., Blow, J.J., Shirahige, K., Nieduszynski, C.A., and Tanaka, T.U. (2013). Kinetochores coordinate pericentromeric cohesion and early DNA replication by Cdc7-Dbf4 kinase recruitment. Mol Cell *50*, 661-674.

Negrini, S., Gorgoulis, V.G., and Halazonetis, T.D. (2010). Genomic instability--an evolving hallmark of cancer. Nat Rev Mol Cell Biol *11*, 220-228.

Newlon, C.S., and Theis, J.F. (1993). The structure and function of yeast ARS elements. Curr Opin Genet Dev *3*, 752-758.

Nguyen, V.Q., Co, C., Irie, K., and Li, J.J. (2000). Clb/Cdc28 kinases promote nuclear export of the replication initiator proteins Mcm2-7. Curr Biol *10*, 195-205.

Nguyen, V.Q., Co, C., and Li, J.J. (2001). Cyclin-dependent kinases prevent DNA re-replication through multiple mechanisms. Nature *411*, 1068-1073.

Nieduszynski, C.A., Blow, J.J., and Donaldson, A.D. (2005). The requirement of yeast replication origins for pre-replication complex proteins is modulated by transcription. Nucleic Acids Res *33*, 2410-2420.

Nishitani, H., and Nurse, P. (1995). p65cdc18 plays a major role controlling the initiation of DNA replication in fission yeast. Cell *83*, 397-405.

Nugroho, T.T., and Mendenhall, M.D. (1994). An inhibitor of yeast cyclin-dependent protein kinase plays an important role in ensuring the genomic integrity of daughter cells. Mol Cell Biol *14*, 3320-3328.

Nyberg, K.A., Michelson, R.J., Putnam, C.W., and Weinert, T.A. (2002). Toward maintaining the genome: DNA damage and replication checkpoints. Annu Rev Genet *36*, 617-656.

Oshiro, G., Owens, J.C., Shellman, Y., Sclafani, R.A., and Li, J.J. (1999). Cell cycle control of Cdc7p kinase activity through regulation of Dbf4p stability. Mol Cell Biol *19*, 4888-4896.

Ozeri-Galai, E., Lebofsky, R., Rahat, A., Bester, A.C., Bensimon, A., and Kerem, B. (2011). Failure of origin activation in response to fork stalling leads to chromosomal instability at fragile sites. Mol Cell *43*, 122-131.

Pappas, D.L., Jr., Frisch, R., and Weinreich, M. (2004). The NAD(+)-dependent Sir2p histone deacetylase is a negative regulator of chromosomal DNA replication. Genes Dev *18*, 769-781.

Pasero, P., Bensimon, A., and Schwob, E. (2002). Single-molecule analysis reveals clustering and epigenetic regulation of replication origins at the yeast rDNA locus. Genes Dev *16*, 2479-2484.

Pasero, P., Duncker, B.P., Schwob, E., and Gasser, S.M. (1999). A role for the Cdc7 kinase regulatory subunit Dbf4p in the formation of initiation-competent origins of replication. Genes Dev *13*, 2159-2176.

Patel, P.K., Arcangioli, B., Baker, S.P., Bensimon, A., and Rhind, N. (2006). DNA replication origins fire stochastically in fission yeast. Mol Biol Cell *17*, 308-316.

Patel, P.K., Kommajosyula, N., Rosebrock, A., Bensimon, A., Leatherwood, J., Bechhoefer, J., and Rhind, N. (2008). The Hsk1(Cdc7) replication kinase regulates origin efficiency. Mol Biol Cell *19*, 5550-5558.

Perkins, G., Drury, L.S., and Diffley, J.F. (2001). Separate SCF(CDC4) recognition elements target Cdc6 for proteolysis in S phase and mitosis. EMBO J *20*, 4836-4845.

Piatti, S., Lengauer, C., and Nasmyth, K. (1995). Cdc6 is an unstable protein whose de novo synthesis in G1 is important for the onset of S phase and for preventing a 'reductional' anaphase in the budding yeast Saccharomyces cerevisiae. EMBO J *14*, 3788-3799.

Poli, J., Tsaponina, O., Crabbe, L., Keszthelyi, A., Pantesco, V., Chabes, A., Lengronne, A., and Pasero, P. (2012). dNTP pools determine fork progression and origin usage under replication stress. EMBO J *31*, 883-894.

Polo, S.E., and Jackson, S.P. (2011). Dynamics of DNA damage response proteins at DNA breaks: a focus on protein modifications. Genes Dev *25*, 409-433.

Prendergast, J.G., Campbell, H., Gilbert, N., Dunlop, M.G., Bickmore, W.A., and Semple, C.A. (2007). Chromatin structure and evolution in the human genome. BMC Evol Biol *7*, 72.

Putnam, C.D., and Kolodner, R.D. (2010). Determination of gross chromosomal rearrangement rates. Cold Spring Harb Protoc *2010*, pdb prot5492.

Raghuraman, M.K., and Brewer, B.J. (2010). Molecular analysis of the replication program in unicellular model organisms. Chromosome Res *18*, 19-34.

Raghuraman, M.K., Brewer, B.J., and Fangman, W.L. (1997). Cell cycle-dependent establishment of a late replication program. Science *276*, 806-809.

Raghuraman, M.K., Winzeler, E.A., Collingwood, D., Hunt, S., Wodicka, L., Conway, A., Lockhart, D.J., Davis, R.W., Brewer, B.J., and Fangman, W.L. (2001). Replication dynamics of the yeast genome. Science *294*, 115-121.

Randell, J.C., Fan, A., Chan, C., Francis, L.I., Heller, R.C., Galani, K., and Bell, S.P. (2010). Mec1 is one of multiple kinases that prime the Mcm2-7 helicase for phosphorylation by Cdc7. Mol Cell *40*, 353-363.

Rane, S.G., Cosenza, S.C., Mettus, R.V., and Reddy, E.P. (2002). Germ line transmission of the Cdk4(R24C) mutation facilitates tumorigenesis and escape from cellular senescence. Mol Cell Biol *22*, 644-656.

Rao, H., and Stillman, B. (1995). The origin recognition complex interacts with a bipartite DNA binding site within yeast replicators. Proc Natl Acad Sci U S A *92*, 2224-2228.

Reed, S.I. (1992). The role of p34 kinases in the G1 to S-phase transition. Annu Rev Cell Biol *8*, 529-561.

Reish, O., Orlovski, A., Mashevitz, M., Sher, C., Libman, V., Rosenblat, M., and Avivi, L. (2003). Modified allelic replication in lymphocytes of patients with neurofibromatosis type 1. Cancer Genet Cytogenet *143*, 133-139.

Remus, D., Beuron, F., Tolun, G., Griffith, J.D., Morris, E.P., and Diffley, J.F. (2009). Concerted loading of Mcm2-7 double hexamers around DNA during DNA replication origin licensing. Cell *139*, 719-730.

Rhind, N. (2006). DNA replication timing: random thoughts about origin firing. Nat Cell Biol *8*, 1313-1316.

Rhind, N., and Gilbert, D.M. (2013). DNA Replication Timing. Cold Spring Harb Perspect Med *3*, 1-26.

Richardson, H., Lew, D.J., Henze, M., Sugimoto, K., and Reed, S.I. (1992). Cyclin-B homologs in Saccharomyces cerevisiae function in S phase and in G2. Genes Dev *6*, 2021-2034.

Rizzardi, L.F., and Cook, J.G. (2012). Flipping the switch from g1 to s phase with e3 ubiquitin ligases. Genes Cancer *3*, 634-648.

Ross, K.E., and Cohen-Fix, O. (2003). The role of Cdh1p in maintaining genomic stability in budding yeast. Genetics *165*, 489-503.

Rowley, A., Cocker, J.H., Harwood, J., and Diffley, J.F. (1995). Initiation complex assembly at budding yeast replication origins begins with the recognition of a bipartite sequence by limiting amounts of the initiator, ORC. EMBO J *14*, 2631-2641.

Ryba, T., Battaglia, D., Chang, B.H., Shirley, J.W., Buckley, Q., Pope, B.D., Devidas, M., Druker, B.J., and Gilbert, D.M. (2012). Abnormal developmental control of replication-timing domains in pediatric acute lymphoblastic leukemia. Genome Res *22*, 1833-1844.

Ryba, T., Hiratani, I., Lu, J., Itoh, M., Kulik, M., Zhang, J., Schulz, T.C., Robins, A.J., Dalton, S., and Gilbert, D.M. (2010). Evolutionarily conserved replication timing profiles predict long-range chromatin interactions and distinguish closely related cell types. Genome Res *20*, 761-770.

Sambrook, J., Fritsch, E.F., and Maniatis, T. (1989). Molecular Cloning: a laboratory manual. Cold Spring Harbor Laboratory Press.

Santamaria, D., Viguera, E., Martinez-Robles, M.L., Hyrien, O., Hernandez, P., Krimer, D.B., and Schvartzman, J.B. (2000). Bi-directional replication and random termination. Nucleic Acids Res *28*, 2099-2107.

Santocanale, C., and Diffley, J.F. (1996). ORC- and Cdc6-dependent complexes at active and inactive chromosomal replication origins in Saccharomyces cerevisiae. EMBO J *15*, 6671-6679.

Santocanale, C., and Diffley, J.F. (1998). A Mec1- and Rad53-dependent checkpoint controls late-firing origins of DNA replication. Nature *395*, 615-618.

Santocanale, C., Sharma, K., and Diffley, J.F. (1999). Activation of dormant origins of DNA replication in budding yeast. Genes Dev *13*, 2360-2364.

Sarkar, S., Ma, W.T., and Sandri, G.H. (1992). On fluctuation analysis: a new, simple and efficient method for computing the expected number of mutants. Genetica *85*, 173-179.

Schneider, B.L., Yang, Q.H., and Futcher, A.B. (1996). Linkage of replication to start by the Cdk inhibitor Sic1. Science *272*, 560-562.

Schwab, M., Lutum, A.S., and Seufert, W. (1997). Yeast Hct1 is a regulator of Clb2 cyclin proteolysis. Cell *90*, 683-693.
Schwob, E. (2004). Flexibility and governance in eukaryotic DNA replication. Curr Opin Microbiol *7*, 680-690.
Schwob, E., Bohm, T., Mendenhall, M.D., and Nasmyth, K. (1994). The B-type cyclin kinase inhibitor p40SIC1 controls the G1 to S transition in S. cerevisiae. Cell *79*, 233-244.
Schwob, E., and Nasmyth, K. (1993). CLB5 and CLB6, a new pair of B cyclins involved in DNA replication in Saccharomyces cerevisiae. Genes Dev *7*, 1160-1175.
Sclafani, R.A. (2000). Cdc7p-Dbf4p becomes famous in the cell cycle. J Cell Sci *113 (Pt 12)*, 2111-2117.
Sclafani, R.A., and Holzen, T.M. (2007). Cell cycle regulation of DNA replication. Annu Rev Genet *41*, 237-280.
Shen, Z. (2011). Genomic instability and cancer: an introduction. J Mol Cell Biol *3*, 1-3.
Sherr, C.J. (2000). Cell cycle control and cancer. Harvey Lect *96*, 73-92.
Sherr, C.J., and McCormick, F. (2002). The RB and p53 pathways in cancer. Cancer Cell *2*, 103-112.
Sheu, Y.J., and Stillman, B. (2010). The Dbf4-Cdc7 kinase promotes S phase by alleviating an inhibitory activity in Mcm4. Nature *463*, 113-117.
Shirahige, K., Hori, Y., Shiraishi, K., Yamashita, M., Takahashi, K., Obuse, C., Tsurimoto, T., and Yoshikawa, H. (1998). Regulation of DNA-replication origins during cell-cycle progression. Nature *395*, 618-621.
Siddiqui, K., On, K.F., and Diffley, J.F. (2013). Regulating DNA replication in eukarya. Cold Spring Harb Perspect Biol *5*.
Sidorova, J.M., and Breeden, L.L. (2003). Precocious G1/S transitions and genomic instability: the origin connection. Mutat Res *532*, 5-19.
Simpson, R.T. (1990). Nucleosome positioning can affect the function of a cis-acting DNA element in vivo. Nature *343*, 387-389.
Siow, C.C., Nieduszynska, S.R., Muller, C.A., and Nieduszynski, C.A. (2012). OriDB, the DNA replication origin database updated and extended. Nucleic Acids Res *40*, D682-686.
Skotheim, J.M., Di Talia, S., Siggia, E.D., and Cross, F.R. (2008). Positive feedback of G1 cyclins ensures coherent cell cycle entry. Nature *454*, 291-296.
Stamatoyannopoulos, J.A., Adzhubei, I., Thurman, R.E., Kryukov, G.V., Mirkin, S.M., and Sunyaev, S.R. (2009). Human mutation rate associated with DNA replication timing. Nat Genet *41*, 393-395.
Stevenson, J.B., and Gottschling, D.E. (1999). Telomeric chromatin modulates replication timing near chromosome ends. Genes Dev *13*, 146-151.
Stinchcomb, D.T., Struhl, K., and Davis, R.W. (1979). Isolation and characterisation of a yeast chromosomal replicator. Nature *282*, 39-43.
Stuart, D., and Wittenberg, C. (1995). CLN3, not positive feedback, determines the timing of CLN2 transcription in cycling cells. Genes Dev *9*, 2780-2794.
Surana, U., Robitsch, H., Price, C., Schuster, T., Fitch, I., Futcher, A.B., and Nasmyth, K. (1991). The role of CDC28 and cyclins during mitosis in the budding yeast S. cerevisiae. Cell *65*, 145-161.
Sutherland, G.R., and Richards, R.I. (1995). The molecular basis of fragile sites in human chromosomes. Curr Opin Genet Dev *5*, 323-327.
Tak, Y.S., Tanaka, Y., Endo, S., Kamimura, Y., and Araki, H. (2006). A CDK-catalysed regulatory phosphorylation for formation of the DNA replication complex Sld2-Dpb11. EMBO J *25*, 1987-1996.
Takeuchi, Y., Horiuchi, T., and Kobayashi, T. (2003). Transcription-dependent recombination and the role of fork collision in yeast rDNA. Genes Dev *17*, 1497-1506.
Tanaka, S., and Araki, H. (2010). Regulation of the initiation step of DNA replication by cyclin-dependent kinases. Chromosoma *119*, 565-574.

Tanaka, S., and Araki, H. (2013). Helicase activation and establishment of replication forks at chromosomal origins of replication. Cold Spring Harb Perspect Biol *5*, a010371.

Tanaka, S., and Diffley, J.F. (2002). Deregulated G1-cyclin expression induces genomic instability by preventing efficient pre-RC formation. Genes Dev *16*, 2639-2649.

Tanaka, S., Nakato, R., Katou, Y., Shirahige, K., and Araki, H. (2011a). Origin association of Sld3, Sld7, and Cdc45 proteins is a key step for determination of origin-firing timing. Curr Biol *21*, 2055-2063.

Tanaka, S., Umemori, T., Hirai, K., Muramatsu, S., Kamimura, Y., and Araki, H. (2007). CDK-dependent phosphorylation of Sld2 and Sld3 initiates DNA replication in budding yeast. Nature *445*, 328-332.

Tanaka, T., Umemori, T., Endo, S., Muramatsu, S., Kanemaki, M., Kamimura, Y., Obuse, C., and Araki, H. (2011b). Sld7, an Sld3-associated protein required for efficient chromosomal DNA replication in budding yeast. EMBO J *30*, 2019-2030.

Tavormina, P.A., Wang, Y., and Burke, D.J. (1997). Differential requirements for DNA replication in the activation of mitotic checkpoints in Saccharomyces cerevisiae. Mol Cell Biol *17*, 3315-3322.

Tazumi, A., Fukuura, M., Nakato, R., Kishimoto, A., Takenaka, T., Ogawa, S., Song, J.H., Takahashi, T.S., Nakagawa, T., Shirahige, K.*, et al.* (2012). Telomere-binding protein Taz1 controls global replication timing through its localization near late replication origins in fission yeast. Genes Dev *26*, 2050-2062.

Teixeira, L.K., Wang, X., Li, Y., Ekholm-Reed, S., Wu, X., Wang, P., and Reed, S.I. (2015). Cyclin E deregulation promotes loss of specific genomic regions. Curr Biol *25*, 1327-1333.

Tercero, J.A., and Diffley, J.F. (2001). Regulation of DNA replication fork progression through damaged DNA by the Mec1/Rad53 checkpoint. Nature *412*, 553-557.

Tercero, J.A., Labib, K., and Diffley, J.F. (2000). DNA synthesis at individual replication forks requires the essential initiation factor Cdc45p. EMBO J *19*, 2082-2093.

Tercero, J.A., Longhese, M.P., and Diffley, J.F. (2003). A central role for DNA replication forks in checkpoint activation and response. Mol Cell *11*, 1323-1336.

Theis, J.F., Irene, C., Dershowitz, A., Brost, R.L., Tobin, M.L., di Sanzo, F.M., Wang, J.Y., Boone, C., and Newlon, C.S. (2010). The DNA damage response pathway contributes to the stability of chromosome III derivatives lacking efficient replicators. PLoS Genet *6*, e1001227.

Thoma, F., Bergman, L.W., and Simpson, R.T. (1984). Nuclease digestion of circular TRP1ARS1 chromatin reveals positioned nucleosomes separated by nuclease-sensitive regions. J Mol Biol *177*, 715-733.

Toone, W.M., Aerne, B.L., Morgan, B.A., and Johnston, L.H. (1997). Getting started: regulating the initiation of DNA replication in yeast. Annu Rev Microbiol *51*, 125-149.

Torres-Rosell, J., De Piccoli, G., and Aragon, L. (2007a). Can eukaryotic cells monitor the presence of unreplicated DNA? Cell Div *2*, 19.

Torres-Rosell, J., De Piccoli, G., Cordon-Preciado, V., Farmer, S., Jarmuz, A., Machin, F., Pasero, P., Lisby, M., Haber, J.E., and Aragon, L. (2007b). Anaphase onset before complete DNA replication with intact checkpoint responses. Science *315*, 1411-1415.

Torres-Rosell, J., Sunjevaric, I., De Piccoli, G., Sacher, M., Eckert-Boulet, N., Reid, R., Jentsch, S., Rothstein, R., Aragon, L., and Lisby, M. (2007c). The Smc5-Smc6 complex and SUMO modification of Rad52 regulates recombinational repair at the ribosomal gene locus. Nat Cell Biol *9*, 923-931.

Toyn, J.H., Johnson, A.L., and Johnston, L.H. (1995). Segregation of unreplicated chromosomes in Saccharomyces cerevisiae reveals a novel G1/M-phase checkpoint. Mol Cell Biol *15*, 5312-5321.

Tuduri, S., Tourriere, H., and Pasero, P. (2010). Defining replication origin efficiency using DNA fiber assays. Chromosome Res *18*, 91-102.

Tye, B.K. (1999). MCM proteins in DNA replication. Annu Rev Biochem *68*, 649-686.

Tyers, M., Tokiwa, G., and Futcher, B. (1993). Comparison of the Saccharomyces cerevisiae G1 cyclins: Cln3 may be an upstream activator of Cln1, Cln2 and other cyclins. EMBO J *12*, 1955-1968.

Vaze, M.B., Pellicioli, A., Lee, S.E., Ira, G., Liberi, G., Arbel-Eden, A., Foiani, M., and Haber, J.E. (2002). Recovery from checkpoint-mediated arrest after repair of a double-strand break requires Srs2 helicase. Mol Cell *10*, 373-385.

Vaziri, C., Saxena, S., Jeon, Y., Lee, C., Murata, K., Machida, Y., Wagle, N., Hwang, D.S., and Dutta, A. (2003). A p53-dependent checkpoint pathway prevents rereplication. Mol Cell *11*, 997-1008.

Venditti, P., Costanzo, G., Negri, R., and Camilloni, G. (1994). ABFI contributes to the chromatin organization of Saccharomyces cerevisiae ARS1 B-domain. Biochim Biophys Acta *1219*, 677-689.

Verma, R., Feldman, R.M., and Deshaies, R.J. (1997). SIC1 is ubiquitinated in vitro by a pathway that requires CDC4, CDC34, and cyclin/CDK activities. Mol Biol Cell *8*, 1427-1437.

Vogelauer, M., Rubbi, L., Lucas, I., Brewer, B.J., and Grunstein, M. (2002). Histone acetylation regulates the time of replication origin firing. Mol Cell *10*, 1223-1233.

Vujcic, M., Miller, C.A., and Kowalski, D. (1999). Activation of silent replication origins at autonomously replicating sequence elements near the HML locus in budding yeast. Mol Cell Biol *19*, 6098-6109.

Wang, Y., Vujcic, M., and Kowalski, D. (2001). DNA replication forks pause at silent origins near the HML locus in budding yeast. Mol Cell Biol *21*, 4938-4948.

Ward, T.R., Hoang, M.L., Prusty, R., Lau, C.K., Keil, R.L., Fangman, W.L., and Brewer, B.J. (2000). Ribosomal DNA replication fork barrier and HOT1 recombination hot spot: shared sequences but independent activities. Mol Cell Biol *20*, 4948-4957.

Watanabe, Y., Abe, T., Ikemura, T., and Maekawa, M. (2009). Relationships between replication timing and GC content of cancer-related genes on human chromosomes 11q and 21q. Gene *433*, 26-31.

Watanabe, Y., Fujiyama, A., Ichiba, Y., Hattori, M., Yada, T., Sakaki, Y., and Ikemura, T. (2002). Chromosome-wide assessment of replication timing for human chromosomes 11q and 21q: disease-related genes in timing-switch regions. Hum Mol Genet *11*, 13-21.

Watanabe, Y., and Maekawa, M. (2010). Spatiotemporal regulation of DNA replication in the human genome and its association with genomic instability and disease. Curr Med Chem *17*, 222-233.

Weber, J.M., Irlbacher, H., and Ehrenhofer-Murray, A.E. (2008). Control of replication initiation by the Sum1/Rfm1/Hst1 histone deacetylase. BMC Mol Biol *9*, 100.

Wilmes, G.M., and Bell, S.P. (2002). The B2 element of the Saccharomyces cerevisiae ARS1 origin of replication requires specific sequences to facilitate pre-RC formation. Proc Natl Acad Sci U S A *99*, 101-106.

Wu, J.R., and Gilbert, D.M. (1995). Rapid DNA preparation for 2D gel analysis of replication intermediates. Nucleic Acids Res *23*, 3997-3998.

Wu, P.Y., and Nurse, P. (2009). Establishing the program of origin firing during S phase in fission Yeast. Cell *136*, 852-864.

Xu, J., Yanagisawa, Y., Tsankov, A.M., Hart, C., Aoki, K., Kommajosyula, N., Steinmann, K.E., Bochicchio, J., Russ, C., Regev, A.*, et al.* (2012). Genome-wide identification and characterization of replication origins by deep sequencing. Genome Biol *13*, R27.

Yabuki, N., Terashima, H., and Kitada, K. (2002). Mapping of early firing origins on a replication profile of budding yeast. Genes Cells *7*, 781-789.

Yaffe, E., Farkash-Amar, S., Polten, A., Yakhini, Z., Tanay, A., and Simon, I. (2010). Comparative analysis of DNA replication timing reveals conserved large-scale chromosomal architecture. PLoS Genet *6*, e1001011.

Yamashita, M., Hori, Y., Shinomiya, T., Obuse, C., Tsurimoto, T., Yoshikawa, H., and Shirahige, K. (1997). The efficiency and timing of initiation of replication of multiple replicons of Saccharomyces cerevisiae chromosome VI. Genes Cells *2*, 655-665.

Yamazaki, S., Ishii, A., Kanoh, Y., Oda, M., Nishito, Y., and Masai, H. (2012). Rif1 regulates the replication timing domains on the human genome. EMBO J *31*, 3667-3677.

Yekezare, M., Gomez-Gonzalez, B., and Diffley, J.F. (2013). Controlling DNA replication origins in response to DNA damage - inhibit globally, activate locally. J Cell Sci *126*, 1297-1306.

Yeong, F.M., Lim, H.H., Padmashree, C.G., and Surana, U. (2000). Exit from mitosis in budding yeast: biphasic inactivation of the Cdc28-Clb2 mitotic kinase and the role of Cdc20. Mol Cell *5*, 501-511.

Yoshida, K., Poveda, A., and Pasero, P. (2013). Time to be versatile: regulation of the replication timing program in budding yeast. J Mol Biol *425*, 4696-4705.

Zappulla, D.C., Sternglanz, R., and Leatherwood, J. (2002). Control of replication timing by a transcriptional silencer. Curr Biol *12*, 869-875.

Zegerman, P., and Diffley, J.F. (2007). Phosphorylation of Sld2 and Sld3 by cyclin-dependent kinases promotes DNA replication in budding yeast. Nature *445*, 281-285.

Zhang, Y., Moqtaderi, Z., Rattner, B.P., Euskirchen, G., Snyder, M., Kadonaga, J.T., Liu, X.S., and Struhl, K. (2009). Intrinsic histone-DNA interactions are not the major determinant of nucleosome positions in vivo. Nat Struct Mol Biol *16*, 847-852.

Zhu, J., Newlon, C.S., and Huberman, J.A. (1992). Localization of a DNA replication origin and termination zone on chromosome III of Saccharomyces cerevisiae. Mol Cell Biol *12*, 4733-4741.

Zou, L., and Stillman, B. (1998). Formation of a preinitiation complex by S-phase cyclin CDK-dependent loading of Cdc45p onto chromatin. Science *280*, 593-596.

Zou, L., and Stillman, B. (2000). Assembly of a complex containing Cdc45p, replication protein A, and Mcm2p at replication origins controlled by S-phase cyclin-dependent kinases and Cdc7p-Dbf4p kinase. Mol Cell Biol *20*, 3086-3096.

APPENDIX 1

Supplementary Figures

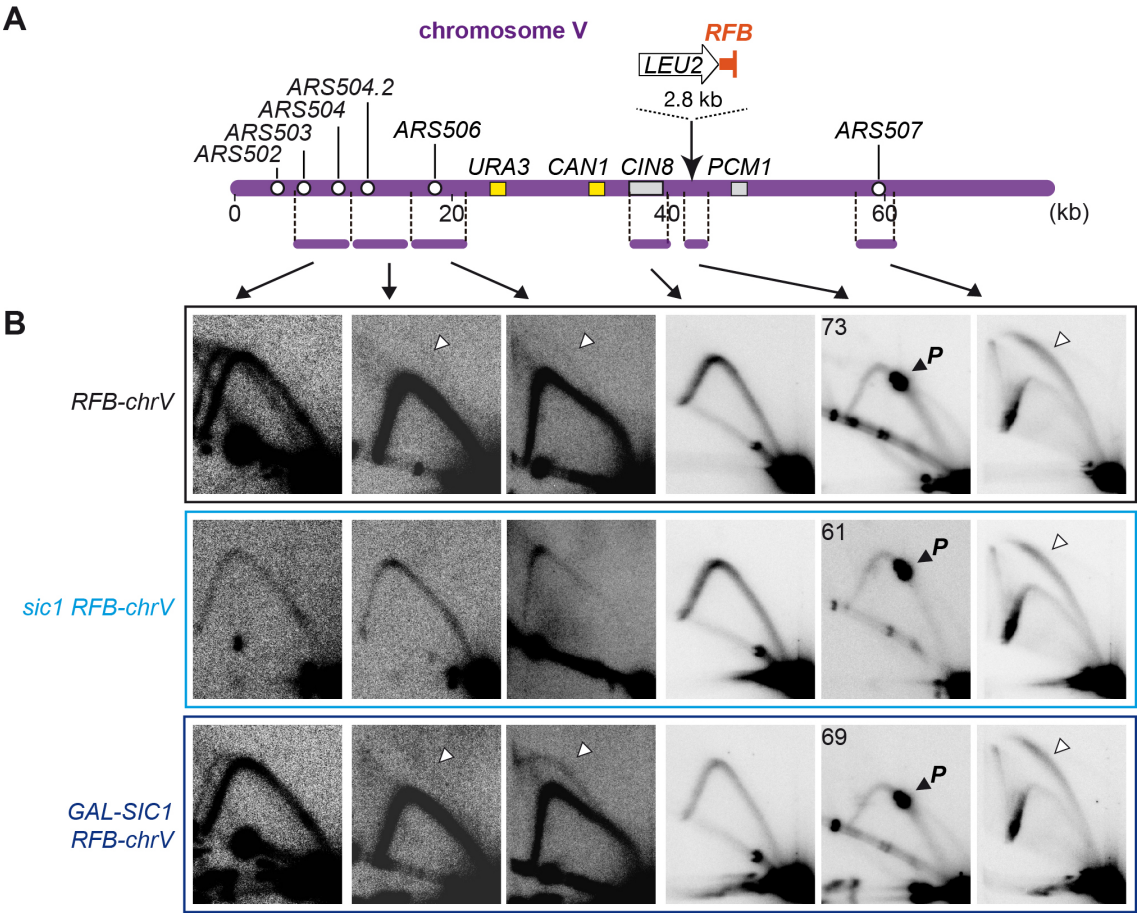

Supplemental Figure 1: Cells lacking Sic1 fail in dormant-origin firing in response to a transiently pause of forks at the RFB in W303-1a strains. (A) Schematic view of the first 100 kb of chromosome V left arm. The insertion of the *LEU2-RFB* cassette is indicated (red). Horizontal bars flanked by dashed lines represent the restriction fragments analysed. **(B)** 2D gel analysis of replication intermediates along the indicated fragments in W303-1a *RFB-chrV* (YAC1164) and *sic1* (YAC1190) glucose-grown (*sic1 RFB-chrV*) or raffinose-galactose-grown cells (*GAL-SIC1 RFB-chrV*). Restriction enzyme digestions, fragments sizes and probes are described in Material and Methods. White arrowheads denote origin-firing and black arrowheads indicate loss of origin-firing efficiency. '*P*' points to forks paused at the RFB (pausing-spot). The percentage of paused forks at the RFC was estimated from the ratio between intermediates in the pausing-spot and intermediates along the Y-arc, and is indicated in the upper left corner of the respective 2D blot.

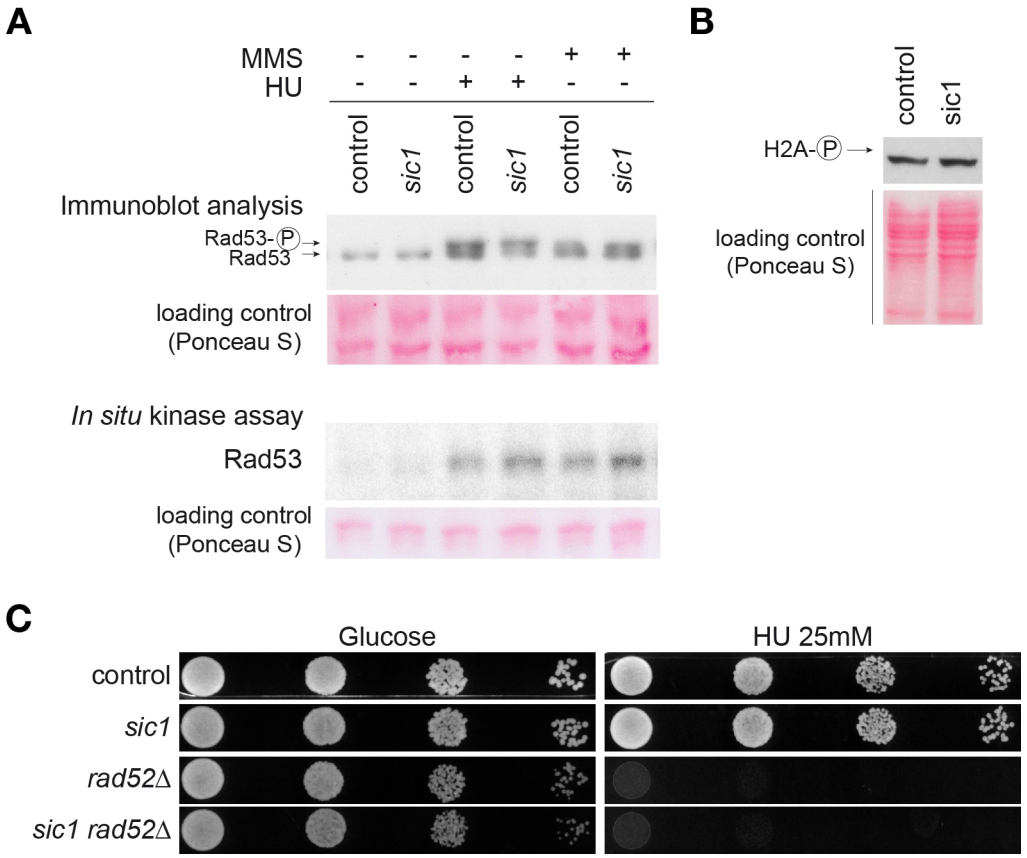

Supplemental Figure 2: Checkpoint responses are not activated in *sic1* cells. (A) Detection of Rad53 hyperhosphorylation by Western blotting and Rad53 autophosporylation by *in situ* kinase assay performed as described (Vaze et al., 2002) in W303-1a control and *sic1* cells growing in normal conditions or after a 2 hours exposure to 0.03% methyl methanesulfonate **(**MMS) or 0.2M hydroxyurea (HU). (B) Detection of histone H2A hyperhosphorylation (H2A-P) by Western blotting. (C) Dilution spotting assay. The indicated strains were plated in YPAD (left panel) or YPAD supplemented with 25mM hydroxyurea (right panel).

Supplemental Table 1: Rates of gross chromosomal rearrangements on chromosome 5 (*CAN^r FOA^r*) obtained in the GCR assay.

Relevant Genotype	GCR rate	95% Confidence Intervals Limits	Fold Increase	
			vs. wt	vs. *sic1*
wt [1]	1.6 X 10^{-9}	[0.1 – 2.4] X 10^{-9}	1	-
RFB-chrV	3.0 X 10^{-8}	[1.7 – 4.6] X 10^{-8}	19	-
RFB-chrV empty	2.3 X 10^{-8}	[1.3 – 3.4] X 10^{-8}	14	-
RFB-chrV 7xARSH4	1.1 X 10^{-8}	[0.4 – 2.1] X 10^{-8}	7	-
*clb2*Δ	0.7 X 10^{-9}	[0.1 – 1.7] X 10^{-9}	0.4	-
sic1	3.7 X 10^{-8}	[2.4 – 5.1] X 10^{-8}	23	1
*sic1 ars507*Δ	1.4 X 10^{-7}	[1.0 – 1.9] X 10^{-7}	87	4
*sic1 ars504.2*Δ	1.2 X 10^{-7}	[0.8 – 1.5] X 10^{-7}	75	3
*sic1 ars507*Δ*::ARS305*	1.2 X 10^{-8}	[0.6 – 2.0] X 10^{-8}	7.5	0.3
sic1 empty	5.0 X 10^{-8}	[3.4 – 6.9] X 10^{-8}	31	1.4
sic1 7xARSH4	1.2 X 10^{-8}	[0.6 – 1.9] X 10^{-8}	7.5	0.3
sic1 RFB-chrV	1.3 X 10^{-5}	[1.1 – 1.5] X 10^{-5}	8,125	351
sic1 RFB-chrV empty	1.6 X 10^{-5}	[1.4 – 1.8] X 10^{-5}	10,000	432
sic1 RFB-chrV 7xARSH4	3.6 X 10^{-6}	[3.0 – 4.2] X 10^{-6}	2,250	97
*sic1 clb2*Δ	2.8 X 10^{-9}	[1.0 – 5.0] X 10^{-9}	1.7	0.08

[1] RDKY3615 (Chen and Kolodner, 1999).

APPENDIX 2

List of Publications

Publications related with this thesis:

Loss of G1/S CKI reduces origin redundancy to delay DNA replication completion at specific chromosome regions to cause genomic instability
(*manuscript in preparation*)

The CDK regulators Cdh1 and Sic1 promote efficient usage of DNA replication origins to prevent chromosomal instability at a chromosome arm
Pilar Ayuda-Durán, Fernando Devesa, **Fábia Gomes**, Joana Sequeira-Mendes, Carmelo Ávila-Zarza, María Gómez, Arturo Calzada
Nucleic Acids Res. 42(11): 7057–7068. Published online 2014 April 21.

Other publication:

Transcriptionally Driven DNA Replication Programme of the Human Parasite Leishmania major
Rodrigo Lombraña, Alba Álvarez, José Miguel Fernández-Justel, Ricardo Almeida, César Poza, **Fábia Gomes**, Arturo Calzada, José María Requena and María Gómez
(*manuscript submitted for publication*)